TARGETING DNA DOUBLE-STRAND BREAK REPAIR TO POTENTIATE RADIO- AND CHEMO THERAPY OF GLIOBLASTOMA

APPROVED BY SUPERVISORY COMMITTEE

_____
Sandeep Burma, Ph.D. (Mentor)
Associate Professor, Radiation Oncology

_____
Robert M. Bachoo, M.D., Ph.D.
Assistant Professor, Neurology

_____
David A. Boothman, Ph.D.
Professor, Pharmacology

_____
Michael A. White, Ph.D.
Professor, Cell Biology

DEDICATION

I dedicate my work to all the patients that have or are currently fighting against cancer. You are the reason I am doing this.

TARGETING DNA DOUBLE-STRAND BREAK REPAIR TO POTENTIATE RADIO- AND CHEMO THERAPY OF GLIOBLASTOMA

by

CARLOS RODRIGO GIL DEL ALCAZAR

DISSERTATION

Presented to the Faculty of the Graduate School of Biomedical Sciences

The University of Texas Southwestern Medical Center at Dallas

In Partial Fulfillment of the Requirements

For the Degree of

DOCTOR OF PHILOSOPHY

The University of Texas Southwestern Medical Center at Dallas

Dallas, Texas

August, 2015

ACKNOWLEDGEMENTS

I thank:

my Ph.D. mentor, Dr. Sandeep Burma, for accepting me in his laboratory and providing numerous opportunities for me to grow as a scientist;

my lab mates, Bipasha, Nozomi, Cristel, Brian, Mariya, Pavlina, and Molly for their constant help and for making the time in the lab more enjoyable;

my parents, Carlos Emilio Gil Loor and Maria Soledad del Alcazar Granda, grandmother, Maria Soledad Granda Centeno, and sisters, Maria Soledad, Carla Emilia, and Maria Isabel Gil del Alcazar for their support and encouragement.

And finally my wife, Pei-hsuan Chen, with whom I have shared this important step of our careers as scientists. I am eternally grateful for all the understanding, encouragement and love you have given me.

TARGETING DNA DOUBLE-STRAND BREAK REPAIR TO POTENTIATE RADIO- AND CHEMO THERAPY OF GLIOBLASTOMA

CARLOS RODRIGO GIL DEL ALCAZAR

The University of Texas Southwestern Medical Center at Dallas, 2015

SANDEEP BURMA, Ph.D.

ABSTRACT

Surgical resection followed by radiation and adjuvant temozolomide (TMZ) is the standard of care for glioblastoma (GBM). Not all GBMs respond to therapy, and most of them quickly acquire resistance to TMZ and recur. In order to develop more effective and rational treatments for GBM, it is crucial to understand the mechanisms underlying radio- and chemo-resistance. We find that protracted TMZ treatment of mice bearing orthotopic tumors (generated by xenografting GBM9 neurospheres) leads to acquired-TMZ resistance resulting in tumor recurrence. In order to understand the basis for therapy-driven TMZ resistance, we generated and functionally characterized ex-vivo cultures from the primary and recurrent tumors. We found that cell lines derived from recurrent (TMZ-treated) tumors were more resistant to TMZ in vitro compared to cell lines derived from primary (untreated) tumors. We also found that the increased resistance to TMZ was due to the augmented repair

of TMZ-induced DNA double strand breaks (DSBs). TMZ induces DNA replication-associated DSBs that are repaired primarily by the homologous recombination (HR) pathway. We found that cell lines from recurrent cultures exhibited faster resolution of Rad51 foci and higher levels of sister chromatid exchanges (SCEs), which indicated that a higher level of HR was contributing to TMZ resistance in these lines. We have recently shown that CDKs 1 and 2 promote HR in S and G2 phases of the cell cycle, in part, by phosphorylating the exonuclease EXO1. We hypothesized, therefore, that blocking CDKs 1 and 2 might be a viable strategy for re-sensitizing recurrent tumors to TMZ. Indeed, we found that CDK inhibitors, AZD5438 and Roscovitine, could attenuate HR in the recurrent TMZ-resistant cell lines resulting in significant chemo-sensitization to TMZ. While HR is primarily involved in the repair of TMZ-induced DSBs, ionizing radiation induced DSBs would be mainly repaired by the non-homologous end joining (NHEJ) pathway. We, therefore, developed another approach to sensitize these tumors to both radiation and TMZ by using a dual PI3K/mTOR inhibitor, NVP-BEZ235, to block both DNA-PKcs and ATM, key enzymes in the NHEJ and HR pathways, respectively. We found that NVP-BEZ235 inhibited both DNA-PKcs and ATM in tumors generated in mice from GBM9 neurospheres, thus blocking the repair of TMZ- and IR-induced DSBs, and resulting in significant chemo- and radio-sensitization. Next, we established that NVP-BEZ235 can cross the blood-brain barrier and recapitulated its radiosensitizing effects in an intracranial GBM model. We found that NVP-BEZ235, administered with IR, can attenuate DSB repair in these intracranial tumors, attenuate tumor growth, and extend survival of tumor-bearing mice. Importantly,

attenuation of DSB repair was more pronounced in tumor cells compared to normal brain cells, thereby providing a larger therapeutic window. In sum, this study indicates that augmented DNA repair may underlie therapy resistance in GBM and provides support for the potential use of DNA repair inhibition as an effective strategy for improving the efficacy of GBM therapy.

TABLE OF CONTENTS

PUBLICATIONS

Gil del Alcazar, C.R., Todorova, P., Mukherjee, B., Tomimatsu, N., Burma, S. Augmented homologous recombination repair mediates acquired temozolomide resistance in a glioblastoma in vivo model of tumor recurrence. [Manuscript in preparation]

Camacho, C.V., Todorova, P.K., Hardebeck, M.C., Tomimatsu, N., **Gil del Alcazar, C.R.**, Ilcheva, M., Mukherjee, B., McEllin, B., Vemireddy, V., Hatanpaa, K., et al. (2014). DNA double-strand breaks cooperate with loss of Ink4 and Arf tumor suppressors to generate glioblastomas with frequent Met amplification. Oncogene.

Gil del Alcazar, C.R., Hardebeck, M.C., Mukherjee, B., Tomimatsu, N., Gao, X., Yan, J., Xie, X.-J., Bachoo, R., Li, L., Habib, A.A., et al. (2014). Inhibition of DNA double-strand break repair by the dual PI3K/mTOR inhibitor NVP-BEZ235 as a strategy for radiosensitization of glioblastoma. Clin. Cancer Res. *20*, 1235–1248. (Highlighted in issue)

LIST OF FIGURES

LIST OF ABBREVIATIONS

53BP1	p53 binding protein 1
AKT	Thymoma viral oncogene homolog 1
ATM	Ataxia telangiectasia mutated
ATR	ATM and Rad3-related protein
BBB	Blood brain barrier
BEZ	NVP-BEZ235
BLI	Bioluminescence imaging
CDK	Cyclin-dependent kinase
CPT	Camptothecin
CO2	Carbon dioxide
DAPI	4', 6-diamidino-2-phenylindole
DDR	DNA damage response
DMEM	Dulbecco's modified eagle medium
DMSO	Dimethyl sulfoxide
DNA	Deoxyribonucleic acid
DNA-PKcs	DNA-dependent protein kinase catalytic subunit
DSB	Double-strand break
EGF	Epidermal growth factor
EGFR	Epidermal growth factor receptor
Epo	Etoposide

GBM	Glioblastoma
Gy	Gray
H2AX	Histone 2A variant X
HR	Homologous recombination
IDH1	Isocitrate dehidrogenase 1
IF	Immunofluorescence
IR	Ionizing radiation
MET	Hepatocyte growth factor receptor
MNNG	N-methyl-N'-nitro-N-nitrosoguanidine
MRI	Magnetic resonance imaging
MRN	Mre11/Rad50/Nbs1 complex
MSI	Microsatellite instability
mTOR	Mammalian target of rapamycin
NF1	Neurofibromatosis
NHEJ	Non-homologous end joining
PBS	phosphate buffered saline
PCR	Polymerase chain reaction
PDGFRA	Platelet derived growth factor receptor
PFA	Paraformaldehyde
PTEN	Phosphate and tensin homolog
RNA	Ribonucleic acid
RTK	Receptor tyrosine kinase

SGZ	Subgranular zone
SVZ	Subventricular zone
TCGA	The cancer genome atlas
TMZ	Temozolomide
TUNEL	Terminal deoxyribonucleic transferase-mediated dUTP-digoxigenin nick and labeling
WHO	World health organization
WT	Wild-type

CHAPTER ONE
General introduction

Glioblastoma

Glioblastomas (GBM) are unfortunately both the most common and deadly type of brain tumors. Patients with GBM exhibit median survival times of only about 15 months and a 5-year survival of less than 10% even with aggressive, multimodal treatment regimens (Stupp et al., 2009a). Although GBM have relatively low incidence, with about 10000 new cases every year (mainly in the older population), they are one of the most devastating cancers, as they are invariably lethal (Dunn et al., 2012). The World Health Organization (WHO) classifies GBM as grade IV diffuse gliomas (Louis et al., 2007) solely based on the histological resemblance to glial cells. Presence of necrosis or microvascular proliferation determines the grade IV glioma diagnosis (Miller and Perry, 2007).

GBM can be further classified into primary or secondary GBM. Primary GBM arise *de novo*, whereas secondary GBM initially arise as grade II or III gliomas and develop into GBM over time through the acquisition of additional mutations (Johnson et al., 2014a). Interestingly, primary GBM account for about 90% of all GBM and have a higher incidence in older patients, whereas secondary GBM account for the remaining 10% and have higher incidence in younger patients. It is important to note that although these two subclasses of GBM are histopathologically indistinguishable, they represent

two very distinct tumor entities with different natural histories, age distributions, genetic signatures, and prognosis (Ohgaki et al., 2014) (**Fig. 1.1**). A salient feature of secondary GBMs is the distinct presence of *TP53* and *IDH1* mutations, which interestingly resemble the Proneural subtype of GBM (see below).

With the advent of the original Cancer Genome Atlas (TCGA) study for GBM (TCGA, 2008), in which the recurrent genomic alterations in more than 200 tumors were identified, four distinct GBM subtypes were defined based on their genomic signature: Classical, Mesenchymal, Neural, and Proneural (Verhaak et al., 2010). The Classical subtype displays the most common recurrent genomic alterations of GBM including Chromosome 7 amplifications and Chromosome 10 deletions, *EGFR* amplifications, and homozygous deletions spanning the *Ink4a/Arf* locus. Notably, this subtype in general lacks additional alterations in *TP53, NF1, PDGFRA, or IDH1*. As the flipside of the Classical subtype, the Proneural subtype does not present Chromosome 7 amplifications and Chromosome 10 deletions as frequently and displays high frequency of *TP53*, *PDGFRA* and *IDH1* alterations. Of clinical relevance, this subtype shows no evidence of therapeutic advantage to high intensity therapies, such as concomitant radiation and chemotherapy. Samples of the Mesenchymal subtype have high expression or mesenchymal markers such as *CHI3LA* and *MET*. This subtype is also marked by either homozygous loss, mutations, or simply low expression of *NF1*. The Neural subtype of GBM most closely resembles the expression pattern of normal brain tissue, with clear overlaps with neuronal and astrocytic gene signatures.

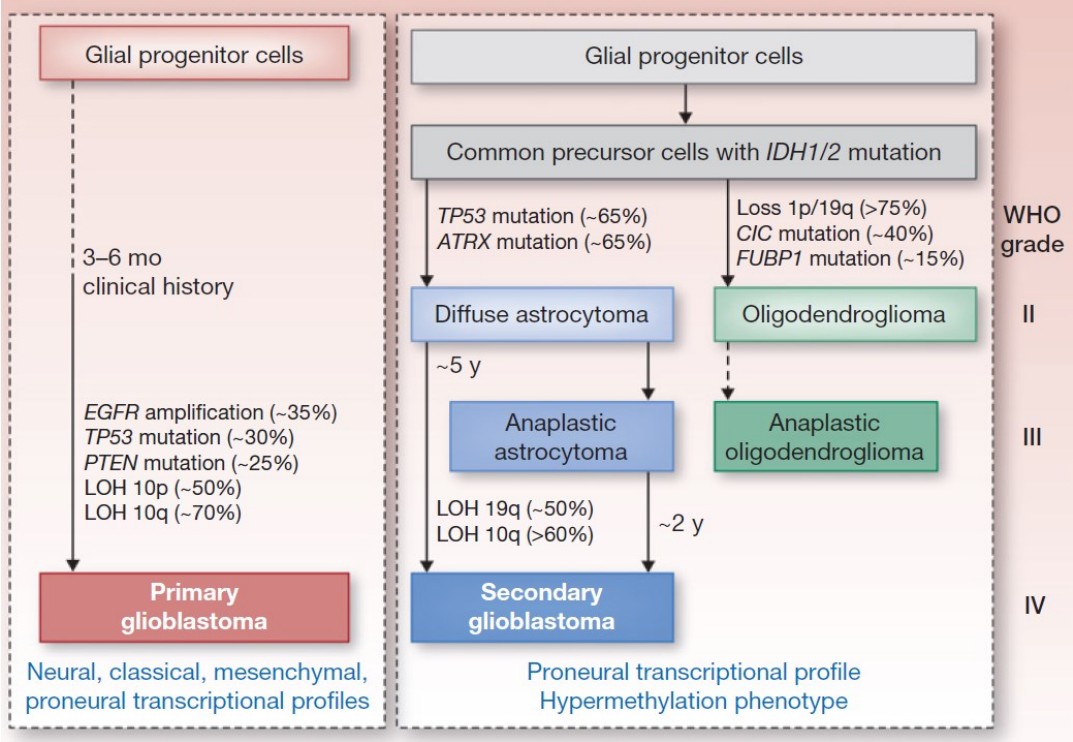

Figure 1.1. Classification of GBM. Primary GBM arise de novo from precursor cells whereas secondary GBM develop from lower grade astrocytomas over time. All subtypes of GBM (neural, classical, mesenchymal and proneural) are represented in the primary GBM, whereas the secondary GBM are all of the proneural subtype, and display *IDH1/2* mutations and a hypermethylation phenotype. Figure modified from Ohgaki et al., 2014.

Glioblastoma treatment

No contemporary treatment is curative. The standard of care of GBM consists of maximal, safe surgical resection followed by radiotherapy and chemotherapy. Significant progress has been made in understanding the biology of GBM, but unfortunately this knowledge has not translated in better treatments in the clinic. One of the major difficulties hindering treatment efficacy, and what makes GBM a very unique type of tumor, is its location. As opposed to other types of tumors, a simple biopsy represents a major brain surgery. Also local growth control is majorly restricted by both the difficulty in performing major tumor resections and by its infiltration into vital nervous tissue. Additionally, limiting drug availability, GBMs hide behind the blood-brain barrier. In addition to its location, its remarkable inter- and intratumoral heterogeneity make GBM multiple diseases at the same time, each potentially with its own resistance and vulnerability, making tumor relapse a given. Indeed multiple subtypes have been identified within the same patient's GBM (Sottoriva et al., 2013). Furthermore, the existence of heterogeneous clones with varying sensitivities to chemotherapy has been confirmed within a single tumor (Meyer et al., 2015).

Surgery. Since the first brain tumor was surgically removed in 1884 (Kirkpatrick, 1984), the field of neurosurgery has dramatically evolved. It soon became evident that surgery, even as radical as whole hemisphere removal, did not cure the cancer. In modern surgeries the goals are to obtain biopsies for pathological diagnosis, relief mass effect, and maximize removal of the tumor. Special attention is taken to spare speech and motor

centers, through the use of awake surgeries, electrodes, and MRI before and during the surgery. Multiple studies have documented the benefits of surgery and its extent (Ammirati et al., 1987; Fadul et al., 1988; Keles et al., 1999; Ryken et al., 2008; Sanai and Berger, 2008). One study with a population size of more than 400 patients, found that a significant survival advantage was associated with resection of 98% or more of the tumor volume with median survival of 13 months vs. 8.8 months in patients with <98% resection (Lacroix et al., 2001). Recurrent GBM are rarely surgically resected as patients may not be eligible for surgery, and the benefit in performing the surgery has not been determined. This makes tumor evolution and resistance studies difficult due to the dearth of matched primary vs. recurrent tumors.

Radiotherapy. Paradoxically, radiation exposure is the only known risk factor for gliomagenesis and also the backbone of GBM treatment. Radiotherapy is usually given concomitantly with temozolomide (see below) or alone in elderly patients (Keime-Guibert et al., 2007). Postoperative radiotherapy has been shown to increase the median survival of GBM patients compared to surgery alone from 14 to 36 weeks (Walker et al., 1978). A dose escalation study showed that giving a higher radiation dose extended the survival from 9 months in the 45Gy regimen to 12 months in the 60Gy regimen (Bleehen and Stenning, 1991). Also when analyzing radiological data, it was determined that 90% of the tumors recurred within a 2cm margin of the originally resected tumors (Liang et al., 1991). Therefore, currently the recommended scheme for postoperative radiotherapy includes a maximum cumulative dose of 60Gy, given in 2Gy daily fractions, and directed towards the radiographically defined T1 contrast-enhancing (by MRI) area plus a 1-2cm

margin (Buatti et al., 2008). Although there are other radiotherapy modalities such as interstitial brachytherapy, they are rarely used and their effectiveness remains to be tested.

Chemotherapy. As it became clear that surgery, even with the radiation adjuvant was not curative, oncologists started experimenting with cytotoxic chemotherapy. As mentioned above, a major hindrance to the use of chemotherapeutic agents for GBM is the blood-brain barrier (BBB), which effectively excludes many agents from the CNS. Therefore, intracranial drug delivery methods are currently under development to go around this issue so that drug toxicities can be reduced as lower doses would be needed to achieve the desired concentrations in the brain tumor. Though not the case anymore, nitrosoureas (BCNU or CCNU) were the major chemotherapeutic agents for GBM treatment, as they apparently had modest increases in survival (Chang et al., 1983). However, the use of such agents remained controversial as results were not conclusive. Recently, a study by Stupp et al. (2005) showed conclusively that temozolomide (TMZ), an alkylating agent (see **Chapter Two** for mechanism of action), was able to extend the median survival of GBM patients from ~12 to ~14 months. Patients also saw significant increase in 2, 3, 4 and 5 year survivals from 27.2%, 16.0%, 12.1%, and 9.8%, respectively, with radiotherapy plus temozolomide, versus 10.9%, 4.4%, 3.0%, and 1.9% with radiotherapy alone (Stupp et al., 2009). Temozolomide was approved by the FDA in 2005 for the treatment of newly diagnosed GBMs and has since then remained part of the mainstay of treatment.

Targeted therapy. With the identification of recurrent genomic alterations in primary GBM, numerous clinical trials testing potential targets are underway. However, for a large fraction of patients clinical response to these agents is either insignificant or short-lived. The epidermal growth factor receptor gene (*EGFR*) is a very attractive candidate for targeted therapy as it is amplified in ~50% of GBM (TCGA, 2008)(Parsons et al., 2008), and a significant fraction of tumors also displays gain-of-function mutated versions such as *EGFRvIII* (Huang et al., 2009). Also overexpression of PDGFR has been documented in GBMs (TCGA, 2008). These events significantly activate PI3K and downstream effectors and result in proliferation and pro-survival signals. Despite the well-justified expectations for inhibitors targeting the kinase domain of EGFR and EGFR mutants, erlotinib and gefitinib showed disappointing clinical benefits (Franceschi et al., 2007; Kesavabhotla et al., 2012; Raizer et al., 2010; van den Bent et al., 2009; Yung et al., 2010). Also imatinib, a kinase inhibitor of PDGFR, showed no benefit in recurrent GBM (Razis et al., 2009). Since GBM are characterized by sustained angiogenesis, there was an interest in targeting this process by inhibiting its key regulator, VEGF. A humanized, monoclonal antibody targeting VEGF, Bevacizumab, has been tested clinically and shows modest activity against primary GBM but no increase in survival when given in combination with standard therapy (Gilbert et al., 2014; Peters et al., 2015). Interestingly, Bevacizumab showed a modest but significant benefit in survival in recurrent GBM and has been approved for treatment (Friedman et al., 2009; Vredenburgh et al., 2007).

DNA repair and resistance

GBMs invariably recur. Despite aggressive treatment and initial response, GBM tumors eventually stop responding to conventional and targeted treatment. It is becoming increasingly clear that GBMs display patterns of branched evolution where cells from the founding population can acquire different mutations and follow different evolutionary paths (Sottoriva et al., 2013). Such branching creates heterogeneity and multiple paths to resistance, which may partly explain the failure of targeted therapies. Moreover, it has been shown that glioma treatment may propel the evolution of these tumors by introducing characteristic mutations (C>T mutations in the case of TMZ) and selecting for resistant clones (Johnson et al., 2014). Very few shared mutations among the initial glioma and its recurrences are observed (**Fig. 1.2**) (Johnson et al., 2014a). However, the relative contribution of TMZ therapy to this diversification it is not clear from these studies , since the progression of tumors alone also introduces new mutations. Since surgical resection is almost complete in a high proportion of patients, it is likely that the recurrent tumors may originate from residual cells representing minor clones that remained undetected in the initial tumors. The study of the evolutionary trees of GBM tumors has identified the presence of both subclonal mutations, late occurring events that are present in a few cells, and clonal events which occur in the trunk of the evolutionary tree. These truncal events represent more attractive targets as they are shared among a bigger group of cells and are more likely to be present in the recurrences. Although an

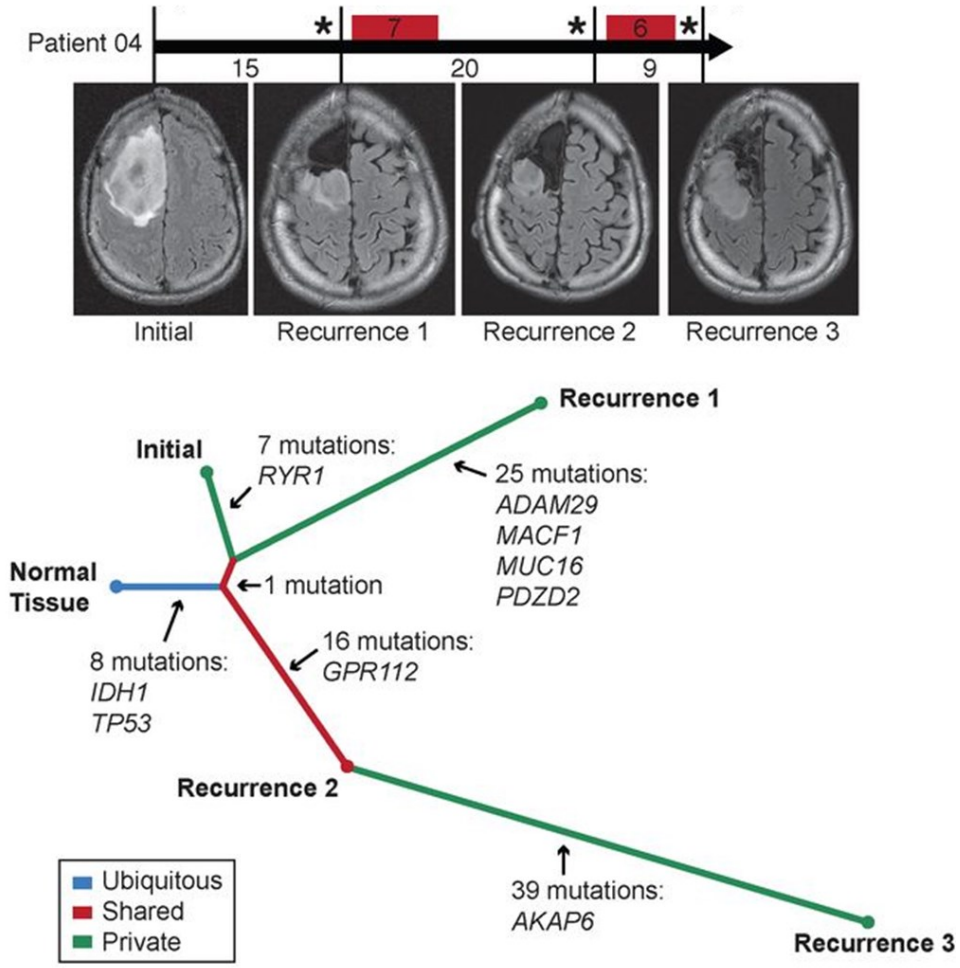

Figure 1.2. Branched evolution of gliomas. Gliomas display a branched evolution during progression and treatment. In the case of this patient, recurrences contained a high number of mutations unshared (private) to each recurrence making it evident that the initial tumor and its recurrences are very different diseases. Modified from Johnson et al., 2014.

enormous amount of research has been done in order to understand the driving oncogenic events and vulnerabilities of primary tumors, this knowledge may have limited utility as recurrent GBM are very different.

In the past decade, data has accumulated to support a hierarchical organization of solid tumors including GBM (Chen et al., 2010; Reya et al., 2001; Singh et al., 2004), in which the so called stem-like cells can give rise to the heterogeneous cells within a tumor. These cancer stem-like cells have been proposed to represent a population of therapy-resistant cells that give rise to recurrences despite tumor response to treatment. As such, cancer stem-like cells would represent the evolving unit of the tumor. Intrinsic and acquired mechanisms of resistance in GBM cancer stem-like cells that limit both radio- and chemotherapy are therefore important to study. The underlying mechanism for such augmented resistance of these cells has been attributed to overexpression of ATP-binding cassette transporters (Dean et al., 2005), activation of survival pathways (Hambardzumyan et al., 2008), and greater DNA-damage repair (Bao et al., 2006). Given that the mechanism of action of TMZ and radiation (the backbone of GBM therapy) is generation of DNA damage, DNA-damage repair is of special importance in treatment failure.

Cells, including cancer cells, are the target of tens of thousands of lesions in the DNA per day. These lesions, if not properly repaired, can impair transcription and replication, or even lead to mutations or gross chromosomal aberrations that can result in aberrant signaling and cell death (Jackson and Bartek, 2009). DNA damage can range from base damage, mismatches, or base loss to strand breaks such as single strand breaks

(SSB). Single strand breaks can give rise to double strand breaks (DSB), the most toxic type of DNA lesion, if they are located very close to each other or if encountered by a replication fork. Given that cancer cells are under a higher level of replication stress due to increased levels of proliferation, they usually have an altered DNA damage response (DDR). Activation of oncogenes and loss of tumor suppressor genes allow cancer cells to suppress cell cycle checkpoint activation and pro-apoptotic signaling allowing them to survive with disturbingly high levels of genomic instability (Halazonetis et al., 2008). In the context of radiotherapy and TMZ treatment, both of which result in multiple types of DNA lesions including DSBs, multiple genetic and epigenetic alterations related to the DDR have been identified that help the cells resist therapy.

Heightened DSBs repair capabilities have been reported before as mechanisms of resistance to genotoxic therapies in glioma cells. One mechanism is upregulation of non-homologous end-joining (NHEJ), one of the two pathways that the cell uses to repair DSBs. This heightening of NHEJ has been shown to occur by over-activation of the DNA repair apical kinase, DNA-PKcs, by Akt in glioma cells with upregulated PI3K/Akt signaling (Mukherjee et al., 2009). Additionally, it has been shown that radiation treatment enriches for glioma stem cells, and these stem cells show a higher activation of ATM, another apical kinase in the DSB repair, and more efficient repair (Bao et al., 2006). Heightened DSB repair can also occur due to upregulation of downstream effectors in the DDR. For instance Rad51, a key protein in the process of homologous recombination (HR), the other pathway used to repair DSBs, has been shown to be overexpressed in several cancers, and this correlated with heightened resistance to

genotoxic therapies including radiation and TMZ (Kiyohara et al., 2012; Raderschall et al., 2002; Short et al., 2011). Therefore targeting the DDR has been proposed as a strategy for sensitizing cancers to both radiation and genotoxic agents.

Targeting the DNA damage response

Not all GBMs respond to radiotherapy, and most of them quickly acquire resistance to TMZ and recur. In order to develop more effective and rational treatments for GBM, it is crucial to understand the mechanisms underlying radio- and chemo-resistance. The work presented here sets out to gain a better understanding of the underlying mechanisms of temozolomide resistance. Using this knowledge, we set to show in a proof of principle manner, that inhibiting two important apical kinases in the DNA damage response (DDR), ATM and DNA-PKcs, could be used as an effective strategy to both chemo- and radio-sensitize GBM. This work can thus be summarized as follows:

1) Development of an orthotopic mouse model of tumor recurrence after TMZ chemotherapy **(Chapter Two)**.
2) Establishing the mechanism(s) of TMZ-resistance in the aforementioned model **(Chapter Two)**.
3) Designing rational strategies for therapeutic sensitization by targeting HR with CDK 1 and 2 inhibitors **(Chapter Two)** and by inhibiting both HR and

NHEJ with an ATM and DNA-PKcs inhibitor **(Chapter Three)** – *in vitro* studies.

4) Validation of DNA repair inhibition as a viable strategy for sensitizing tumors to TMZ and radiotherapy **(Chapter Three)** – *in vivo* studies.

CHAPTER TWO
Mechanisms of resistance to temozolomide

Introduction

Glioblastomas (GBMs) are incurable, malignant brain tumors (Dunn et al., 2012). The median survival of patients with GBM is only slightly above a year and the 5-year survival is less than 10% despite aggressive treatment regimens (Stupp et al., 2009b). The current mainstay of treatment is surgical resection, followed by radiation therapy combined with concomitant and adjuvant temozolomide chemotherapy (Stupp et al., 2009b). Addition of temozolomide to standard therapy increases the survival rates significantly, though minimally (Stupp et al., 2009b). This lack of effectiveness is mostly due to intrinsic and acquired resistance of tumors to TMZ (Sarkaria et al., 2008). With only three drugs ever being approved for clinical use for treatment of GBM (McNeill et al., 2014) patients are virtually left without treatment options after tumor recurrence; therefore, it is crucial to find the mechanisms of resistance in order to find strategies to re-sensitize these tumors to TMZ.

TMZ is an alkylating agent that methylates DNA at the N^7 position of guanine, the O^3 position of adenine and the O^6 position of guanine (Friedman et al., 2000). Cytotoxicity from TMZ is mostly derived from the O^6-methyl guanine (O^6-meG) (Dolan et al., 1991; Wedge et al., 1996a; Wedge et al., 1996b). If not reversed by direct enzymatic repair of O^6-methylguanine methyl transferase (MGMT), O^6-meG mismatches

with thymine during replication. The mismatch is recognized by the DNA mismatch repair (MMR) machinery, which promotes the excision of the newly synthesized strand leaving the parental strand with the O^6-meG lesion intact (Friedman et al., 2000). O^6-meG can then mismatch again with thymine leading to repeated cycles of repair attempts and persistent single strand stretches (Fu et al., 2012). During the following round of replication, the replication fork encounters single stranded DNA, and a single-ended double strand break (DSB) is formed (Ochs and Kaina, 2000). DSBs are extremely toxic to the cell and can lead to cell death if not repaired accurately by homologous recombination repair, the dominant DSB repair pathway in the S/G2 (replicative phases) of the cell cycle (Jackson and Bartek, 2009).

Though TMZ-induced DSBs are very toxic, TMZ's efficacy is greatly limited by both inherent and acquired resistance mechanisms developed by the cell. MGMT can directly reverse the O^6-meG lesions; therefore, high expression of the protein leads to TMZ resistance. MGMT promoter methylation (which silences expression of MGMT) correlates with better response to TMZ (Hegi et al., 2005a; Wiewrodt et al., 2008). Conversely, acquired resistance has been correlated to heightened expression of MGMT in recurrent tumors in clinical and mouse xenograft studies (Felsberg et al., 2011; Happold et al., 2012; Kitange et al., 2012; Sarkaria et al., 2008). Another reported mechanism of acquired resistance is loss of MMR (Cahill et al., 2007; Felsberg et al., 2011; Happold et al., 2012; Hunter et al., 2006; Johnson et al., 2014b; Nguyen et al., 2014; Sarkaria et al., 2008; Yip et al., 2009). The basic principle being that without MMR, single stranded DNA stretches are not generated and consequently no DSBs are

formed at replication forks. In this case the cells are able to survive with the resulting C>T/A>G mutations. In both cases no DSBs are induced.

Though important, MGMT and MMR status do not account for resistance to TMZ in all cases (2008; Happold et al., 2012). About half of patients express MGMT (Hegi et al., 2005a) and only a fraction exhibit evidence of MMR deficiency (2008; Cahill et al., 2007; Felsberg et al., 2011), making it evident that there must be yet undiscovered mechanisms of resistance. Here, we report that protracted treatment with TMZ of MGMT deficient, orthotopic GBM tumors can result in acquired TMZ resistance due to heightened DSB repair of TMZ-induced DSBs. This resistance can be attributed to augmented homologous recombination repair, a pathway that can be targeted for chemosensitizing GBM.

Methods

*Cell culture and in vitro TMZ treatments***.** Neurosphere cultures were maintained as described (Estrada-Bernal et al., 2011). Briefly, GBM9 spheres were maintained in DMEM/F12 1:1 media (Life Technologies) supplemented with B27 without Vitamin A (Life Technologies), 10 ng/mL EGF, and 10 ng/mL bFGF (Peprotech). Monolayer human glioma lines were maintained in DMEM media with 5% FBS, 5% NCS, 1% P/S. U138 was supplemented with non-essential amino acids. HSFs were maintained in αMEM supplemented with 20% FBS. All cells were kept in humidified incubators at 37^{o}C with 5% CO_2. All cells were tested to be *Mycoplasma* free. To generate temozolomide

resistant lines, GBM9 spheres, and U251, U87MG, LN229, T98G, U138 monolayer cultures were treated with 50μM temozolomide and replenished every other day for 24 days.

Animal injections, treatments, and ex-vivo culture generation. Animal studies were performed in accordance of the UT Southwestern IACUC-approved protocol #2010-0077. Intracranial tumors were generated by injecting 5×10^5 GBM9 cells in 5 μL of growth media into the right corpus striatum (Mukherjee et al., 2009) of Nu/Nu nude mice (Charles River, Stock#88). Treatment was initiated 7 days after injections. Mice were treated every other day with 20mg/kg temozolomide by oral gavage (*vehicle:* polyethylene glycol 300, Sigma-Aldrich) a total of 12 times. Mice bearing intracranial tumors were sacrificed when they became moribund. Brains were removed and tumors dissected. Ex-vivo cultures were generated by triturating tumor tissue with trypsin and placing the mixture in plastic flasks with DMEM 10% FBS media.

Colony survival. Cells were plated in triplicate onto 60-mm dishes (1,000 cells per dish), and treated either with ionizing radiation, temozolomide, N-methyl-N'-nitro-N-nitrosoguanidine, Camptothecin, or Etoposide at the indicated doses. At 48 hours after TMZ or MNNG, 2hr after CPT, or 1hr after Epo addition, drug-containing medium was replaced with drug-free medium. For the chemosensitization experiments, TMZ-containing media was replaced with either 5μM Roscovitine or 0.25μM AZD5438

containing media for 48hr. Surviving colonies were stained with crystal violet approximately 10 to 14 days later as described before (Mukherjee et al., 2012).

Western Blot. Cells were mock irradiated or irradiated with 10Gy of IR. Cell lysates were prepared 0.5hr after irradiating and Western blotted as described before (Mukherjee et al., 2012). Antibodies used were as follows: Actin, Sigma, 1:1000; Chk1, Cell Signaling, 1:500; Chk1 (Ser317) Cell Signaling, 1:500; Chk2, Cell Signaling, 1:500; Chk2 (Thr68), Cell Signaling, 1:500; MGMT, Millipore, 1:1000; MLH1, BD Biosciences, 1:500; MSH2, BD Biosciences, 1:500; MSH3, Assay Biotech, 1:1000; MSH6, Assay Biotech, 1:1000.

Microsatellite Instability. Genomic DNA was obtained from high passage ex-vivo cultures by using the DNeasy Tissue and Blood kit (Qiagen). Microsatellite-containing loci were amplified by PCR and products ran in 8% polyacrylamide gels to determine their relative sizes. PCR reaction conditions and primers were used as described (Dietmaier et al., 1997b).

DNA repair assay. For monitoring DSB repair**,** cells in chamber slides were pulsed with TMZ (10μM) for 48hr, MNNG (1μM) for 48hr, CPT (50nM) for 2hr, Epo (2μM) for 1hr, or irradiated with 1Gy of IR. Cells were fixed at the indicated times and processed for immunofluorescence staining as described (Mukherjee et al., 2012) using antibodies

against 53BP1 (Santa Cruz, 1:1000), or Rad51 (Santa Cruz, 1:1000). Foci were counted manually in more than 50 cells and average values were calculated.

Flow cytometry. Cells were treated with 10uM TMZ for 48hr, or irradiated with 10Gy of IR, fixed at the specified timepoints and processed for propidium idodide staining and flow cytometry (McEllin et al., 2010).

Resection assays. For the BrdU incorporation assay, cells were grown in BrdU (40ug/mL) for 2 days (1 cell division) before addition of CPT. For both assays, BrdU incorporation and RPA foci staining, cells were pulsed with CPT (50nM) for 2hr, and fixed at indicated timepoints. Cells were extracted and processed for staining as described (Tomimatsu et al., 2014).

Sister Chromatid Exchanges. To visualize SCEs, cells were incubated in the presence of BrdU (BD Biosciences, 20μM) and DMSO or CPT (50nM) for two cell divisions (4 days), after which metaphases were prepared as described before (McEllin et al., 2010). SCEs were counted and normalized to the total number of chromosomes per spread for 25 metaphase spreads per treatment group.

Results

Temozolomide treatment leads to acquired TMZ-resistance in MGMT negative cells. Temozolomide (TMZ) chemotherapy is part of the backbone of GBM treatment;

however, these tumors inevitably become resistant to temozolomide. Given the universality of tumor recurrence, more studies are desperately needed to address mechanisms of chemoresistance in glioblastoma (GBM). As a prelude to *in vivo* studies, we treated human glioma cells with 50μM TMZ (12 doses over 24 days), as this is lower than measured plasma concentrations and around the predicted concentrations in the tumors of GBM patients. We used the MGMT-expressing, adherent cell lines, T98G and U138, the MGMT-negative, adherent lines U251, U87MG, LN229, and the MGMT-negative sphere-forming ("stem-like cells") GBM9. The MGMT-expressing lines were initially very resistant to TMZ (**Fig. 2.1A** and **B**). Not surprisingly, the resulting lines after prolonged TMZ-treatment (T98G-T12 and U138-T12) were also very resistant. On the other hand, the MGMT-negative lines U87MG and LN229 stopped dividing after the 6-8th dose of TMZ and remained senescent. In contrast, the U251 and GBM9 cells, even though initially sensitive, became more resistant to TMZ after prolonged treatment with TMZ (**Fig. 2.1C** and **D**). Importantly, this acquired resistance in cells U251-T12 and GBM9-T12 was not accompanied by overexpression of MGMT. This result suggests that other mechanisms of resistance may be in action that either impede the formation of double-strand breaks (DSB) or aide the cells in handling or responding to DSBs to avoid cell death. In order to further understand the acquired TMZ-resistance, we decided to use a more realistic, *in vivo* orthotopic model.

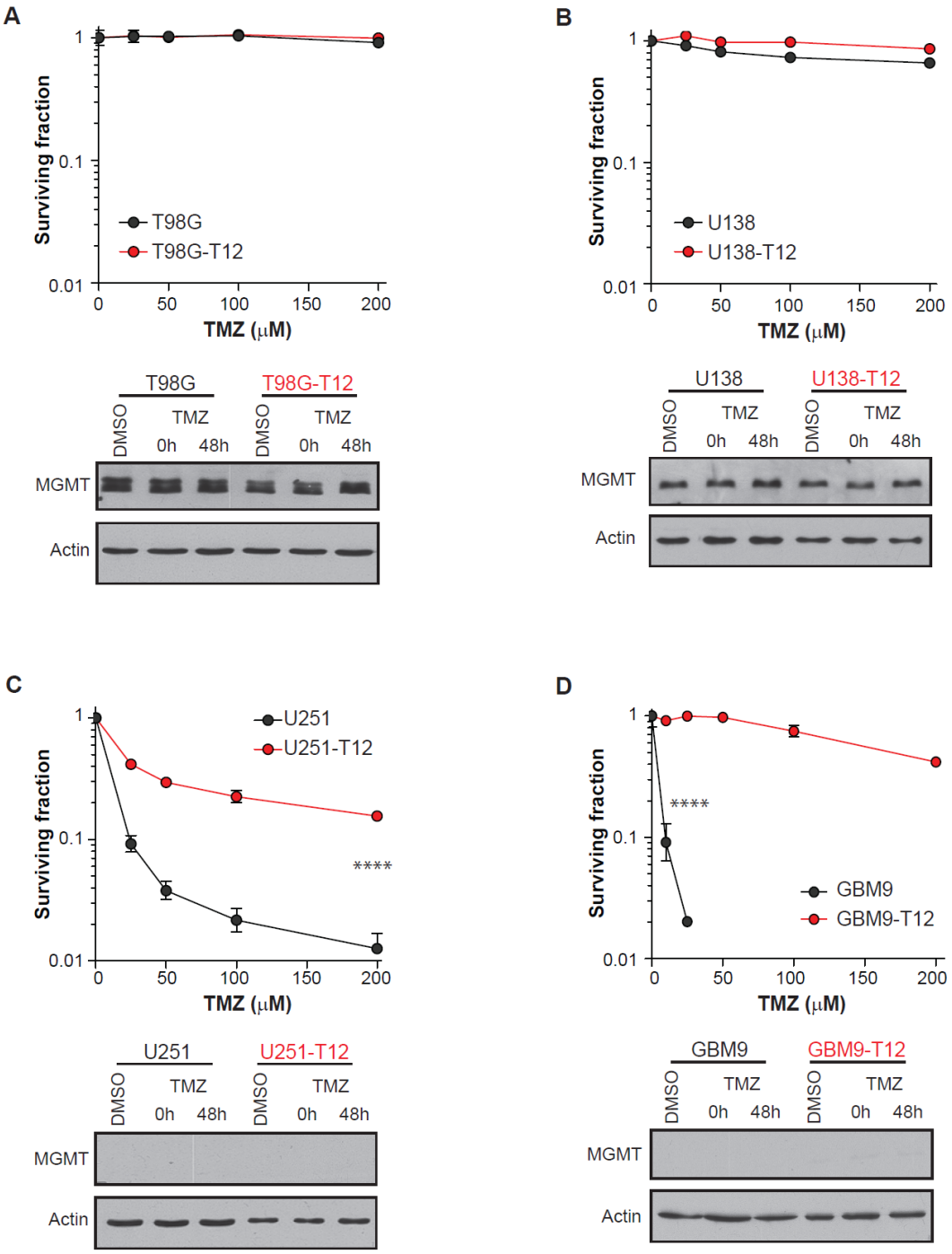

Figure 2.1. Acquired resistance does not correlate with increased MGMT. A-D. T98G, U138, U251 and GBM9, and their long-term treated counterparts (T12) were used in a colony survival assay with increasing concentrations of TMZ. Error bars, S.D. ****, P<0.0001. Cell lysates treated with DMSO or TMZ were probed for MGMT expression.

GBM orthotopic mouse model generation. One reason for the lack of studies addressing TMZ resistance is the lack of matched primary and recurrent patient samples/cell lines, and the lack of good experimental models to study acquired resistance. In this study, we have generated an *in vivo* model of acquired resistance to address this need. We first surgically implanted GBM9 sphere-forming cells into the brain of nude mice. GBM9 were obtained from a treatment naïve patient and established as cultures in serum free media. These growing conditions have allowed these cells to maintain an undifferentiated state, which is key to maintain important genomic signatures from the original tumor (such as EGFR overexpression in GBM9) (Estrada-Bernal et al., 2011). Therefore, this line forms tumors in the brain that closely resemble the original tumor. Seven days after implantation, mice remained untreated or were treated with TMZ repeatedly (20mg/kg, 12 doses every other day), mimicking the adjuvant phase of treatment in the clinic. When the mice became moribund due to brain tumor burden, ex-vivo cultures were generated from each independently evolving tumor. In this model the untreated tumors represent the original, treatment-naïve, primary tumor, and the tumors after TMZ treatment represent the recurrent tumor of an isogenic, matched tumor pair (**Fig. 2.3A**). Importantly, mice bearing GBM9 tumors treated with TMZ had a longer survival than untreated mice, showing that the GBM9 cells were initially sensitive and acquired TMZ-resistance during the course of TMZ treatment (**Fig. 2.2**). Furthermore, when we performed clonogenic assays with increasing doses of TMZ, we found that recurrent GBM9 ex-vivo cultures (shown in green) were generally more resistant to TMZ than the primary GBM9 ex-vivo cultures (shown in black; **Fig. 2.3B**). Two cultures, 419

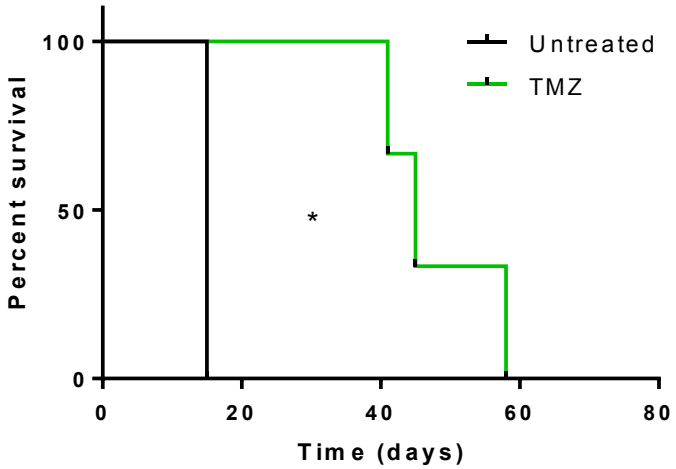

Figure 2.2. GBM9 tumors respond to TMZ. GBM9 cells were injected in the brain of nude mice and allowed to form tumors. The TMZ arm received 12 doses of 20mg/kg TMZ every other day. *, P=0.0253

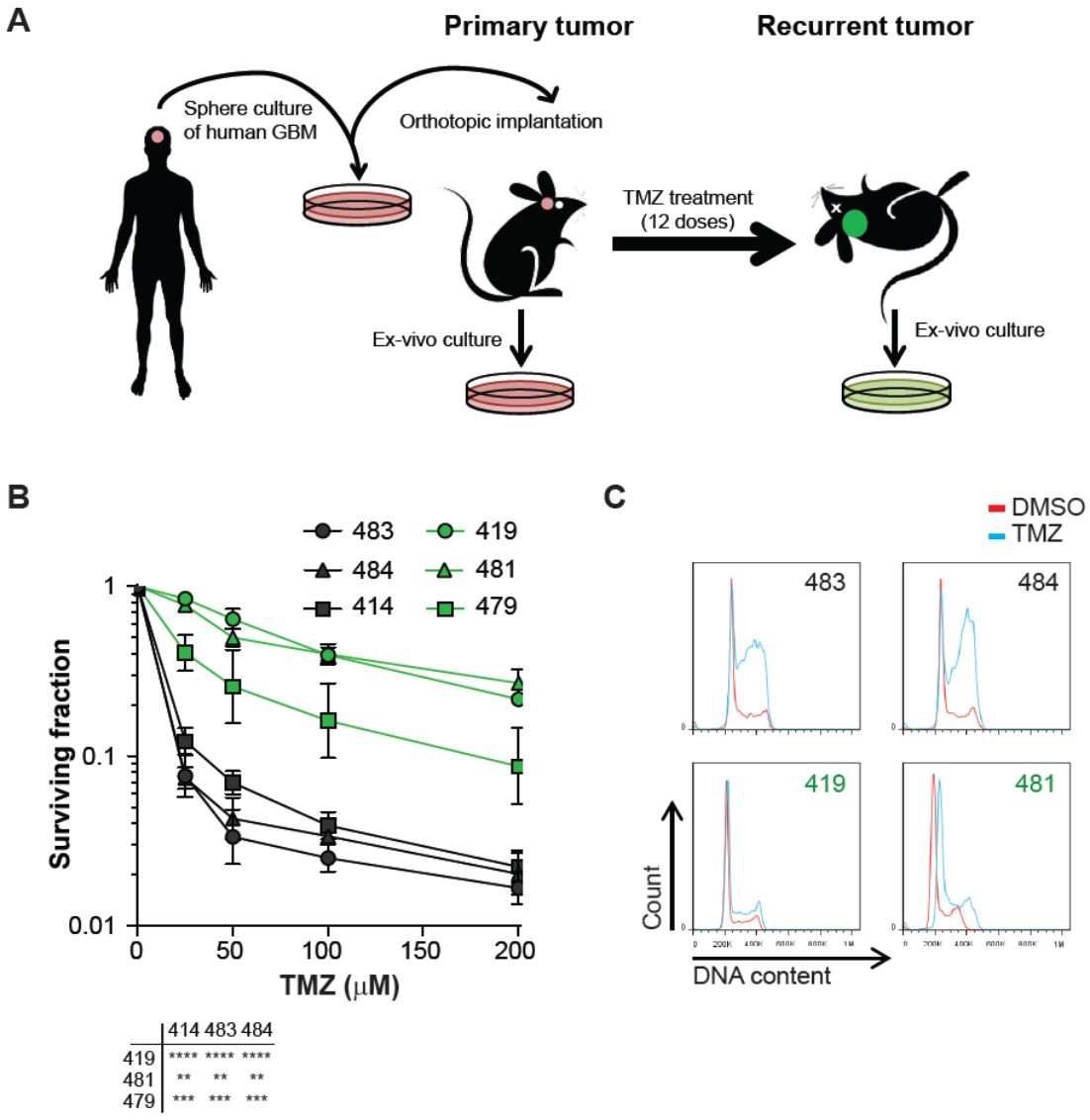

Figure 2.3. Acquired TMZ-resistance arises after protracted in vivo treatment. A. GBM9 neurosphere cultures of a patient sample were expanded in culture and injected intracranially in nude mice. Brain tumors from untreated (primary) and TMZ treated mice (recurrent) were harvested and ex-vivo cultures were generated for further characterization. **B.** Primary (shown in black: 414, 483 and 484) and recurrent (shown in green: 419, 479 and 481) cultures were used in a colony survival assay with increasing concentrations of TMZ. Error bars, S.D. ****, P<0.0001. **, P=0.0017. **C.** Primary (483 and 484) and recurrent (419 and 481) cultures were treated with 50μM TMZ for 48hr, stained using PI, and intensity of 10000 cells measured by flow cytometry.

and 481, were exceptionally chemoresistant and were therefore chosen for further analysis. Two sensitive cultures (483 and 484) were chosen as the primary controls. We observed a normal S/G2 arrest in response to TMZ treatment in the primary cultures but not in the recurrent ones, further showing the dichotomous sensitivities between these two groups (**Fig. 2.3C**). Importantly, this was not due to an abrogated checkpoint activation in the recurrent cultures, as we did observe a robust arrest in G2 and phosphorylation of checkpoint proteins Chk1 and Chk2 in these cells upon irradiation (**Fig. 2.4**).

Augmented DNA repair via HR is the basis of acquired TMZ-resistance. We next wanted to find out the mechanism of this acquired TMZ-resistance in the recurrent tumors. As mentioned above, the main mechanisms of resistance seen in patients are re-expression of MGMT and loss of MMR proficiency, both of which impede the generation of DSBs in the tumor cells. MGMT-mediated repair does not play a role in the observed resistance, as neither the original GBM9 spheres, the primary, nor the recurrent ex-vivo cultures express MGMT (**Fig. 2.5A**). To assess MMR status, we looked at four MMR proteins whose expression levels have been shown to decrease after TMZ treatment (Cahill et al., 2007; Felsberg et al., 2011). There was no difference in protein levels between the original GMB9 cells and ex-vivo cultures suggesting these cells are MMR proficient (**Fig. 2.5B**). However, this does not rule out mutations in these genes which are also believed to render cells MMR deficient (Cahill et al., 2007; Hunter et al., 2006; Johnson et al., 2014b; Nguyen et al., 2014; Yip et al., 2009). Therefore, we looked at the

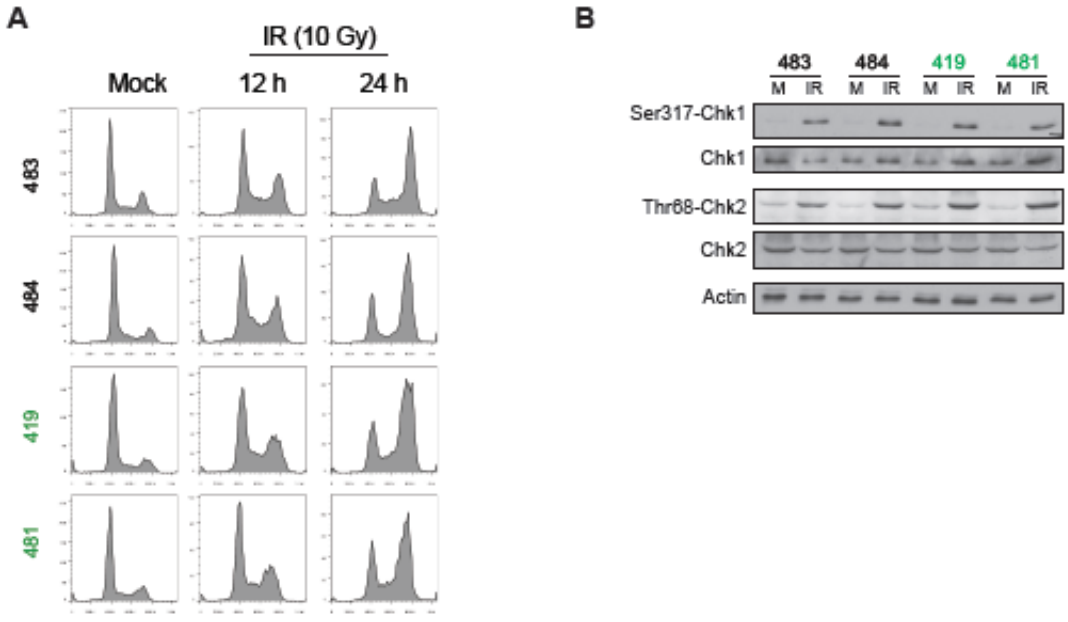

Figure 2.4. Primary and recurrent cultures can arrest in G2. A. Primary and recurrent cultures were irradiated with 10Gy IR and stained with PI for flow cytometry at 12 and 24hr post-irradiation. **B.** Chk1 and Chk2 phosphorylation levels were assessed as a means of determining their activation 30 min after irradiating primary and recurrent cultures with 10Gy IR.

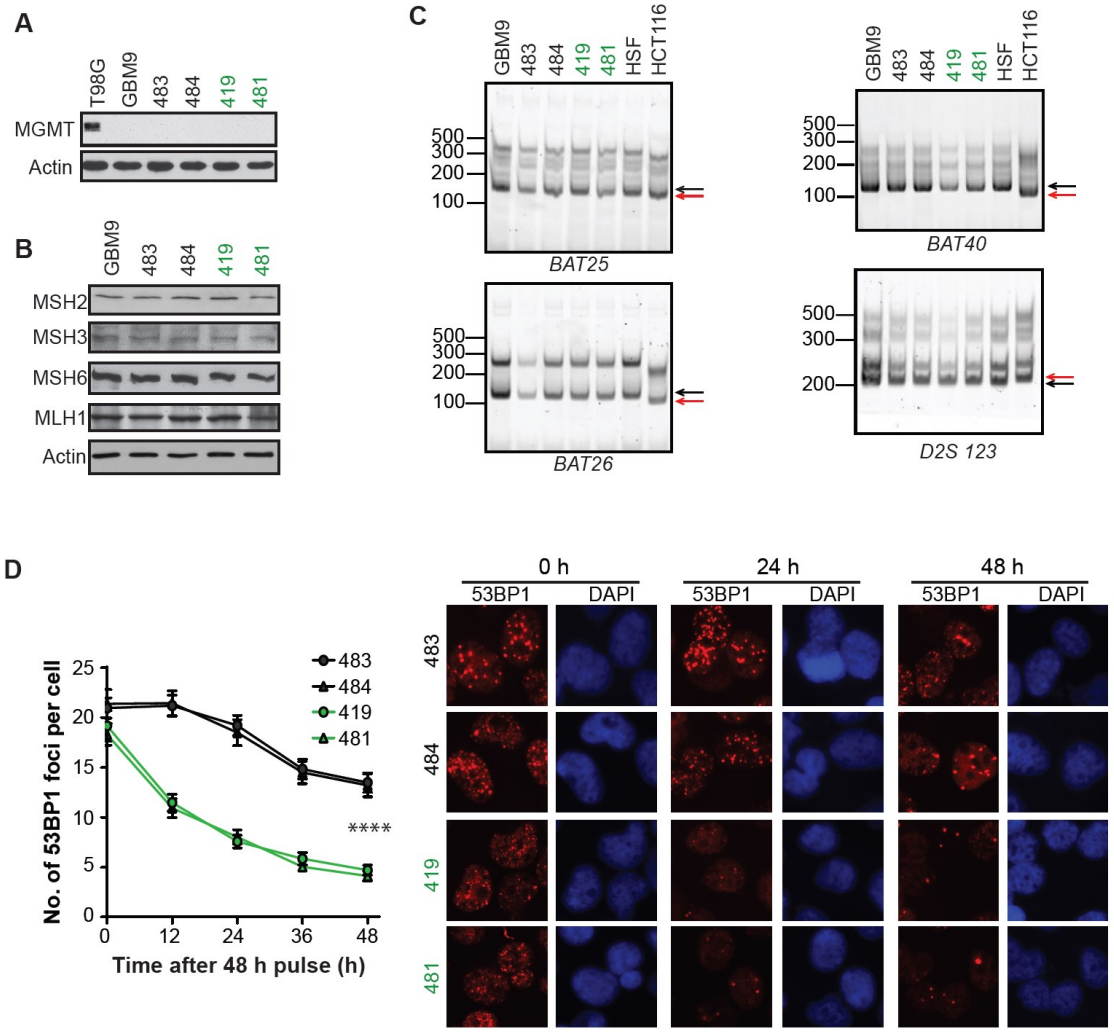

Figure 2.5. TMZ generates DSBs in ex-vivo cultures. A-B. Whole cell lysates were obtained and probed for MGMT (A) and MMR proteins (B). **C.** MSI was assayed by PCR of regions in loci BAT 25, BAT26, BAT40 and D2S123 encompassing microsatellites to asses MMR proficiency. **D.** Primary (483 and 484) and recurrent cultures (419 and 481) were pulsed with 10μM TMZ for 48hr, fixed at the indicated timepoints, immunofluorescence stained for 53BP1 foci (red) and imaged at 40X magnification to obtain the DNA repair kinetics upon TMZ treatment. Nuclei are stained with DAPI (blue). 53BP1 foci in 50 nuclei per timepoint were counted and plotted. Error bars, S.E.M. ****, P<0.0001 (any recurrent *versus* any primary culture at 48hr).

presence of microsatellite instability (MSI), which is a functional consequence indicative of MMR deficiency (Dietmaier et al., 1997a) . MSI was assayed by amplifying the region within the loci containing microsatellites and then determining whether the product has insertions/deletions by looking at amplicon size by gel electrophoresis. We used low passage human skin fibroblasts (HSFs) as a MMR-proficient control and the colon cancer line, HCT116, as a MMR-deficient control (Bhattacharyya et al., 1994). As pointed by the red arrows, HCT116 samples have PCR products that are either higher or lower than those of the HSF samples (black arrows) indicating indels and MSI. In contrast we found there were no indels and therefore no MSI in either the original GBM9 or the ex-vivo cultures at four commonly unstable loci (**Fig. 2.5C**). In agreement with these data showing lack of MGMT expression and a proficient MMR, we saw that TMZ induced a statistically comparable ($P>0.08$) amount of 53BP1 foci, a marker for DNA breaks, between any primary and any recurrent culture. The induction of DSBs underscores the fact that MMR is proficient in these cultures. Importantly, the recurrent cultures exhibited a faster kinetics of resolution for 53BP1 foci (**Fig. 2.5D**), which could explain acquired TMZ-resistance.

If accelerated DSB repair was the basis for the acquired TMZ-resistance, then the recurrent cultures should be cross-resistant to other genotoxic agents. To test this idea, we used ionizing radiation (IR), etoposide (Epo), N-methyl-N'-nitro-N-nitrosoguanidine (MNNG) and camptothecin (CPT), all of which generate DSBs, albeit through different mechanisms. IR can directly ionize DNA and also ionize water which results in radicals that then react with DNA to induce DSBs independently of the cell cycle. Epo is a

TOPO2 isomerase poison which locks the DNA bound enzyme after it has cut the DNA at both strands and therefore also induces DSBs irrespective of the cell cycle. MNNG is a functional analog of TMZ and depends on a proficient MMR to create nicks in the DNA that are then converted into DSBs during replication. CPT is a TOPO1 isomerase poison which blocks the DNA bound enzyme after it has made its single strand cut in the DNA, and therefore it generates DSBs after these single strand nicks encounter a replication fork. Hence, MNNG- and CPT-induced breaks, just like TMZ-induced breaks, are replication associated. Interestingly, we found that the recurrent cultures were not cross-resistant to IR or Epo (**Fig. 2.6A-B**) and repaired IR- or Epo-induced breaks at a rate similar to that of the primary cultures (**Fig. 2.7A-B**). On the other hand, the recurrent cells were cross-resistant to both MNNG and CPT (**Fig. 2.6C-D**) and repaired the replication-associated MNNG- and CPT-induced breaks at a much faster rate compared to the primary cultures (**Fig. 2.7C-D**). Since the augmented DSB repair was specific to replication associated breaks, we hypothesized that the recurrent cultures exhibit heightened DSB repair via homologous recombination (HR), which is active only during the S and G2 phases when a sister chromatid is available and serves as a template for recombination. Importantly, when we compared the CPT-induced break repair capabilities of normal human astrocytes (NHA) to the ex-vivo cultures, we saw NHAs were comparable to the primary ($P=0.0870$, $P=0.1183$; NHA versus 483 and 484, respectively) and different from recurrent cultures ($P=0.0004$, $P=0.0013$; NHA versus 419 and 481, respectively) (**Fig. 4D**).

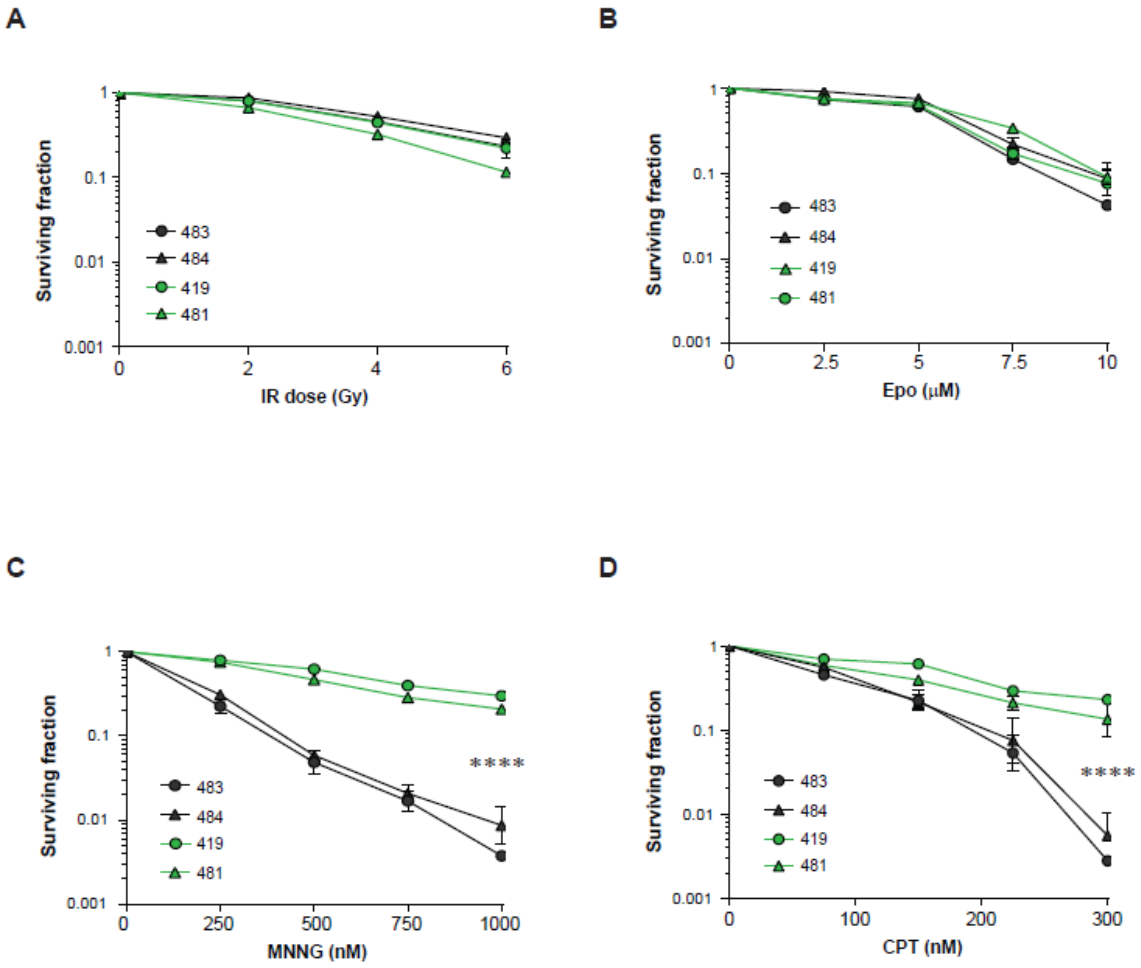

Figure 2.6. Recurrent cultures are cross resistant to MNNG and CPT but not to IR and Etoposide. A-D. Primary (483 and 484) and recurrent cultures (419 and 481) were seeded for clonogenic assays and irradiated (A), pulsed with Epo for 1hr (B), pulsed with 1 MNNG for 48hr (C), or pulsed with CPT for 2hr (D) at the doses shown.

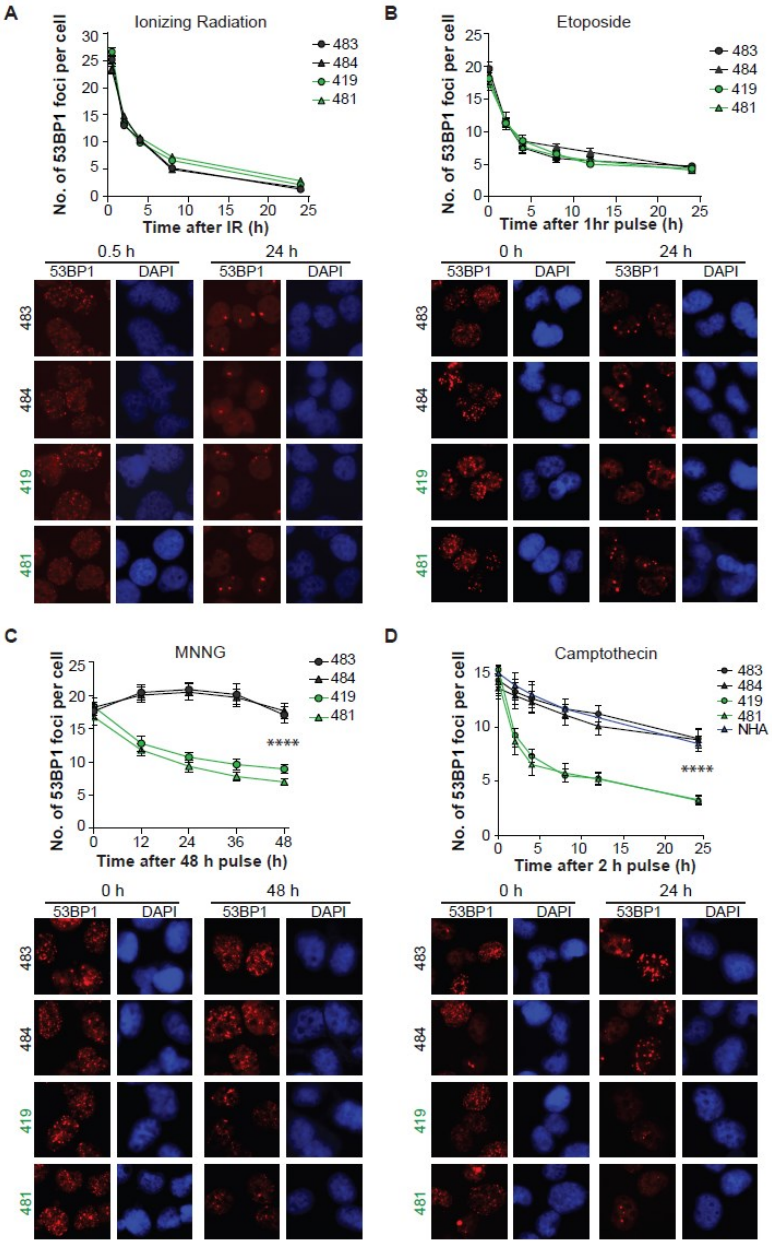

Figure 2.7. Recurrent cultures have heightened repair of replication associated breaks. A-D. Primary (483 and 484) and recurrent cultures (419 and 481) were irradiated with 1Gy (A), pulsed with 2μM Epo for 1hr (B), pulsed with 1μM MNNG for 48hr (C), or pulsed with 50nM CPT for 2hr (D), fixed at the indicated timepoints, immunofluorescence stained for 53BP1 foci (red) and imaged at 40X magnification to obtain the DNA repair kinetics upon DSB induction. Nuclei are stained with DAPI (blue). 53BP1 foci in 50 nuclei per timepoint were counted and plotted. Error bars, S.E.M. ****, P<0.0001 (any recurrent *versus* any primary culture at 48hr in C and 24hr in D).

To confirm augmented HR and mechanistically understand how it is upregulated in the recurrent cultures, we tried to elucidate differences in specific steps of HR between primary and recurrent cultures. For the following experiments we used a short pulse of CPT, which is sufficient to induce damage in cells that are in S phase (as opposed to TMZ which requires two rounds of replication to induce breaks). Importantly CPT induces DSBs that are mostly processed by HR as evidenced by the high Rad51 to γH2AX ratio (**Fig. 2.8**). In order for recombination to occur, DNA ends flanking the DSBs need to be resected first (Symington and Gautier, 2011). DNA end resection (5' to 3') results in the formation of a 3'-OH single stranded tail that is first coated with replication protein A (RPA). To look at the progression of resection, we stained the ex-vivo cultures for RPA, but found no significant difference in the amount of RPA foci between recurrent and primary cultures (**Fig. 2.9A**). To substantiate these results, we carried out a BrdU incorporation-based assay in which resection of DNA unmasks the epitope of the incorporated BrdU which can then be stained in the single-stranded DNA around the breaks (Tomimatsu et al., 2014). Again, we found that there was no significant difference in the amount of BrdU foci (**Fig. 2.10**). Next we analyzed Rad51 loading, which is an HR specific protein that displaces RPA from the resected ends of DNA at the break site (Krejci et al., 2012). Rad51 forms nucleoprotein filaments (Conway et al., 2004) that catalyze the homology search and DNA strand exchange (Krejci et al., 2012; Sung, 1994). Induction of Rad51 foci was similar in primary and recurrent cultures; however, the recurrent cultures showed a faster foci resolution (Rad51 dissociation) (**Fig. 2.9B**), an essential step that exposes the 3'-OH required for DNA synthesis and repair

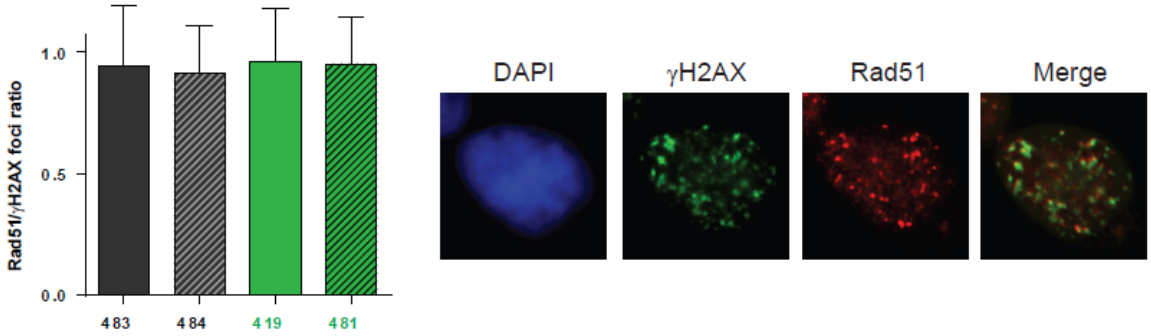

Figure 2.8. CPT induces breaks that are repaired via homologous recombination. Ex-vivo cultures were pulsed with 50nM CPT and stained 2hr after drug removal for Rad51 and gH2AX to assess the fraction of breaks repaired by homologous recombination.

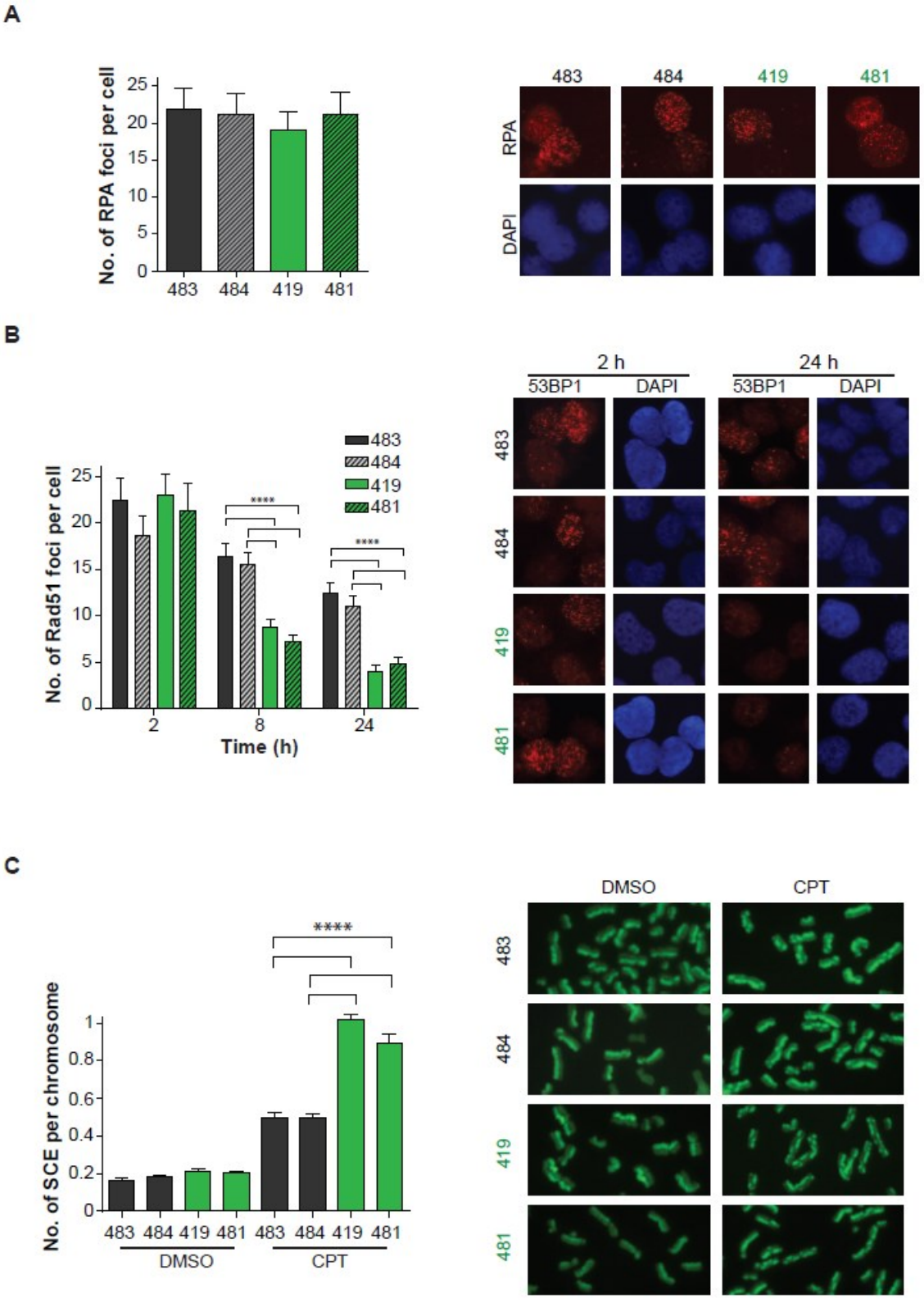
A
No. of RPA foci per cell
25
20
15
10
5
0
483
484
419
481
483
484
419
481
RPA
DAPI
B
No. of Rad51 foci per cell
483
484
419
481
****
****
2
8
24
Time (h)
2 h
24 h
53BP1
DAPI
53BP1
DAPI
483
484
419
481
C
No. of SCE per chromosome
****
1
0.8
0.6
0.4
0.2
0
483 484 419 481 483 484 419 481
DMSO
CPT
DMSO
CPT
483
484
419
481

Figure 2.9. Recurrent cultures have augmented HR and faster Rad51 foci resolution. A. Primary (483 and 484) and recurrent cultures (419 and 481) were pulsed with 50nM CPT for 2hr, and fixed 2hr later. Cells were immunofluorescence stained for RPA foci (red) and imaged at 40X magnification to assess the level of resection. Nuclei are stained with DAPI (blue). RPA foci in 50 nuclei per culture were counted and plotted. Error bars, S.E.M. **B.** Primary (483 and 484) and recurrent cultures (419 and 481) were pulsed with 50nM CPT for 2hr, fixed at the indicated timepoints, immunofluorescence stained for Rad51 foci (red) and imaged at 40X magnification to assess the extent (2hr timepoint) and efficiency (24hr timepoint) of HR. Nuclei are stained with DAPI (blue). Rad51 foci in 50 nuclei per culture were counted and plotted. Error bars, S.E.M. ****, P<0.0001 (any recurrent *versus* any primary culture at 8 or 24hr). **C.** Primary (483 and 484) and recurrent cultures (419 and 481) were labeled with BrdU during two cell cycles while on CPT treatment. Metaphase spreads were prepared from treated and untreated samples, slides were stained with acridine orange (green) and imaged at 40X magnification to quantify the amount of SCE as a measurement of HR. Error bars, S.E.M. ****, P<0.0001 (any recurrent *versus* any primary culture treated with CPT)

completion (Krejci et al., 2012; Miyazaki et al., 2004). Therefore, we believe that the underlying mechanism for augmented HR lies in a step downstream of Rad51 loading and leads to a higher level of recombination. Finally, we checked the extent of recombination, measured as cross-over events, occurring after CPT treatment in the ex-vivo cultures. We quantified the amount of crossovers as a measurement of HR by assessing the frequency of sister chromatid exchanges (SCE) (McEllin et al., 2010). As expected, there was an increased number of SCE in the recurrent cultures compared to the primary tumor cultures, thereby confirming the difference in HR proficiency between these groups (**Fig. 5C**). When we assessed the level of known HR-related proteins, we did not find a significant difference between the primary and recurrent cultures (data not shown). This suggests that probably HR is differentially regulated via post-translational modifications (PTM) rather than by transcriptional or translational modulation of the HR players. PTMs such as phosphorylation have been shown to have essential roles in the

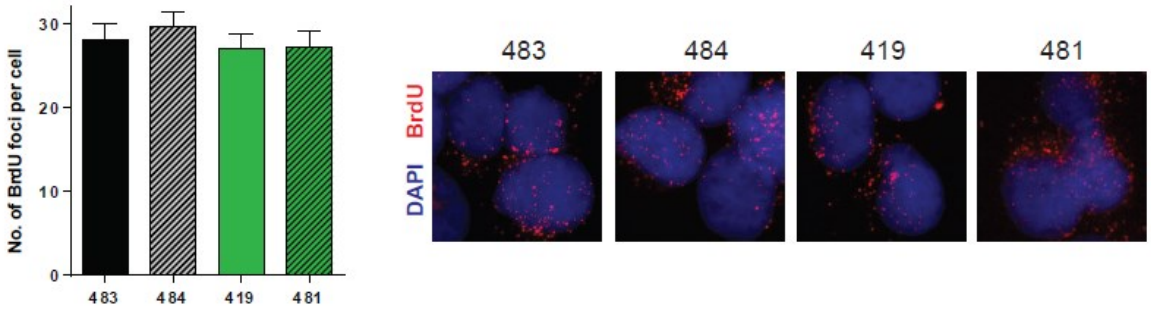

Figure 2.10. Ex-vivo cultures show similar levels of DNA end resection. Cells were cultures in BrdU-containing media for one cell division. Incorporated DNA is exposed upon resection and was visualized by immunofluorescence.

control of HR proteins such as Rad51 either by modulating its recombinase activity or its intracellular localization.

Re-sensitization of recurrent cultures. Honing in on HR deficiency as a possible mechanism of resistance, we wanted to see if we could re-sensitize the recurrent cultures by inhibiting HR. One way to target HR would be by directly inhibiting Rad51; alternatively, one can indirectly block HR by targeting pathways affecting HR (Ward et al., 2015). Although already in development (Budke et al., 2012; Huang et al., 2012; Takaku et al., 2011; Zhu et al., 2013), Rad51 inhibitors are not currently in clinical use. However, CDKs 1 and 2 have been shown by our lab and others to regulate multiple steps during HR (Buis et al., 2012; Davies and Pellegrini, 2007; Esashi et al., 2005; Falck et al., 2012; Huertas and Jackson, 2009; Restle et al., 2008; Tomimatsu et al., 2014; Wang et al., 2013; Yun and Hiom, 2009), such as DNA end resection via phosphorylation of Exo1 (Tomimatsu et al., 2014). As opposed to Rad51, there are multiple CDK1 and 2 inhibitors available already in clinical trials which could be repurposed for HR inhibition; therefore, in light of the nascent link between cell cycle regulation and HR, we used AZD5438 (a potent inhibitor of CDKs 1, 2, and 9) and Roscovitine (a potent inhibitor of CDKs 1, 2, and 5). To determine if CDK inhibition indeed inhibits HR DNA repair in our ex-vivo cultures, we pulsed them with TMZ for 48 hours to induce breaks and then added DMSO, AZD5438, or Roscovitine for another 48 hours. Importantly, very low doses of AZD5438 (0.25μM) and Roscovitine (5μM) were used to limit off-target effects. Cells were stained for 53BP1 in a timecourse experiment to analyze the kinetics of DSB repair.

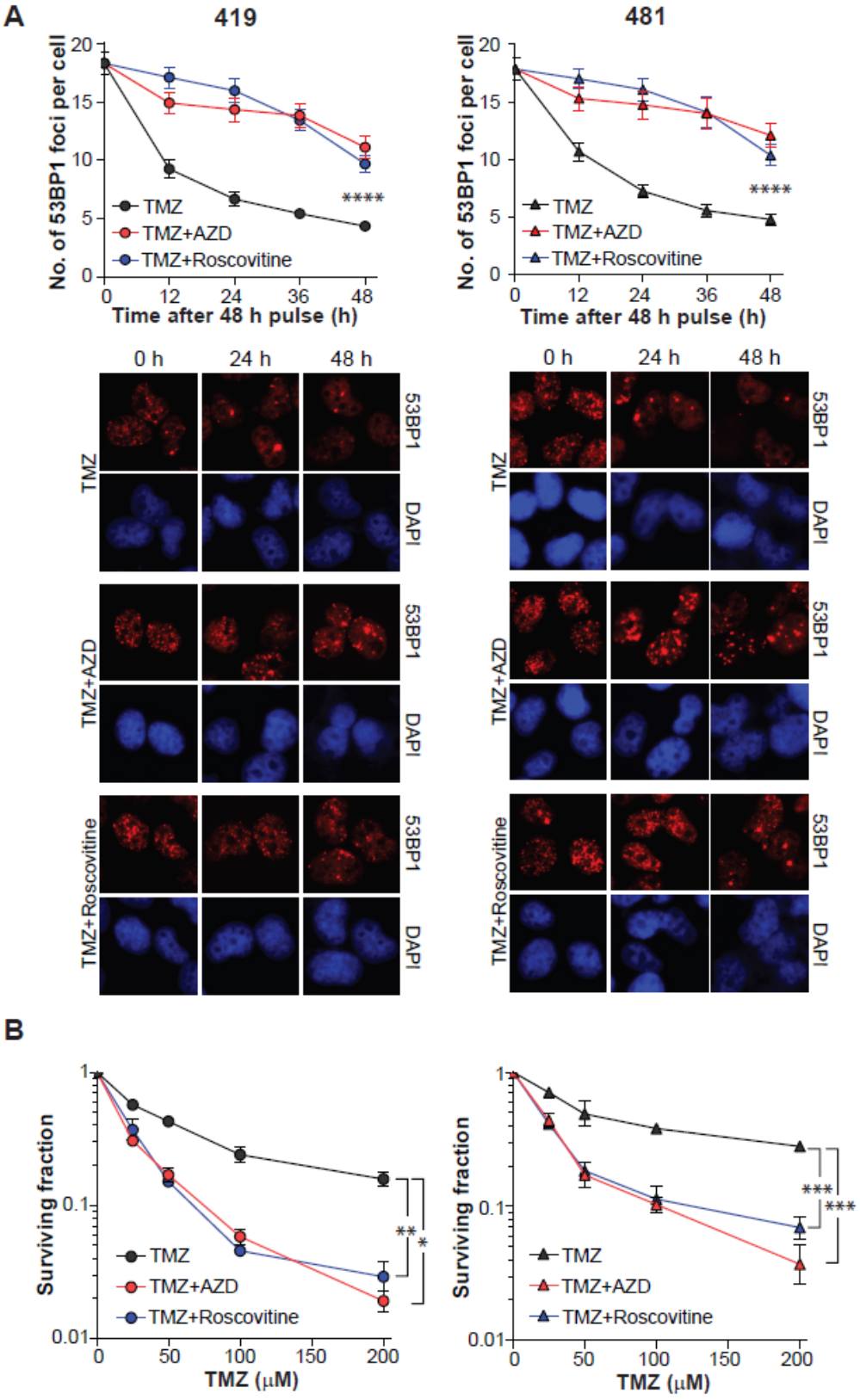
A
419
481
No. of 53BP1 foci per cell
Time after 48 h pulse (h)
TMZ
TMZ+AZD
TMZ+Roscovitine
****
0 h
24 h
48 h
53BP1
DAPI
B
Surviving fraction
TMZ (μM)
**
*
***

Figure 2.11. Inhibition of HR chemosensitizes recurrent cultures to TMZ. A. Recurrent cultures (419 and 481) were pulsed with 10μM TMZ for 48hr, then treated with either DMSO, 0.25μM AZD5438, or 5μM Roscovitine, and finally fixed at the specified timepoints. Cells were immunofluorescence stained for 53BP1 foci (red) and imaged at 40X magnification to the extent of repair inhibition. Nuclei are stained with DAPI (blue). 53BP1 foci in 50 nuclei per culture were counted and plotted. Error bars, S.E.M. ****, P<0.0001 (TMZ versus TMZ+AZD or TMZ+Roscovitine at 48hr). **B.** Recurrent cultures (419 and 481) were plated for colony survival assays in which cells were pulsed with increasing concentrations of TMZ for 48hr and later DMSO, 0.25μM AZD5438 or 5μM Roscovitine were added for another 48hr. Error bars, S.D. *, P=0.0109. **, P=0.0019. ***, P=0.0006.

By 48 hours post-AZD5438 or Roscovitine exposure, a significantly higher number of breaks remained when compared to the DMSO treated samples implying abrogated DNA repair (**Fig. 2.11A**). Notably, this abrogation in DNA repair translated in a significant chemosensitization to

TMZ as demonstrated by clonogenic assays (**Fig. 2.11**). Of note, even though cell doubling would presumably be decreased by CDK inhibition, which would result in TMZ resistance, CDK inhibition still had a striking chemosensitization effect because it was administered only after breaks had been induced by TMZ. This underscores the importance of determining the right schedule for drug administration. Altogether this work suggests that HR can contribute to TMZ-resistance, and that it can be targeted by CDK 1 and 2 inhibition for chemosensitizing recurrent tumors.

Discussion

It is very difficult to study GBM recurrence, mainly because of the dearth of primary and recurrent matched tumor samples since biopsy sampling occurs usually at

diagnosis only. Even with the few available matched pairs, there are limited parameters that can be measured, such as histopathology, and genomic and proteomic profiles; no functional assays can be done without live cell lines. Adding a whole new layer of complexity, GBMs are highly intra-tumorally heterogeneous (Meyer et al., 2015; Patel et al., 2014; Sottoriva et al., 2013); therefore, it is questionable whether a single, small biopsy truly represents the wide genetic heterogeneity observed in GBM. This would make it difficult to assess whether a specific alteration is acquired after treatment or whether it was already present in the primary tumors but not represented in the biopsy.

We generated a model of tumor recurrence that allowed us to assess tumor response by functional assays in matched isogenic samples, as opposed to expression profiles. A caveat of the model is that it starts with a relatively monoclonal population with very little time to allow for heterogeneity to be established; therefore, interdependent and co-operative evolution would be misrepresented. On the other hand, this reductionist model allows us to identify therapy-specific changes as whole tumors are harvested and therefore spatially separated sub clones should be represented in the ex-vivo cultures. An important caveat is that selection may take place during culturing though we have limited this by using low passage (3-5 divisions) cultures. Another caveat is that all the functional assays were carried out *in vitro*; however, here we attempted to model development of TMZ-resistance which did occur *in vivo* in the mouse brain which retains important cancer-microenvironment relations.

While the experiments presented here clearly show that TMZ had a significant effect in shaping the tumors' chemoresistance, they did not determine whether there was

selection of a low frequency, pre-existing resistant clone or whether TMZ-resistance was acquired during treatment. If TMZ resistance was due to an aberrant genomic alteration, and had we identified it, deep sequencing (1000X for variants that are 1% frequent) could be applied to detect the low allelic frequency genomic alterations in the untreated tumors. However, since we do not have a resistance marker to sequence, determining whether TMZ resistance was pre-existing would be difficult. Isolating single cells from the primary cultures, allowing them to form colonies, and comparing the individual sensitivities to the recurrent tumors could identify rare, pre-existing clones. Presence of a range of sensitivities would indicate heterogeneity within the primary cultures which would point to the existence of rare TMZ resistant clones.

Importantly, we found recurrent tumors to have augmented HR, which did not correlate with overexpression of known HR-related proteins, and therefore would have been missed if not using functional assays. Nevertheless, these results are in agreement with other reports in numerous cancers pointing to a role of HR in chemotherapy resistance (Ohba et al., 2014). Though we have narrowed it down to the post-resection phase of HR, it still remains to be determined how exactly HR is upregulated; what are the mediators and effectors involved. It is possible that different molecular mechanisms are active in the individual recurrent tumors leading to heightened HR (convergent evolution). Consistent with this idea, when we analyzed the data of the TCGA (2008), we found all (n=11) recurrent GBMs treated with TMZ to have overexpression of HR related genes in a non-recurrent, almost mutually exclusive fashion.

The fact that HR is augmented upon TMZ-treatment has important clinical implications. First of all, it suggests that re-challenging tumors with TMZ alone would not be beneficial. This is in agreement with the results of a Phase II clinical trial, where re-treatment with TMZ of recurrent tumors had minimal effects on most patients (especially those who had been treated for extended periods of time with TMZ prior to the study) (Perry et al., 2010). Notably, our results expose a drugable vulnerability. Inhibitors of Rad51 are currently in development (Budke et al., 2012; Huang et al., 2012; Takaku et al., 2011; Zhu et al., 2013) and soon such an inhibitor may be available in the clinic. In the meantime, the nascent link between CDK signaling and HR activation can be exploited for chemosensitization purposes, since CDK inhibitors are currently in clinical trials and could be quickly repurposed. For this approach, tumor selectivity may be driven by a higher proliferation level in GBMs and an elevated expression of CDK1 and 2 in tumors compared to normal cells. A caveat of this approach might be the relative similarity among CDKs which makes selective targeting difficult. For instance, Roscovitine and AZD5438 both have additional targets besides CDK1 and CDK2 (albeit with much higher IC50s) that may contribute to increased toxicities. However this drawback is being circumvented by the rational development of specific, next generation inhibitors based on the crystal structures of CDK1 and CDK2 (Brown et al., 2015; Carbain et al., 2014). Importantly, this strategy of combining TMZ with CDK1/2 inhibitors may give an option to patients with recurrent GBMs but is not limited just to this set of patients. Indeed, it would be beneficial for all patients in which TMZ is able to induce breaks as HR is the main pathway by which these breaks are repaired regardless

of whether they are in a recurrent or primary tumor (Short et al., 2011). This approach, besides being very toxic to all tumor cells, would sensitize resistant, rare clones that may be present in the primary tumor before they are selected for and expand.

CHAPTER THREE
Targeting the DDR for chemo- and radio-sensitization

Introduction

Ionizing radiation (IR) induces DNA double-strand breaks (DSB), the most deleterious of all types of DNA lesions, that can lead to cell death if left unrepaired (Jackson and Bartek, 2009). Abrogating the DNA damage response (DDR) to these breaks is, in principle, an attractive strategy to sensitize cancers to radiation and chemotherapy (Begg et al., 2011; Helleday et al., 2008; Lord and Ashworth, 2012). DSBs can be repaired either through the error-prone non-homologous end joining (NHEJ) pathway or the error-free homologous recombination (HR) pathway, in which the PI3K-like kinases, DNA-PKcs and ATM, respectively, are centrally involved (Shiloh and Ziv, 2013; Wang and Lees-Miller, 2013). Therefore, these two apical kinases are very attractive targets for radiosensitization of GBM and other tumors. Research over the past decade has led to the development of specific DNA-PKcs and ATM inhibitors, some of which are quite potent (Finlay and Griffin, 2012). Unfortunately, potent ATM or DNA-PKcs inhibitors that have good bioavailability for pre-clinical tumor studies and that can also cross the blood-brain-barrier (BBB) have not yet been successfully developed (Finlay and Griffin, 2012).

NVP-BEZ235 is a small molecule inhibitor that was originally identified as a dual PI3K/mTOR inhibitor (IC_{50}=4-75nM, IC_{50}=20nM, respectively) (Maira et al., 2008);

reviewed in (Garcia-Echeverria and Sellers, 2008). We reported earlier that NVP-BEZ235 also potently inhibits both ATM and DNA-PKcs, thereby attenuating both HR and NHEJ and resulting in unprecedented radiosensitization in a panel of GBM cell lines (Mukherjee et al., 2012). NVP-BEZ235 was also found to inhibit ATR, another member of the PI3K-like family (Toledo et al., 2011). Unlike specific inhibitors of PI3K-like kinases (Finlay and Griffin, 2012), NVP-BEZ235 is currently in Phase I/II clinical trials as an mTOR inhibitor and has shown great promise in controlling solid tumors in pre-clinical mouse models (Peyton et al., 2011). Thus, this drug provides us with the unique opportunity of carrying out proof-of-principle experiments in pre-clinical mouse models to test the possibility of improving GBM therapy by blocking both DNA-PKcs and ATM.

In this study, we examined whether NVP-BEZ235 could act as a DDR inhibitor in pre-clinical mouse models and, if so, whether combining this drug with IR could be a viable strategy for improving GBM therapy. We find that NVP-BEZ235 can block both DNA-PKcs and ATM and abrogate the repair of IR-induced DSBs in tumors *in vivo*, thereby controlling brain tumor growth and significantly prolonging survival of brain tumor-bearing mice. Our results indicate that GBM therapy could possibly be improved by using a combination of IR and specific inhibitors of DNA-PKcs and/or ATM that are potent and bioavailable.

Materials and methods

Cell culture and drug treatment. U87MG cells ectopically expressing EGFRvIII (U87-

vIII) have been described before (Mukherjee et al., 2009) and were maintained in Dulbecco's Modification of Eagle Medium (DMEM) with 10% fetal bovine serum in a humidified 37°C incubator with 5% CO2. U87-vIII cells expressing luciferase were generated by infection with a lentivirus carrying firefly luciferase under the control of the PGK promoter. Lentivirus was generated by packaging pLenti PGK V5-LUC Puro (Campeau et al., 2009) in 293FT cells using the ViraPower Lentiviral Packaging System (Invitrogen). pLenti PGK V5-LUC Puro was a gift from Dr. Kaufman (Addgene; plasmid #19166). Luciferase-expressing cells were selected with 1 μg/ml Puromycin (GIBCO) and were maintained in medium containing Puromycin. GBM9 neurosphere culture has been described before (Puliyappadamba et al., 2013). Briefly, these cells were maintained in DMEM/F12 1:1 media (Life Technologies) supplemented with B27 without Vitamin A (Life Technologies), 10 ng/ml EGF, and 10 ng/ml bFGF (Peprotech). Once spheres reached a size of ~100 μm, they were dissociated by triturating in Accutase (Sigma-Aldrich) and sub-cultured at a 1:3 dilution. All cells were Mycoplasma free. NVP-BEZ235 (Selleck Chemicals) and TMZ (Sigma-Aldrich) were dissolved in dimethyl sulfoxide (DMSO; Sigma-Aldrich), and 10 mM and 100 mM stocks, respectively, were stored at -20°C. Cells were treated with drugs for 1 hour before irradiation. Cells were irradiated with gamma rays from a 137Cs source (JL Shepherd and Associates) at the indicated doses.

Mouse tumor studies. The Nestin-GFP transgenic mouse (Yamaguchi et al., 2000) was obtained from the Mouse Cancer Models Consortium. Nu/Nu nude mice were obtained

commercially (Charles River, Stock#88). Subcutaneous tumors were generated by injecting 3.00x106 U87-vIII or 1.00x106 GBM9 cells subcutaneously in 50 µL PBS/Matrigel into 6 weeks-old Nu/Nu mice. Tumors were measured at the indicated times with digital calipers (Fisher Scientific), and tumor volumes were calculated (length x width x height x 0.5). For intra-cranial stereotactic injections, 5.00x105 U87-vIII cells were suspended in PBS (7.5µl) and delivered into the left corpus striatum of the brains of 6 weeks-old Nu/Nu nude mice as described before (Mukherjee et al., 2009). Tumor development was monitored by bioluminescence imaging (BLI). Treatment was initiated when the subcutaneous tumors reached an average size of 150-200 mm3, and when the intra-cranial tumors reached a signal of 0.5-1.0x109 photons/s. Mice were treated with NVP-BEZ235, TMZ, or both by oral gavage or with vehicle (N-methyl-2-pyrrolidone/polyethylene glycol 300; 1:9 vol/vol; Sigma-Aldrich) as control; radiation was administered 2 hours after treatment. The treatment regimen consisted of a total of 12 doses of drug and/or IR given every other day. Mice bearing subcutaneous tumors were treated with 50 mg/kg NVP-BEZ235 and/or 20 mg/kg TMZ. Mice bearing intra-cranial tumors were treated with 75 mg/kg NVP-BEZ235. Subcutaneous as well as intra-cranial tumors were irradiated with an X-ray device (X-RAD 320, Precision X-ray; 250 kV, 15 mA, 0.2 min, 1.65 mm Al filter, at 5cm) fitted with a specifically designed collimator providing a 10.08 mm-diameter field size iso-dose exposure for a total dose of 2 Gy per treatment. Subcutaneous tumors were excised after they reached a group mean volume of 1000 mm^3. Mice were perfused with 1X phosphate buffered saline (PBS) followed by 4% paraformaldehyde (PFA) (Sigma-Aldrich). Excised tumors were post-

fixed by immersion in 4% PFA and either embedded in paraffin or processed for cryosectioning. Mice bearing intra-cranial tumors were sacrificed when they became moribund. Symptomatic mice were perfused with PBS followed by 4% PFA. Brains were dissected out, post-fixed by immersion in 4% PFA, embedded in paraffin, and sectioned coronally. Mice were weighed three times per week during the drug-treatment period and afterwards to ensure that weight loss due to drug treatment was less than 20% and that mice regained weight once treatment was stopped. All animal studies were performed under protocols approved by the Institutional Animal Care and Use Committee of UT Southwestern Medical Center.

Non-invasive intra-cranial bioluminescence imaging. Serial bioluminescence images of tumor-bearing mice were obtained using the IVIS Lumina System (Xenogen Corp.) coupled to Living Image data acquisition software (Xenogen Corp.). During imaging, mice were anaesthetized with isoflurane (Baxter International Inc.), and a solution of D-luciferin (180 mg/kg in PBS; total volume: 80 μL; Gold Biotechnology) was administered subcutaneously in the neck region. Images were acquired between 10 and 20 minutes post-luciferin administration and peak luminescence signals were recorded. The BLI signals emanating from the tumors were quantified by measuring photon flux within the region of interest (ROI) using the Living Image software package.

Western blot analyses. Nuclear extracts from irradiated cells were prepared and Western blotted as described before (Peterson et al., 1995). For analysis of DNA-PKcs and ATM

activation in vivo, tumors were allowed to grow to 100 mm3 and treated with NVP-BEZ235 or vehicle and irradiated 2 hours later at the indicated doses. Tumors were excised and snap frozen in liquid nitrogen 30 minutes after irradiation. Tumors were homogenized in hypotonic lysis buffer, nuclear extracts were obtained, and Western blot analysis was carried out as described before(Peterson et al., 1995). Antibodies used were as follows: anti-phospho-Akt(S473), anti-Akt, and anti-phospho-p53(S15) (Cell Signaling); anti-ATM (Sigma-Aldrich); anti-p53, (Santa Cruz Biotechnology); anti-phospho-KAP-1(S824), anti-KAP-1 (Bethyl); anti-phospho-ATM(S1981) (GenScript); anti-phospho-DNA-PKcs(S2056) (Abcam); anti-DNA-PKcs (Thermo Fisher); anti-Ku80 (kind gift from Dr. B. Chen); HRP-conjugated secondary antibodies (Biorad); Alexa488/568-conjugated secondary antibodies (Molecular Probes).

Immunofluorescence staining. Subcutaneous tumors and tumor-bearing brains were cut into 20 μm cryosections or 5-10 μm paraffin sections. Tissue sections were stained according to immunofluorescence protocols as described (Blaiss et al., 2011; Mukherjee et al., 2009). Antibodies used for immunofluorescence staining were as follows: anti-53BP1 (Santa Cruz), anti-Ki67 (Abcam), anti-phospho-S6(S235/236) (Cell Signaling). A Leica DM5500 microscope was used for imaging. Ki67 and pS6 images were taken at 10X magnification and 53BP1 foci were imaged at 40X magnification.

H&E and TUNEL staining. TUNEL staining was performed on paraffin sections using the FragEL™ DNA Fragmentation Detection Kit (Merck KGaA). Hematoxylin and eosin (H&E) staining was done by standard techniques.

Colony formation assays. Cells were plated in triplicate onto 60-mm dishes (1000 cells per dish), treated with the indicated drugs, and irradiated 4 hours later with graded doses of radiation. At 16 hours after irradiation, drug-containing medium was replaced with drug-free medium. Surviving colonies were stained with crystal violet approximately 10 to 14 days later as described (Mukherjee et al., 2009).

DSB repair assays. For monitoring DSB repair in vivo, mice were treated with NVP-BEZ235 (150 mg/kg) or vehicle and irradiated 2 hours later at the indicated doses. Mice were treated when the subcutaneous tumors reached a volume of 100 mm3 or the intra-cranial tumors reached a BLI intensity of 0.5-1 x 109 photons/sec. Tumors were collected at the indicated times and processed for immunofluorescence staining as described above. For quantifying 53BP1 foci, a stack of images along the Z-axis (at 0.5 μm intervals throughout the depth of the tissue) was obtained with a Leica DM5500 microscope and Leica Application Suite software. The Z-stacks were combined (Projection Type: Maximum Intensity) using Image J software and all visible foci were counted manually by the same scorer. Nuclei overlapping with other nuclei were excluded. The number of 53BP1 foci per nucleus (average of >50 nuclei per tumor) was determined for each time

point or treatment and plotted after subtracting background (average number of foci per nucleus of vehicle treated, mock-irradiated mice).

Statistical analysis. DNA repair and cell proliferation data were analyzed by unpaired, two tailed t-tests with Welch's correction using the Graphpad Prism software package. Mouse survival data were plotted using the Kaplan-Meier method and compared using the logrank test. Tumor growth profiles between different groups were compared by the Mixed Model method. An AR(1) covariance structure for repeated tumor volume measures was used in the model. SAS 9.3 for Windows was used for analysis.

Results

NVP-BEZ235 is a potent inhibitor of DNA-PKcs and ATM in tumors in vivo. NVP-BEZ235 has exhibited good bioavailability as well as potent inhibition of its canonical targets, mTOR and PI3K, in pre-clinical mouse models (Brachmann et al., 2009; Chanthery et al., 2012; Chiarini et al., 2010; Cho et al., 2010; Eichhorn et al., 2008; Engelman et al., 2008; Konstantinidou et al., 2009; Liu et al., 2009; Santiskulvong et al., 2011; Schnell et al., 2008; Serra et al., 2008), and is currently in clinical trials for the treatment of solid tumors. We have previously reported that NVP-BEZ235 can also block the PI3K-like kinases, DNA-PKcs and ATM, *in vitro* (Mukherjee et al., 2012). This provides us, for the first time, with a potent DSB repair inhibitor that is bioavailable and that can be used to evaluate whether clinical radiosensitization of GBM may be a viable

option for improving therapy. For our study, we chose U87MG human glioma cells expressing the constitutively active form of EGFR, EGFRvIII (henceforth called U87-vIII). We have previously shown that these cells form radioresistant intra-cranial tumors that are very suitable for radiosensitization studies (Mukherjee et al., 2012). As a prelude to intra-cranial GBM studies, we wanted to determine whether this drug could inhibit DNA-PKcs and ATM in subcutaneous tumors *in vivo*. We first confirmed that NVP-BEZ235 could block DNA-PKcs and ATM in U87-vIII cells in culture leading to acute radiosensitization (**Fig. 3.1**) similar to that reported by us previously for a panel of glioma lines (Mukherjee et al., 2012). It was previously reported that NVP-BEZ235 levels peak in tumors approximately 2 hours after drug administration (Maira et al., 2008). Therefore, we treated mice bearing U87-vIII subcutaneous tumors with increasing downstream signaling events such as KAP-1 and p53 phosphorylation (Shiloh and Ziv, 2013) doses of NVP-BEZ235, focally irradiated the tumors 2 hours later, and harvested them at 0.5 hours post-IR. We then examined IR-induced DNA-PKcs and ATM activation by Western blotting tumor extracts with phospho-specific antibodies that recognize auto-phosphorylated DNA-PKcs or ATM (Shiloh and Ziv, 2013; Wang and Lees-Miller, 2013). We found that NVP-BEZ235 could inhibit IR-induced activation of both ATM and DNA-PKcs in tumors (**Fig. 3.2A**). As also seen *in vitro* (**Fig. 3.1**), phosphorylation of DNA-PKcs in tumors was impaired to a greater extent than that of ATM. Nevertheless, the partial inhibition of ATM in tumors was sufficient to block (**Fig. 3.2A**). Consequently, DSB repair was severely impaired in irradiated tumors as seen in a time course experiment in which tumor sections were immunostained for 53BP1 foci, a

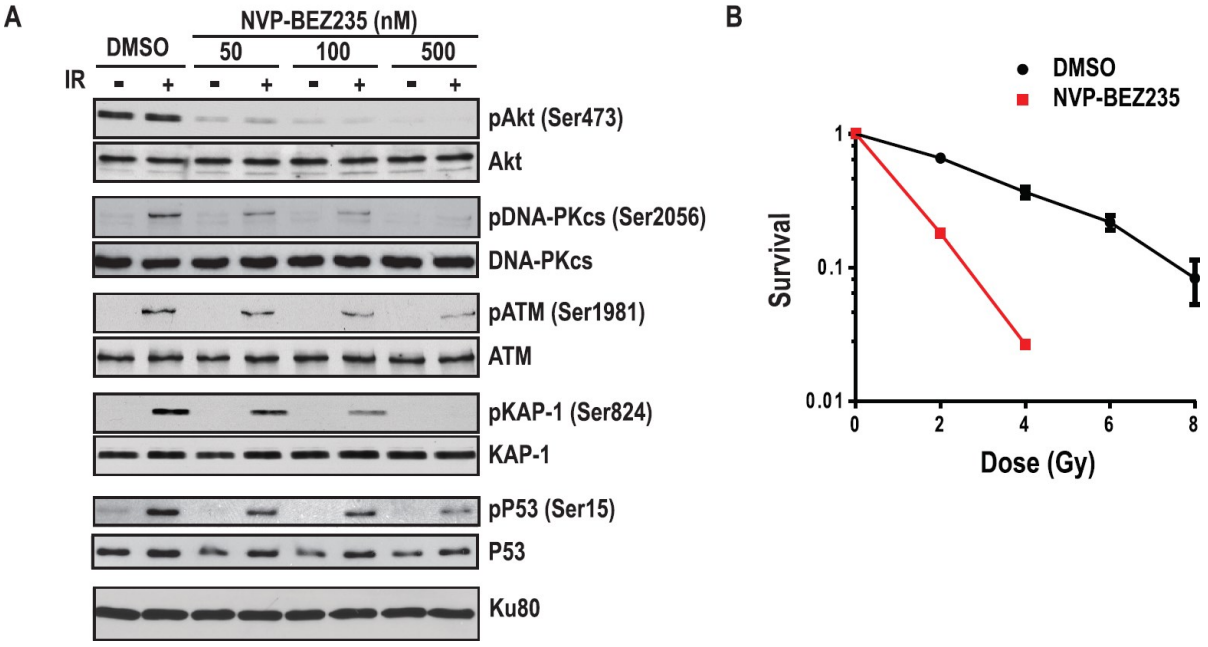

Figure 3.1. NVP-BEZ235 inhibits the DDR in U87-vIII cells. A. Cells were treated for 1 hour with NVP-BEZ235 (indicated doses) or DMSO before irradiation (10Gy). Cells were harvested 30 minutes after irradiation and nuclear extracts were assessed for phosphorylation of proteins by Western blotting with the indicated antibodies. **B.** Survival of U87-vIII cells after treatment with NVP-BEZ235 (100nM) or DMSO and radiation was quantified by colony formation assays. The fraction of surviving colonies (y-axis) was plotted against the corresponding radiation dose (x-axis). Error bars, S.E.M.

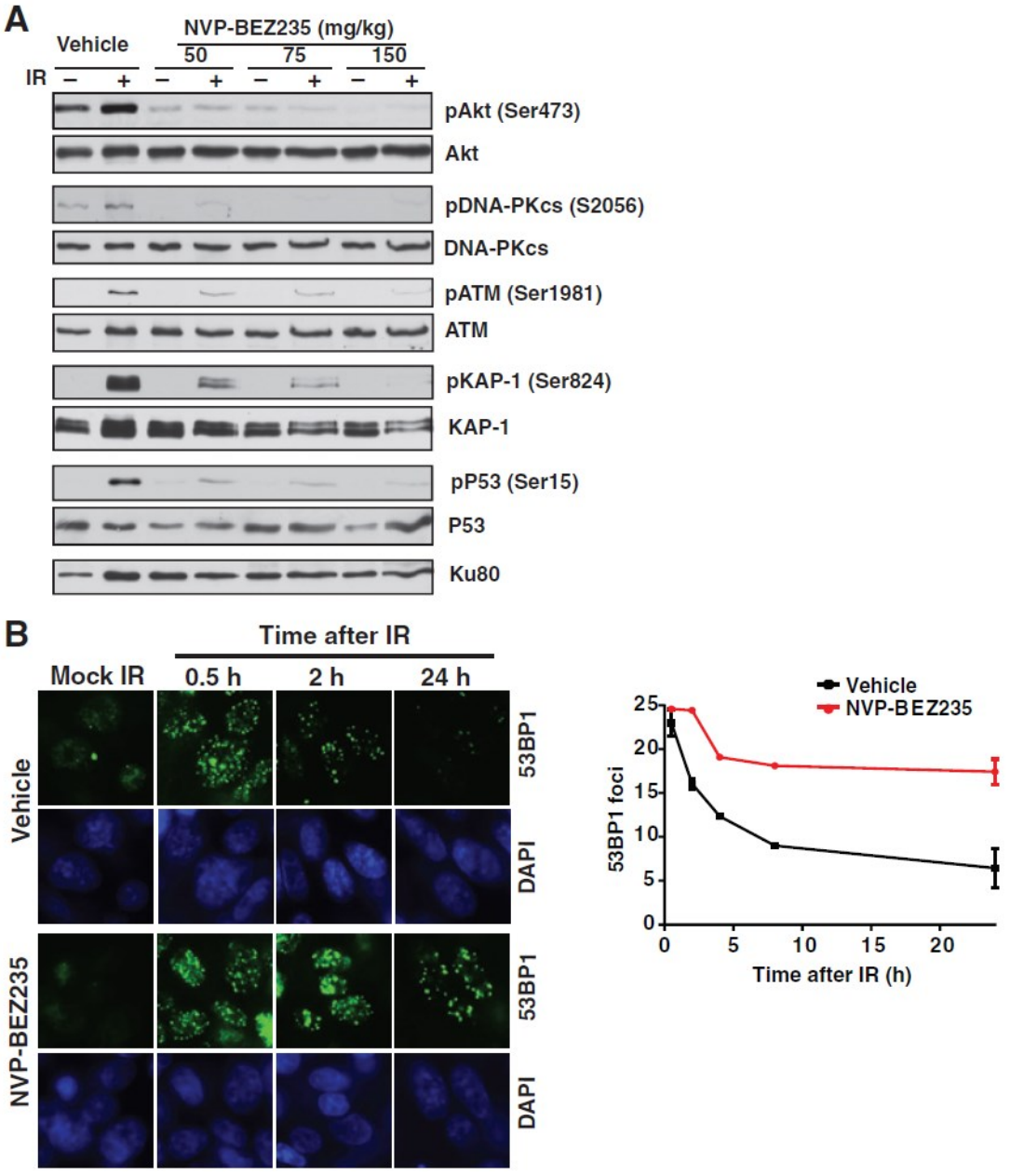

Figure 3.2. NVP-BEZ235 blocks both ATM and DNA-PKcs in tumors and inhibits DSB repair. A. Subcutaneous tumors generated from U87-vIII cells were mock-irradiated or irradiated (IR) with a total dose of 10 Gy. Tumor-bearing mice were treated with the indicated doses of NVP-BEZ235 or with vehicle alone 2 hours prior to irradiation. Tumors were excised 30 minutes after irradiation and tumor extracts were Western blotted with the indicated antibodies. Note attenuation of IR-induced autophosphorylation of DNA-PKcs and ATM and reduced phosphorylation of ATM targets, KAP-1 and p53. **B.** Tumor-bearing mice were treated with NVP-BEZ235 and

irradiated 2 hours later with 4 Gy of IR. Tumors were harvested at 0.5, 2, 4, 8, or 24 hours post-irradiation, and cryosections were immunofluorescence stained for 53BP1 foci (green) and imaged at 40X magnification. Nuclei are stained with DAPI (blue). 53BP1 foci in 50 nuclei per tumor were counted and plotted for each time point. n = 2 tumors per time point. Error bars, S.E.M. Note abrogated DSB repair in NVP-BEZ235-treated tumors.

surrogate marker for DSBs (**Fig. 3.2B**). Thus, it is clear that the pronounced inhibition of these PI3K-like kinases and DSB repair seen *in vitro* can be recapitulated *in vivo*.

DSB repair inhibition by NVP-BEZ235 results in accumulation of DSBs in tumors and striking radiosensitization. In order to determine if inhibition of DSB repair by NVP-BEZ235 would result in radiosensitization and tumor regression, we generated subcutaneous tumors using U87-vIII cells, and allowed the tumors to grow to a volume of 200 mm^3 before initiating treatment. The treatment regimen consisted of twelve doses, given every other day, of 50 mg/kg of NVP-BEZ235 given by oral gavage, followed 2 hr later by 2 Gy of IR localized to the tumor. Six mice were randomly allocated for each treatment group: 1) mock-irradiation and vehicle only (Vehicle), 2) irradiation and vehicle only (IR), 3) mock-irradiation and NVP-BEZ235 (BEZ), and 4) irradiation and NVP-BEZ235 (IR+BEZ) (**Fig. 3.3A**). Mice treated with IR alone exhibited tumor growth profiles that were only slightly delayed compared to untreated animals, demonstrating the highly radioresistant nature of these tumors. The BEZ arm also showed a minor initial response, but the tumors resumed rapid growth which was not unexpected as adaptive resistance to NVP-BEZ235 has been reported before (Muranen et al., 2012). In striking contrast, combinatorial treatment with IR and NVP-BEZ235 resulted in tremendous

radiosensitization as evidenced by inhibition of tumor growth throughout the treatment period and for approximately 60 additional days after treatment was stopped (**Fig. 3.3A, B; Fig. 3.4A**).

In order to determine if the regressing tumors (IR+BEZ arm) carried a greater burden of DSBs compared to the non-responding tumors (the other three arms), three replicate sets of tumor-bearing mice were treated as before, and tumors were harvested at mid-treatment, i.e., 24 hours after dose 7. We detected significant accumulation of 53BP1 foci in tumors treated with both IR and NVP-BEZ235 compared to those treated with either modality alone (**Fig. 3.3C**) which correlated with the tumor response (**Fig. 3.3A**). The IR+BEZ235 tumors also showed a striking reduction in proliferation assessed by Ki67 staining in accord with the greater burden of DSBs in these tumors (**Fig. 3.3D**). The tumors from the different groups did not exhibit significant levels of apoptosis as assayed by TUNEL staining (**Fig. 3.4B**). However, NVP-BEZ235 has been reported to trigger necrosis (Fokas et al., 2012) as well as autophagy (Cerniglia et al., 2012) in irradiated cells *in vitro*, and these processes could also modulate tumor responses *in vivo*. Taken together, our observations indicate that DNA repair inhibition in irradiated tumors results in a high burden of DSBs and inhibition of tumor growth.

NVP-BEZ235 does not interfere with TMZ, an agent co-administered with radiation for GBM treatment. The S_N1-type DNA alkylating drug temozolomide (TMZ) is the only chemotherapeutic agent that offers survival benefit when administered with IR for GBM therapy (Stupp et al., 2009a; Stupp et al., 2005). Thus, any new radiosensitizing

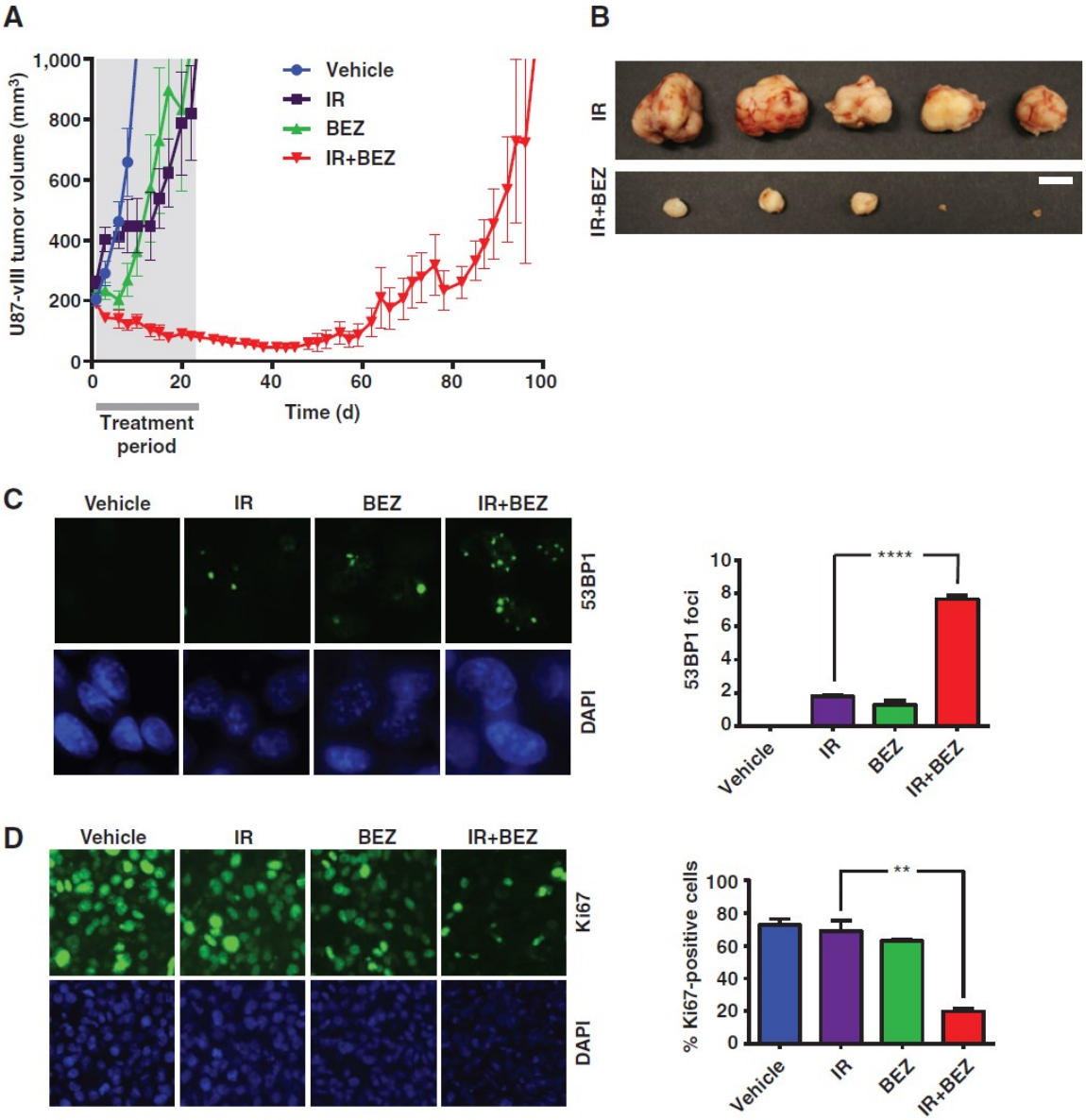

Figure 3.3. Administration of NVP-BEZ235 with radiation results in accumulation of DSBs in tumors and striking radiosensitization. A. Subcutaneous tumors generated from U87-vIII cells were allowed to reach a volume of 200 mm3 following which mice were treated every other day with vehicle, NVP-BEZ235, IR, or NVP-BEZ235 with IR (2 Gy, given 2 hours after drug administration) for a total of 12 doses (shaded area). Tumor growth was monitored until tumors reached 1000 mm3. n = 6 for each treatment group. Error bars, S.E.M. $P < 0.0001$ (IR vs. IR+BEZ). **B.** A set of tumors excised at end of treatment period illustrate the marked reduction in tumor size with combinatorial

treatment. Bar, 10 mm. **C.** A set of tumors was harvested 24 hours after dose 7, and cryosections were immunofluorescence stained for 53BP1 foci (green) and imaged at 40X magnification to obtain a snapshot of the DNA damage load in tumors undergoing treatment. Nuclei are stained with DAPI (blue). 53BP1 foci in 50 nuclei per tumor were counted and plotted. n = 3 tumors per group. Error bars, S.E.M. ****, $P < 0.0001$. **D.** Cryosections were immunofluorescence stained for Ki67 (green) and imaged at 10X magnification. More than 5000 nuclei per tumor were scored using Cell Profiler software and the percentages of Ki67-positive cells were plotted. n = 3 tumors per group. Error bars, S.EM. **, $P = 0.0018$.

approach for GBM needs to be compatible with TMZ. We and others have shown that lethality from S_N1-type alkylating agents is due to secondary DSBs that are generated during DNA replication (Kaina et al., 2007; McEllin et al., 2010; Roos et al., 2007). The anti-proliferative activity of NVP-BEZ235 could attenuate induction of such secondary DSBs and thereby antagonize the effects of TMZ. To rule out this possibility, we generated U87-vIII tumors and allowed them to reach a size of $200mm^3$. We then treated the mice every other day (total of 12 treatments over 24 days; 6 mice per treatment group) with TMZ only (TMZ) or a combination of both TMZ and NVP-BEZ235 (20 mg/kg and 50 mg/kg, respectively) given at the same time by gavage (TMZ+BEZ) (**Fig. 3.5A**). We found that while these tumors regressed upon treatment with TMZ, they always recurred and grew rapidly thereafter. Upon addition of NVP-BEZ235 to the TMZ-treatment regimen, 50% of TMZ+NVP-BEZ235-treated tumors showed no major differences in tumor growth, while the remaining 50% exhibited significantly longer tumor remission compared to TMZ alone (**Fig. 3.6**). This experiment was repeated, and the same split response was observed again. Pooled data from both experiments is shown (**Fig. 3.5A**). It is clear from these data that NVP-BEZ235 does not interfere with the

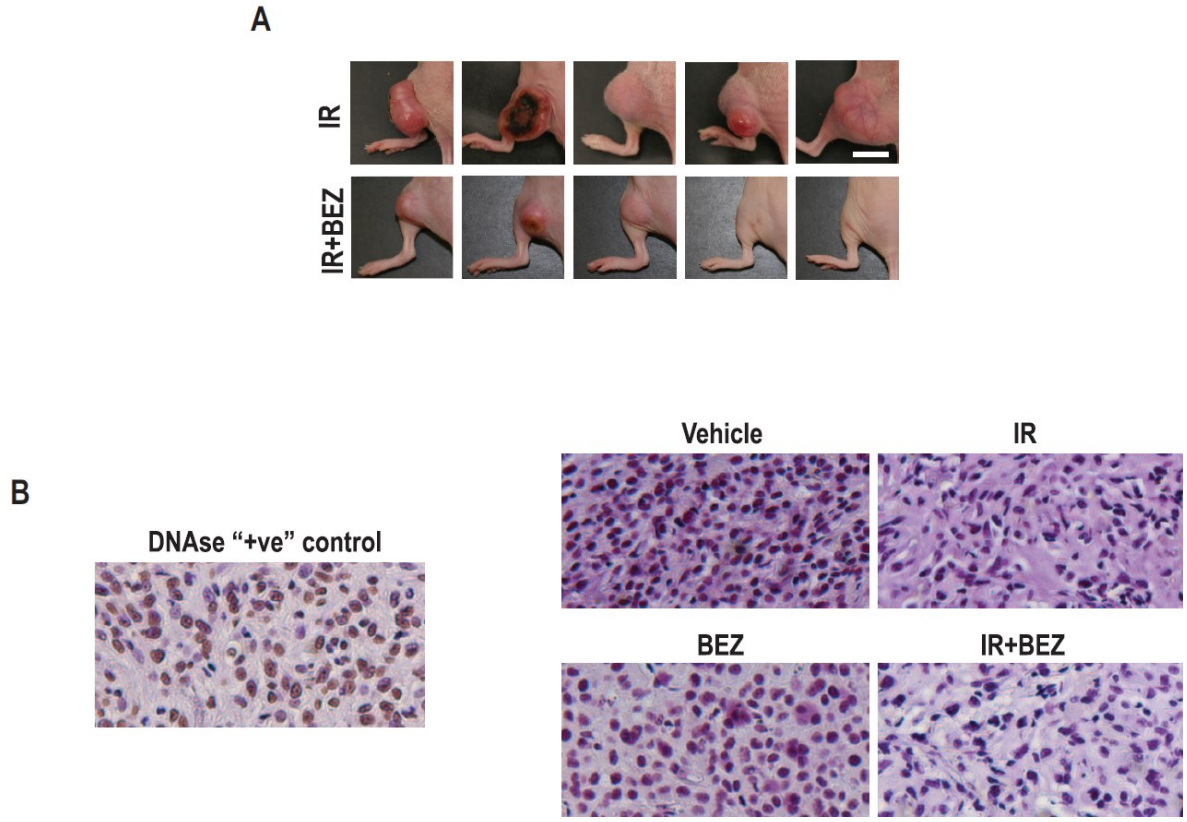

Figure 3.4. NVP-BEZ235 impairs growth of U87-vIII tumors when given in conjunction with IR. A. Subcutaneous tumor-bearing mice at the end of treatment with IR alone or IR with NVP-BEZ235. Bar, 10mm. **B.** Tumors were excised 24 hr after dose 7 and TUNEL staining was performed on paraffin sections to assess levels of apoptosis. As a positive control, a mock-irradiated tumor section was treated with DNAse.

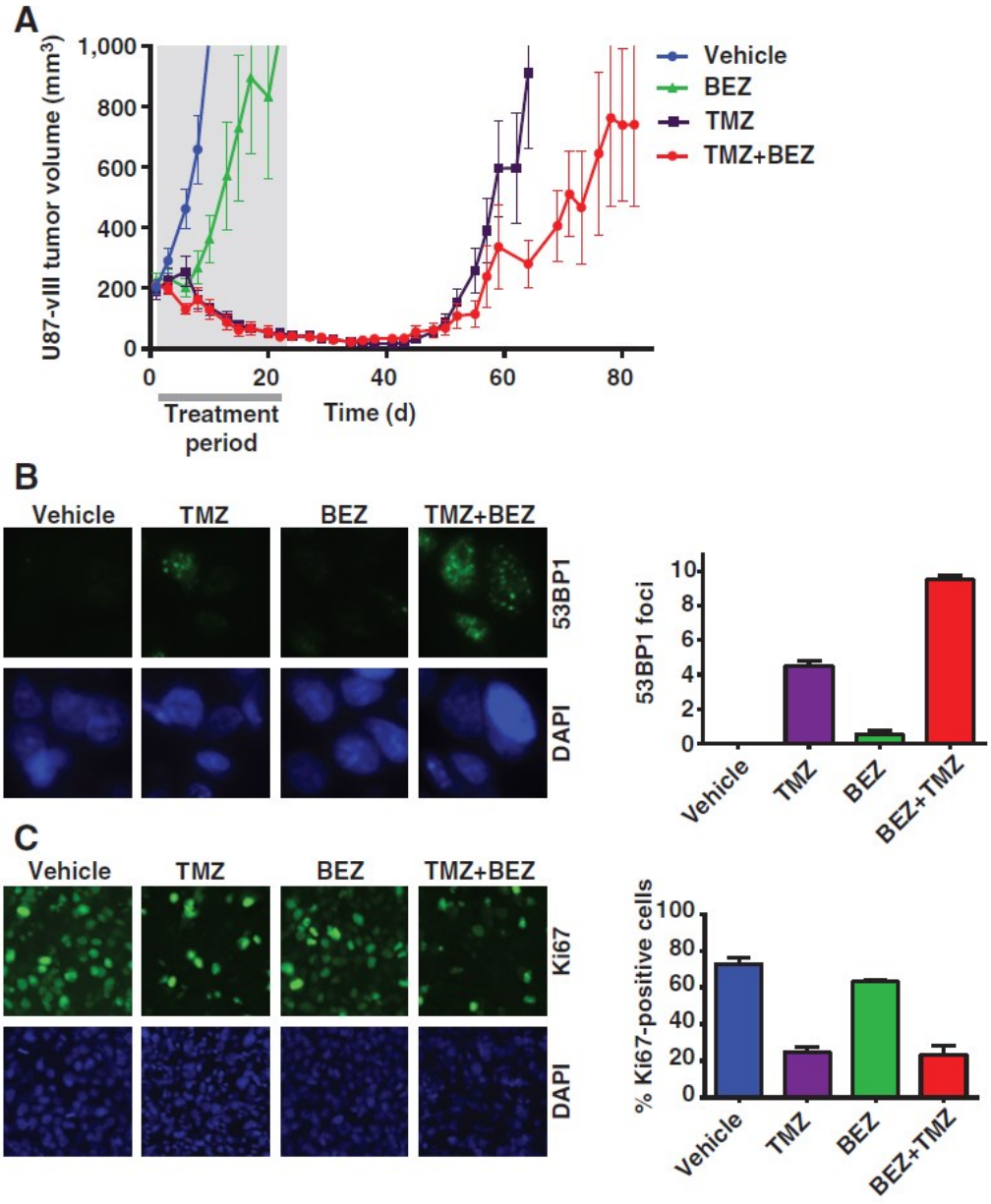

Figure 3.5. NVP-BEZ235 does not interfere with the anti-tumor effects of TMZ. **A**. Subcutaneous tumors generated from U87-vIII cells were allowed to reach a volume of 200 mm^3 and were treated every other day with TMZ, NVP-BEZ235, or a combination of NVP-BEZ235 and TMZ (given at the same time) for 12 doses (shaded area). Tumor growth was monitored until tumors reached a size of 1000 mm^3. Note that the addition of NVP-BEZ235 does not interfere with the effects of TMZ and actually hinders tumor growth further. n = 12 mice per treatment group. Error bars, S.E.M. P = 0.04 (TMZ *vs*. TMZ+BEZ). Vehicle and BEZ plots from Figure 2A are shown for comparison. **B**. A set of tumors was harvested 24 hours after dose 7, and cryosections were

immunofluorescence stained for 53BP1 foci (green) and imaged at 40X magnification to obtain a snapshot of the DNA damage load in tumors undergoing treatment. Nuclei are stained with DAPI (blue). 53BP1 foci in 50 nuclei per tumor were counted and plotted. n = 3 tumors per group. Error bars, S.E.M. **C.** Cryosections were immunofluorescence stained for Ki67 (green) and imaged at 10X magnification. More than 5000 nuclei per tumor were scored using Cell Profiler software and the percentages of Ki67-positive cells were plotted. n = 3 tumors per group. Error bars, S.E.M.

antitumor effects of TMZ, and in a subset of the tumors, dual treatment actually shows an advantage in tumor growth control. A similar synergy between TMZ and NVP-BEZ235 has also been reported before with a different dosing schedule though the underlying mechanism was not elucidated (Maira et al., 2008).

Next, three replicate sets of tumor-bearing mice were treated as before with NVP-BEZ235 and/or TMZ and tumors in the middle of the treatment regimen (i.e., 24 hours after dose 7) from each arm were harvested and immunostained for 53BP1 and for Ki67. We found that the TMZ-treated tumors show an increased number of 53BP1 foci compared to the control tumors (**Fig. 3.5B**), which correlates with a decrease in proliferation (**Fig. 3.5C**). These effects of TMZ are clearly not attenuated by the addition of NVP-BEZ235 to the treatment regimen (**Fig. 3.5B, C**). Taken together, these data indicate that NVP-BEZ235 does not antagonize the anti-tumor effect of TMZ, and in a subset of tumors, actually augments these effects.

NVP-BEZ235 radiosensitizes tumors derived from GBM neurospheres. Next, we wanted to examine if radiosensitization with NVP-BEZ235 could be recapitulated in

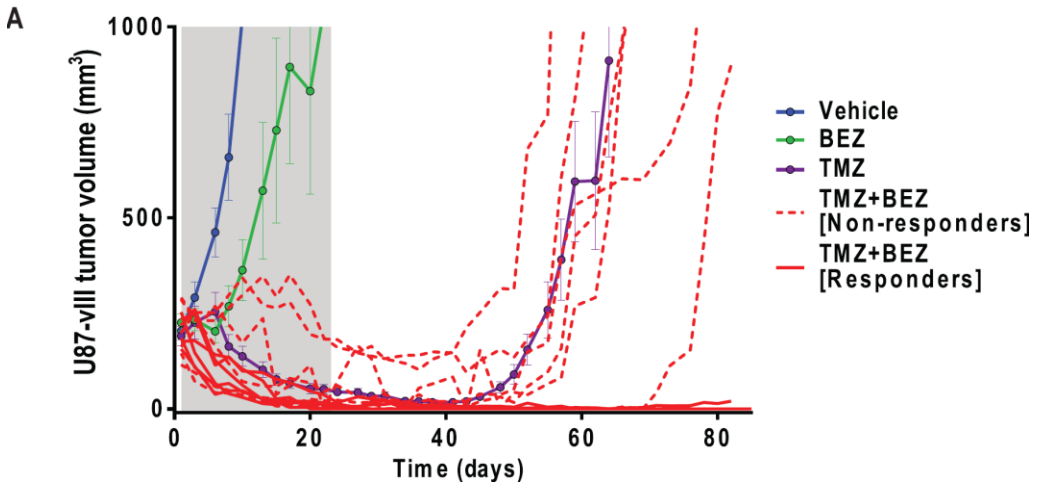

Figure 3.6. NVP-BEZ235 does not interfere with the anti-tumor effects of TMZ in U87-vIII tumors. Data from Figure 3.5A is re-represented to show individual tumor growth profiles for the TMZ+BEZ arm. Please note that 6 tumors (Non-responders; dashed red lines) behave like the TMZ-treated tumors (purple line) while 6 tumors (Responders; solid red lines) exhibit longer tumor regression.

early-passage, primary GBM cells grown as neurospheres. We chose the previously described GBM9 cells for this purpose as these cells retain high levels of amplified EGFRvIII and are thus complementary to the U87-vIII cells used in this study (Puliyappadamba et al., 2013). We found that NVP-BEZ235 could block IR-induced activation of DNA-PKcs and ATM in GBM9 cells in culture leading to acute radiosensitization, similar to that seen with the U87-vIII cells (**Fig. 3.7**). We then generated subcutaneous tumors in Nu/Nu mice using GBM9 cells and found that NVP-BEZ235 could inhibit IR-induced activation of both ATM and DNA-PKcs and phosphorylation of downstream substrates in these tumors (**Fig. 3.8A**). As a result, DSB repair was compromised in irradiated tumors as seen by immunostaining tumor sections for 53BP1 foci (**Fig. 3.8B**).

In order to determine if NVP-BEZ235 could radiosensitize tumors generated from GBM9 cells, we allowed the tumors to grow to a volume of approximately 150 mm^3 before initiating treatment. As with the U87-vIII tumors, the treatment regimen consisted of twelve doses, given every other day, of 50mg/kg of NVP-BEZ235 given by gavage, followed 2 hours later by 2 Gy of IR localized to the tumor. Six mice were randomly allocated to each treatment group. While mice treated with IR or NVP-BEZ235 alone exhibited some delay in tumor growth, combinatorial treatment with both IR and NVP-BEZ235 resulted in striking radiosensitization as evidenced by inhibition of tumor growth throughout the treatment period and for at least 45 additional days after treatment was stopped (**Fig. 3.8C**). Tumor regression was clearly accompanied by a greater burden of DSBs in the tumors as seen by staining a set of tumors at the mid-treatment point for

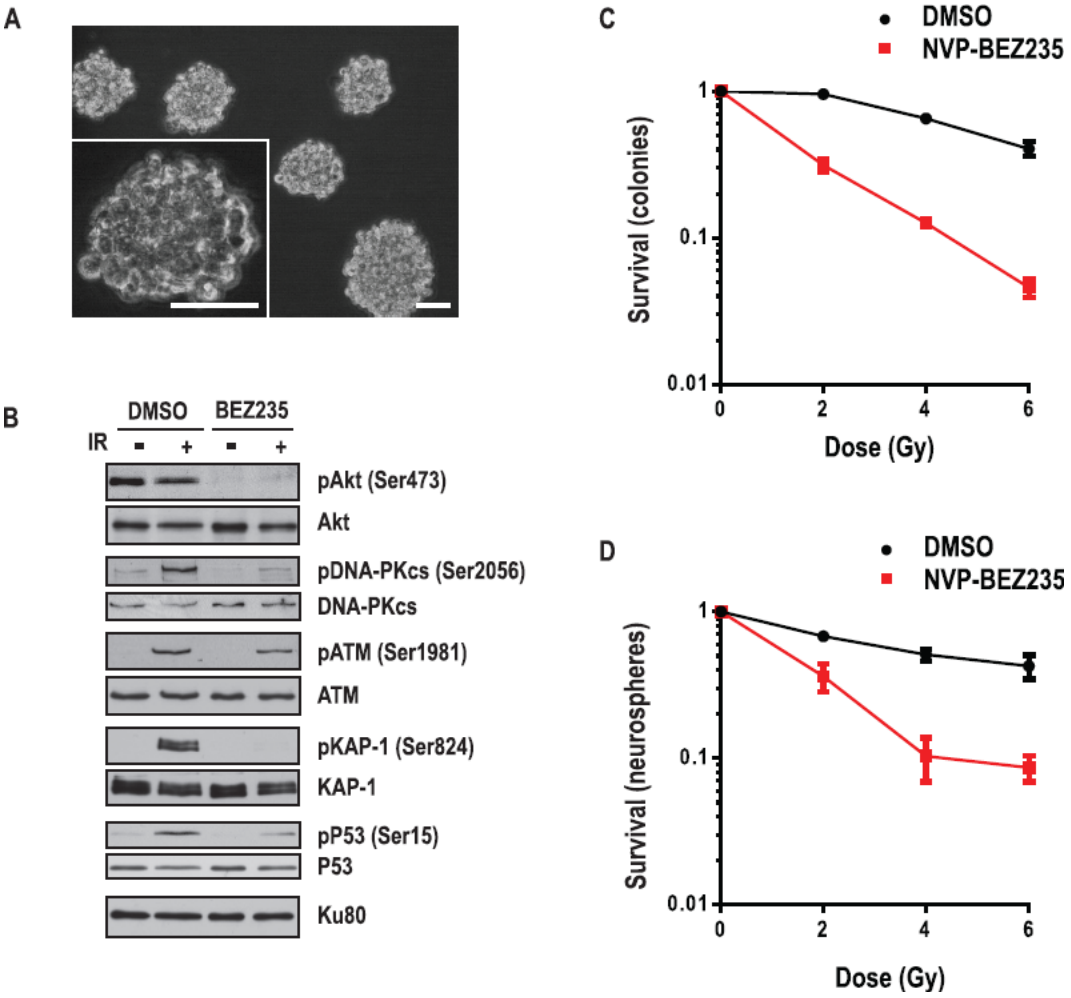

Figure 3.7. NVP-BEZ235 inhibits the DDR in GBM9 neurospheres. A. Bright-field microscopy image of GBM9 neurospheres. Bar, 60 μm. **B.** Neurospheres were treated for 1 hour with NVP-BEZ235 (100 nM) or DMSO before irradiation (10 Gy). Cells were harvested 30 minutes after irradiation and nuclear extracts were analyzed for phosphorylation of proteins by Western blotting with the indicated antibodies. Survival of GBM9 neurospheres after treatment with NVP-BEZ235 (100 nM) or DMSO and radiation was quantified by colony formation (**C**) and sphere formation (**D**) assays. Neurospheres were irradiated at the indicated doses, dissociated into single cells 6 hours after irradiation, and plated onto 6 cm dishes in serum-containing medium for colony formation or suspended as single cells in stem cell medium in 96-well plates for sphere formation. The fraction of colonies or spheres formed (y-axis) was plotted against the corresponding radiation dose (x-axis). Error bars, S.E.M.

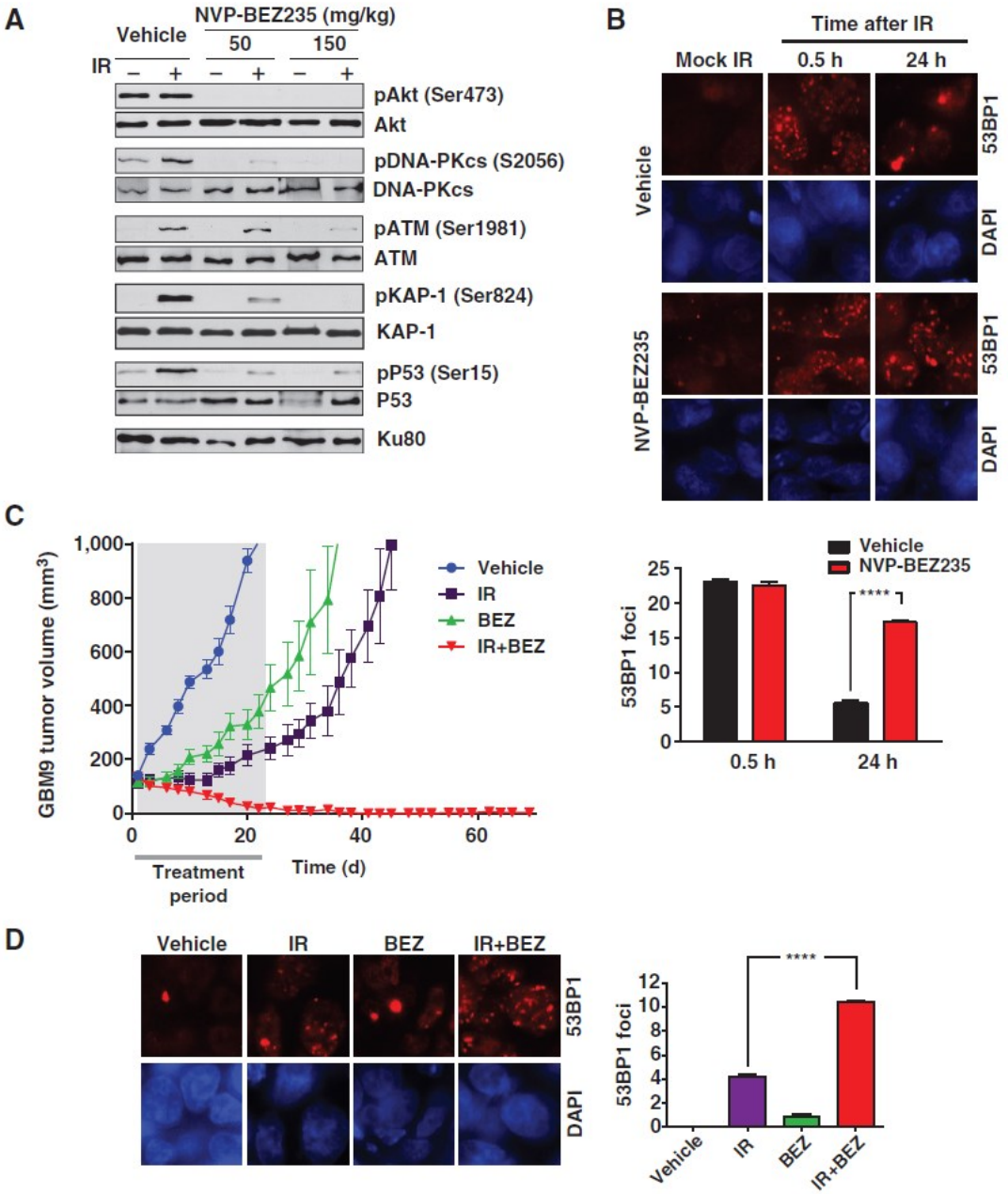

Figure 3.8. NVP-BEZ235 radiosensitizes tumors derived from GBM neurospheres. **A.** Subcutaneous tumors generated from GBM9 neurospheres were mock-irradiated or irradiated (IR) with a total dose of 10 Gy. Tumor-bearing mice were treated with the indicated doses of NVP-BEZ235 or with vehicle alone 2 hours prior to irradiation. Tumors were excised 30 minutes after irradiation and tumor extracts were Western blotted with the indicated antibodies. Note attenuation of IR-induced autophosphorylation of DNA-PKcs and ATM and reduced phosphorylation of ATM targets, KAP-1 and p53. **B.** In order to quantify DSB repair in irradiated tumors, tumor-bearing mice were treated with NVP-BEZ235 and irradiated with 4 Gy of IR after 2 hr. Tumors were harvested at

0.5 or 24 hr post-irradiation, and cryosections were immunofluorescence stained for 53BP1 (red) and imaged at 40X magnification. Nuclei are stained with DAPI (blue). 53BP1 foci in 50 nuclei per tumor were counted and plotted for each time point. n = 3 tumors per time point. Error bars, S.E.M. ****, $P < 0.0001$ **C**. Tumors were allowed to reach a volume of 150 mm^3 following which mice were treated every other day with vehicle, NVP-BEZ235, IR, or NVP-BEZ235 with IR (2 Gy, given 2 hours after drug administration) for a total of 12 doses (shaded area). Tumor growth was monitored until tumors reached a size of 1000 mm^3. n = 6 mice per treatment group. Error bars, S.E.M. $P < 0.0001$ (IR *vs*. IR+BEZ). **D**. A set of tumors was harvested 24 hours after dose 7, and cryosections were immunofluorescence stained for 53BP1 (red) and imaged at 40X magnification. 53BP1 foci in 50 nuclei per tumor were counted and plotted. n = 3 tumors per group. Error bars, S.E.M. ****, $P < 0.0001$.

53BP1 foci (compare IR+BEZ arm with the other three arms) (**Fig. 3.8D**). Our results, showing that NVP-BEZ235 can radiosensitize tumors generated from both U87-vIII cells and GBM9 neurospheres, indicate that DSB-repair inhibitors could have broad utility in GBM therapy.

NVP-BEZ235 crosses the blood-brain-barrier (BBB) and inhibits DSB repair and tumor growth in orthotopic GBM models. A concern with new compounds for the treatment of diseases localized in the central nervous system is whether they will be able to cross the BBB. To see if NVP-BEZ235 can cross the BBB, we treated Nestin-GFP mice (Yamaguchi et al., 2000) with NVP-BEZ235 and sacrificed mice at time points ranging from 0.5 to 16 hours post-treatment. Inhibition of the PI3K-Akt-mTOR pathway by NVP-BEZ235 was assessed by staining for phosphorylation of the ribosomal protein S6 (Engelman et al., 2008). We detected a significant decrease in phospho-S6 staining between 2 to 8 hours post-treatment in most regions of the mouse brain, including the

cortex, cerebellum, and the two neurogenic niches, the subventricular zone (SVZ) and the subgranular zone (SGZ), both marked by nestin promoter-driven GFP expression. (**Fig. 3.9A**). These data clearly indicate that NVP-BEZ235 can cross the BBB making it a very attractive candidate for radiosensitization of GBM.

To test the efficacy of NVP-BEZ235 in blocking DSB repair in an orthotopic GBM model, we stereotactically injected U87-vIII cells intra-cranially into the left corpus striatum of Nu/Nu mice as described before (Mukherjee et al., 2012) and allowed approximately 7 days for tumor development **(Fig. 3.9B)**. We treated tumor-bearing mice with vehicle or NVP-BEZ235 and irradiated them intra-cranially 2 hours later with 2 Gy of IR. Irradiated mice were sacrificed at different times post-IR, and tumor sections were immunofluorescence stained for phospho S6 (Ser236) and for 53BP1 foci. We found ablation of phospho S6 staining upon treatment with NVP-BEZ235 confirming delivery of the drug to these intra- cranial tumors **(Fig. 3.9C)**. 53BP1 staining indicated that the irradiated tumors harbored extensive DNA DSBs at 0.5 hours post-IR. These breaks were almost completely repaired by 12 hours in the vehicle-treated arm, but a significant portion remained unrepaired in the NVP-BEZ235-treated arm (**Fig. 3.9D**). This clearly indicates that NVP-BEZ235 can cross the BBB and block DSB repair in intra-cranial tumors.

To examine if combinatorial treatment with NVP-BEZ235 and IR could control brain tumor growth, intra-cranial tumors were generated in Nu/Nu mice using U87-vIII cellsexpressing luciferase to allow monitoring of tumor growth by bioluminescent imaging (BLI), as described before (Mukherjee et al., 2012). Treatment

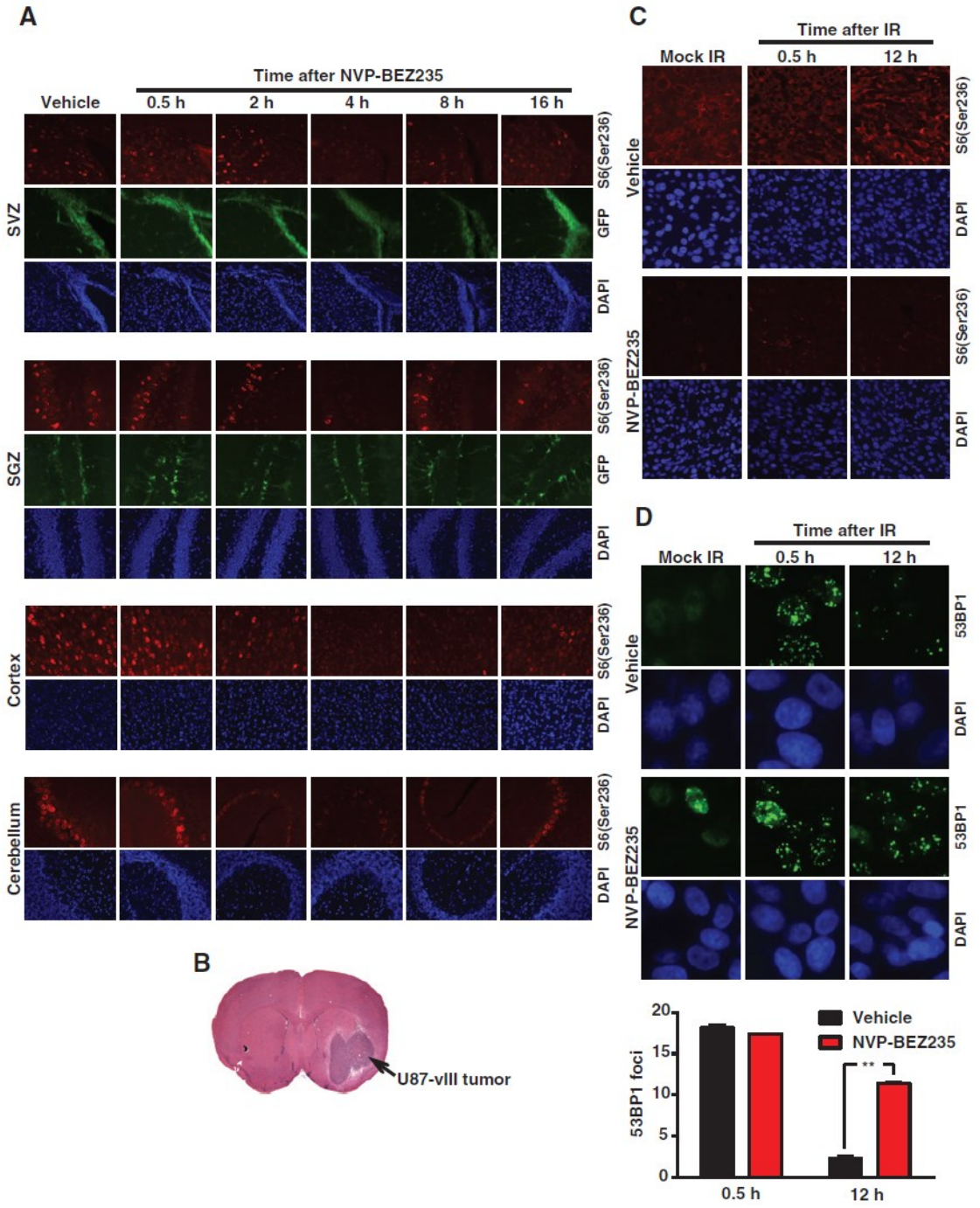

Figure 3.9. NVP-BEZ235 can cross the blood-brain-barrier and inhibit DSB repair in brain tumors. A. Nestin-GFP mice were treated with NVP-BEZ235 and sacrificed at the indicated times post-treatment. Cryosections of the mouse brain were immunofluorescence stained for phospho S6 (red) and imaged at 10X magnification as a measure of inhibition of the PI3K-Akt pathway. The subventricular zone (SVZ),

subgranular zone (SGZ), cortex, and cerebellum were imaged. Stem cell compartments are labeled with GFP (green) and nuclei are stained with DAPI (blue). Note reduction in phospho S6 staining between 2 – 8 hours post-treatment. **B.** U87-vIII cells were injected intra-cranially to generate orthotopic brain tumors. After 7 days, mice were treated with NVP-BEZ235 or vehicle by gavage, intra-cranially irradiated (2 Gy) after 2 hours, and sacrificed at 0.5 or 12 hours post-IR. Intra-cranial tumors were identified in coronal brain sections by H&E staining. **C.** Paraffin sections of tumor-bearing brains were immunofluorescence stained for phospho S6 (red) and imaged at 10X magnification as a measure of inhibition of the PI3K-Akt pathway. **D.** Brain tumor sections were also immunofluorescence stained for 53BP1 foci (green) and imaged at 40X magnification to quantify residual DSBs. n = 2 tumors per time point. Error bars, S.E.M. **, P = 0.002.

was initiated when tumors reached BLI intensities in the 0.5 - 1.0 x 10^9 photons/sec range and were presumably of similar size at time of treatment. As with the subcutaneous tumors, we followed a 12-dose regimen with treatments given every other day. Each dose consisted of vehicle or NVP-BEZ235 (75 mg/kg) followed after 2 hours by mock-irradiation or 2 Gy of IR delivered intra-cranially. BLI radiance was recorded and plotted over time, and mice were sacrificed once they became moribund due to the brain tumor burden. Intra-cranial irradiation (IR) or NVP-BEZ235 (BEZ) alone had little effect on tumor growth rates compared to non-treated tumors (Vehicle) (**Fig. 3.10A**). Strikingly, combinatorial treatment with both modalities (IR+BEZ) resulted in reduced tumor growth rates, and in the case of one mouse (out of a cohort of 6), complete ablation of BLI signal was observed around day 30 post-treatment with no recurrence for at least 12 months post-treatment. There was very little improvement in overall survival (Kaplan-Meier plots) when the mice were treated with either modality alone **(Fig. 3.10B)**. In contrast, combinatorial treatment significantly prolonged survival of tumor bearing mice: treatment with IR or NVP-BEZ235 alone resulted in an increase of only 5.5 and 5 days in

median survival, respectively, whereas combined treatment extended median survival by 35.5 days. Thus, as with the subcutaneous tumor model, we see striking synergy between NVP-BEZ235 and IR in brain tumor growth control, as well as in the median survival of tumor-bearing mice.

To examine if this synergy correlated with a greater burden of DSBs in the tumors receiving combinatorial treatment, additional sets of orthotopic tumors were treated as before, and tumors were harvested at mid-treatment, i.e., 24 hours after dose 7. Upon staining for 53BP1 foci, we observed that tumors treated with both IR and NVP-BEZ235 harbored higher numbers of DSBs than tumors treated with either modality alone **(Fig. 3.10C)**. Importantly, the DSB load was much greater in tumors compared to the normal areas of the irradiated mouse brain. This indicates that there might exist a therapeutic window in which combinatorial treatment could result in greater damage to the tumor relative to the normal brain thereby minimizing collateral damage due to radiosensitization. Taken together, our pre-clinical results clearly indicate that significant improvement of GBM radiotherapy may become possible in the clinic with potent and bioavailable DDR inhibitors such as NVP-BEZ235.

Discussion

GBMs remain one of the most lethal of all tumors for which no effective treatment exists despite decades of research (Dunn et al., 2012). Thus, there is an urgent

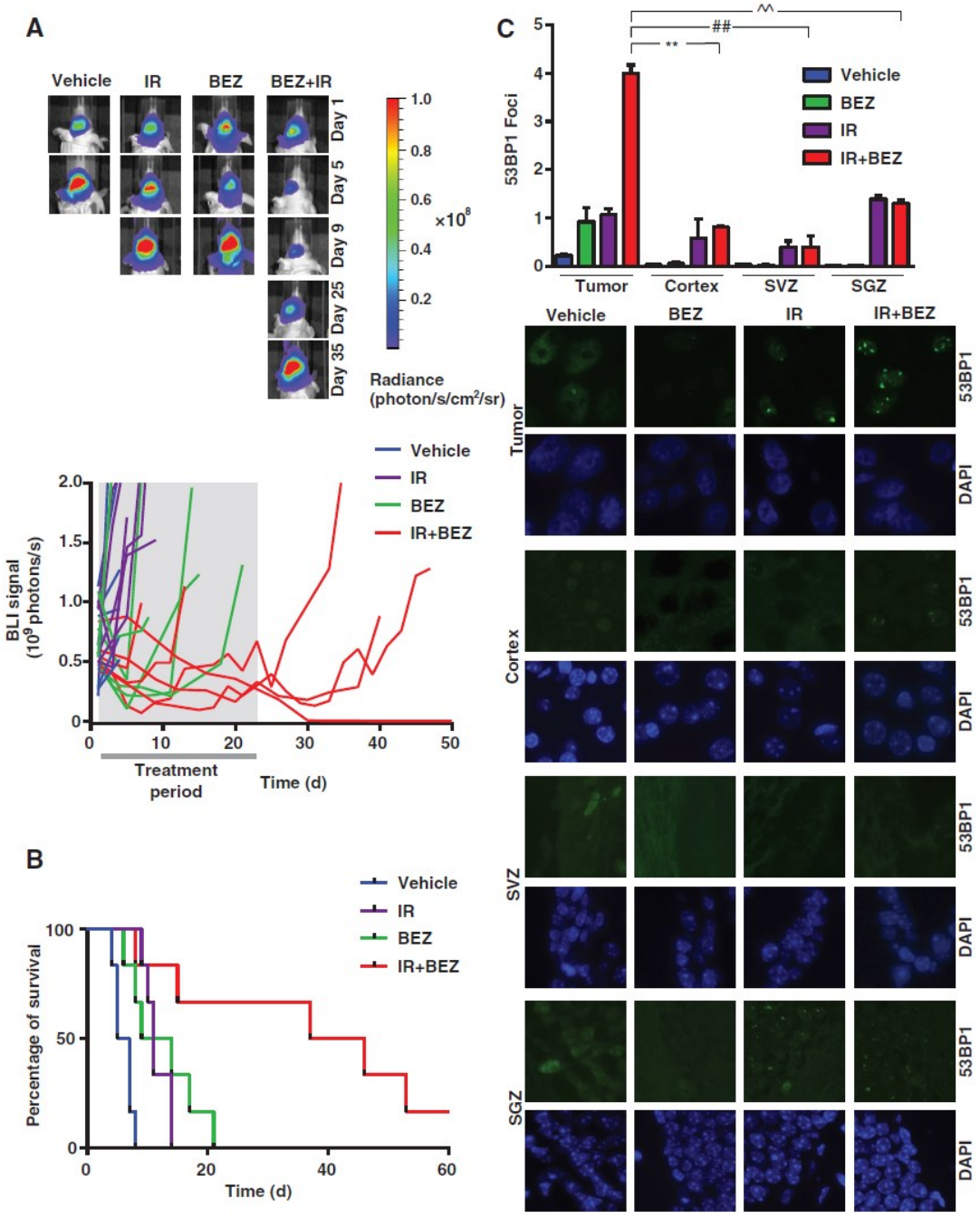

Figure 3.10. NVP-BEZ235 sensitizes brain tumors to radiation and prolongs survival of tumor-bearing mice. A. U87-vIII cells expressing firefly luciferase were injected intra-cranially to generate orthotopic brain tumors (6 mice per treatment group) that were monitored by BLI. Once tumors reached a signal of 0.5-1.0X109 photons/s, mice were treated every other day with vehicle alone, NVP-BEZ235, IR (2Gy), or NVP-BEZ235 in combination with IR (2 Gy given 2 hours after drug administration) for a total

of 12 doses. Upper panel shows tumor progression in a representative mouse for each treatment arm. Lower panel shows quantifications of all measurements. Each curve represents an individual brain tumor. Scale, 0-2x108 protons/s/cm2/sr. $P < 0.0001$ (IR vs. IR+BEZ). Note delay in reappearance of BLI signals in IR+BEZ arm. **B.** Survival of brain tumor-bearing mice was recorded and represented in a Kaplan-Meier plot. n = 6 mice per group. $P = 0.0152$ (IR vs. IR+BEZ). Note improved survival of IR+BEZ mice. **C.** A set of brain tumor-bearing mice was sacrificed at 24 hours after dose 7 and paraffin sections of the whole brain were obtained. Sections were immunofluorescence stained for 53BP1 (green) and imaged at 40X magnification, and 53BP1 foci in 50 nuclei within each tumor were quantified. Nuclei are stained with DAPI (blue). 53BP1 foci were also quantified in the cortex, SVZ, and SGZ and plotted. n = 2 brains per group. Error bars, S.E.M. **, $P = 0.003$. ##, $P = 0.0064$. ^^, $P = 0.0046$.

need for the development of new therapeutic modalities for GBM. The standard-of-care for GBM is surgical resection followed by IR and concomitant and adjuvant TMZ (Stupp et al., 2005). As both IR and TMZ induce DSBs (Jackson and Bartek, 2009; Kaina et al., 2007), blocking the DNA damage response to these breaks is, in principle, a rational approach for sensitizing GBMs and other cancers (Begg et al., 2011; Helleday et al., 2008; Lord and Ashworth, 2012). More than ten years of research efforts focused on the development of potent DNA-PKcs and ATM inhibitors have yielded specific compounds, some of which are very useful in the laboratory for cell-based studies (Finlay and Griffin, 2012). Unfortunately, no single compound shows the necessary potency, bioavailability, and ability to cross the BBB that would allow their evaluation in pre-clinical mouse GBM models. Against this backdrop, our results, demonstrating that NVP-BEZ235 potently inhibits both ATM and DNA-PKcs in tumors, are exciting as they open up new therapeutic possibilities for GBM.

In our study, using pre-clinical mouse models and a drug that is bioavailable and in clinical trials, we show that radio- and chemo-sensitization of GBM may be a viable option for improving therapeutic outcomes. We have previously shown that NVP-BEZ235, a dual PI3K/mTOR inhibitor, can also inhibit both DNA-PKcs and ATM *in vitro* at low doses (in the nanomolar range) (Mukherjee et al., 2012). Here, we have established the *in vivo* utility of this drug as a radiosensitizer in pre-clinical mouse GBM models. We show that this drug can block the phosphorylation of both ATM and DNA-PKcs in subcutaneous tumors and attenuate the repair of IR-induced DSBs. Importantly, we show that the drug can cross the BBB and inhibit DSB repair in intra-cranial tumors. Therefore, a striking efficacy in controlling tumor growth was observed in both subcutaneous and orthotopic tumor models when the drug was administered in combination with IR. Consequently, the addition of NVP-BEZ235 to the irradiation schedule resulted in a significant increase in survival of mice bearing intra-cranial tumors.

Notably, upon analyzing mouse brains during the middle of the IR+BEZ treatment regimen, we observed that the normal brain tissue harbored a lower burden of DSBs compared to the tumor. This hints at the existence of a therapeutic window wherein DNA damage in the tumor may be higher than in the normal brain. This differential inhibition of DSB repair could possibly be attributed to the aberrant hyperproliferation of tumor cells resulting in replication stress and DSBs (Bartkova et al., 2010; Jackson and Bartek, 2009), which could be compounded by the effects of NVP-BEZ235. Heightened activation of DSB repair pathways has been observed in glioma cell lines (Mukherjee et

al., 2009) and human glioma stem cells (Bao et al., 2006) by us and others; reviewed in (Mukherjee et al., 2010). Thus, it is possible that glioma cells may be more dependent on these repair pathways, a phenomenon referred to as "non-oncogene addiction" (Luo et al., 2009). Non-oncogene addiction to DSB repair pathways, in addition to oncogene addiction to the PI3K-Akt-mTOR pathway, both of which would be targeted by NVP-BEZ235, may render tumor cells particularly vulnerable to this drug. Hence, NVP-BEZ235 might have a more drastic effect on tumor cells than on normal brain cells resulting in a greater burden of DSBs in the tumor *versus* the normal brain during therapy. Such a differential effect was also seen *in vitro* in preliminary experiments in which we found that normal human astrocytes (Sonoda et al., 2001) were radiosensitized to a lesser extent by NVP-BEZ235 (**Fig. 3.11**) compared to human glioma cell lines (see Supplementary Fig. S1 and S4 and (Mukherjee et al., 2012)). These differential effects on normal *versus* tumor cells, as well as the effects of NVP-BEZ235 on glioma initiating cells and the tumor microenvironment merit further investigation in the future.

Administration of TMZ is integral to the current GBM therapeutic regimen and constitutes the only significant advance in the treatment of GBM in decades, improving median survival by 2 months compared to IR only and increasing the 5 year survival from 2 to 10 % (Hegi et al., 2005b; Stupp et al., 2009a). Therefore, it is very important that new therapeutic modalities be compatible with TMZ. We find that NVP-BEZ235 does not interfere with the antitumor effects of TMZ. Rather, NVP-BEZ235 and TMZ

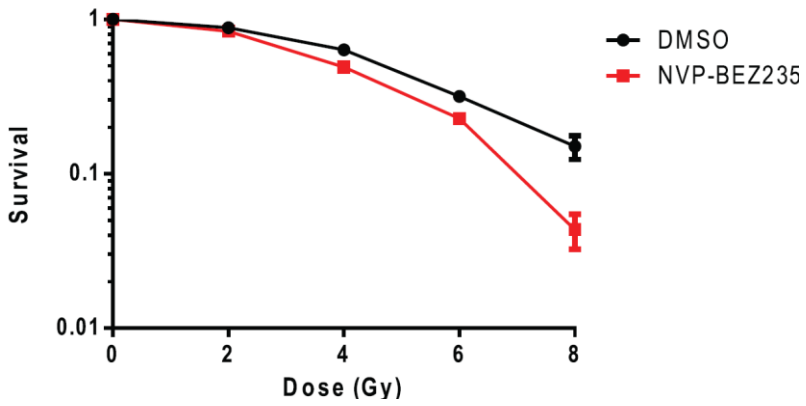

Figure 3.11. Radiosensitization of normal human astrocytes (NHA) with NVP-BEZ235. NHAs were irradiated at the indicated doses and plated out for colony formation. The fraction of colonies formed (y-axis) was plotted against corresponding radiation dose (x-axis). Error bars, S.E.M. Please note lesser extent of radiosensitization, especially in the 2-6 Gy dose range, when compared to U87-vIII or GBM9 cells.

seemed to synergize in at least half of the combinatorially-treated tumors. Potentiation of the effects of TMZ could be due to the inhibition of repair of breaks that are secondarily induced by TMZ (Kaina et al., 2007; McEllin et al., 2010; Roos et al., 2007). However, further experiments are clearly needed to understand why this synergy was only seen in a subset of tumors. Regardless, the potentiating effect of NVP-BEZ235 on TMZ treatment has important clinical implications since NVP-BEZ235 could possibly be given in the clinic both concomitantly with IR and TMZ, and as an adjuvant with TMZ.

A few recent studies have evaluated the radiosensitizing effects of specific DNA-PKcs or ATM inhibitors *in vivo* (Batey et al., 2013; Biddlestone-Thorpe et al., 2013; Munck et al., 2012; Shinohara et al., 2005; Zhao et al., 2006); however, none of these compounds have reached clinical trials. In contrast, NVP-BEZ235 is currently in phase I/II clinical trials for the treatment of advanced solid tumors as a monotherapeutic agent and shows good pharmacokinetics *in vivo* (Garcia-Echeverria and Sellers, 2008; Maira et al., 2008; Peyton et al., 2011). Moreover, NVP-BEZ235 shows a significantly greater radiosensitizing effect *in vivo* compared to the specific DNA-PKcs or ATM inhibitors tested thus far (Batey et al., 2013; Biddlestone-Thorpe et al., 2013; Munck et al., 2012; Shinohara et al., 2005; Zhao et al., 2006), possibly because it potently inhibits both DNA-PKcs and ATM. GBM radioresistance is a pressing and intractable problem with no possibility of improvement currently in sight. While we await the development of better clinically-suitable DDR inhibitors, our proof-of-principle experiments indicate that it could be possible to significantly improve GBM therapy in the future by combining radiation with DNA-PKcs and ATM inhibitors.

CHAPTER FOUR
Conclusions and recommendations

In the past decades, the only significant advance in the treatment of GBMs has been the addition of temozolomide to radiotherapy regimens. However, this treatment modality increases survival only minimally (Stupp et al., 2009a) due to recurrences. Therefore, a better understanding of resistance to TMZ to find new treatment modalities is urgently needed. Mechanisms of resistance causing therapeutic failure to TMZ have mostly been identified as MGMT re-expression and loss of functional mismatch repair, but these account for treatment resistance in only a fraction of the patients. We find that extended TMZ treatment can lead to acquired TMZ-resistance both *in vitro* as well as in orthotopic tumors. Whether this effect was due to TMZ-directed mutagenesis or selection of existing resistant clones remains to be determined. We found that the mechanism of resistance in these tumors was not re-expression of MGMT or abrogation of MMR. Instead we found that TMZ induces DSBs in the primary and recurrent tumor cultures; however, these breaks are repaired at a much faster rate in the recurrent cultures compared to the primary tumor cultures. Interestingly, this augmented repair capability was observed only for TMZ-, MNNG-, and CPT-induced breaks, which are replication associated. Therefore we hypothesized that the mechanism of resistance is augmented HR. Supporting this notion, the recurrent cultures exhibited faster resolution of Rad51 foci and a higher level of recombination as measured by sister chromatid exchanges.

Given the nascent connection between CDK signaling and modulation of HR, as a translational approach, we used the CDK 1 and 2 inhibitors, AZD5438 and Roscovitine, to indirectly inhibit HR. TMZ-induced break repair was abrogated after CDK inhibition resulting in a significant chemosensitization to TMZ in the recurrent cultures. We conclude that augmented HR contributes to temozolomide resistance and therefore recommend exploring HR inhibition in combination with TMZ treatment as a strategy for re-sensitization of recurrent tumors. It is important to point out that we expect this strategy to be effective only if DSBs are generated upon TMZ-treatment. This would be an important aspect to determine in the clinic, as a big fraction of GBMs are TMZ-resistant via DSB formation avoidance either by overexpression of MGMT or mutation/silencing of MMR genes. As TMZ-induced breaks are mainly repaired by HR, we expect this strategy to be effective in primary tumors as well. Indeed, it may potentiate initial responses to TMZ and avoid expansion of existing clones that have upregulated HR. However, it still remains to be determined if such a strategy would promote or speed up the emergence of other mechanisms of resistance. This outcome is possible as this strategy would eliminate competing clones that would otherwise limit the space and nutrients available for expansion of fitter clones.

Future directions of this part include 1) to identify the key molecular players involved in HR upregulation and 2) determine how universal this mechanism of resistance is or whether it correlates with other genomic/epigenomic alterations. To identify the key players involved in HR, a sequence analysis could be carried out to compare the primary to the recurrent cultures. For such analysis, sequencing of HR

related genes with enough coverage to detect mutations could be carried out. However, a whole genome sequencing strategy might reveal more differences as novel, non-DNA repair pathways could impinge on HR. It is also possible that alterations may not be present at the genomic level, but rather at the proteomic or epigenomic level. In that case, high throughput assays such as bisulfite sequencing or mass spectrometry could be used to detect differences in DNA methylation or differences in post-translational modifications of specific proteins. The usefulness of identifying the specific alteration would depend on how frequent it is, therefore it is crucial to first investigate the frequency at which tumors develop upregulated HR. To do this, a model like the one proposed here could be used in a large scale study where a big array of confirmed GBM tumors could be induced to develop TMZ-resistance in the mouse brain. The multidimensional analysis of such samples and correlation of gene expression signatures with mechanisms of resistance in recurrence could possibly yield a set of predictive markers.

Augmented NHEJ has also been shown to result in treatment resistance (Mukherjee et al., 2009), specifically radioresistance, as IR-induced breaks in asynchronous cells are repaired by NHEJ for the most part (Branzei and Foiani, 2008). Because of HR's role in TMZ-induced break repair and NHEJ's role in IR-induced break repair, it is a more effective strategy to inhibit both repair pathways by targeting the DDR's apical kinases, ATM, DNA-PKcs, and ATR. Inhibitors of the DDR have great potential for radiosensitization of numerous cancers including GBM. However, compounds with the necessary specificity, potency, bioavailability, and ability to cross

the blood brain barrier have not yet reached the clinic. Previously, we demonstrated that the dual PI3K/mTOR inhibitor NVP-BEZ235 can potently inhibit the two central DDR kinases, DNA-PKcs and ATM, *in vitro* (Mukherjee et al., 2012). Additionally, ATR was also shown to be targeted by NVP-BEZ235 *in vitro* (Toledo et al., 2011). The work presented here shows that NVP-BEZ235 potently inhibited both DNA-PKcs and ATM kinases and attenuated the repair of IR-induced DNA damage in tumors. Importantly, this resulted in striking tumor radiosensitization, which extended the survival of brain tumor-bearing mice. NVP-BEZ235 also sensitized subcutaneous tumors to TMZ; however this occurred in only approximately 50% of the tumors. It remains to be determined why some of the tumors did not respond to NVP-BEZ235 and had responses similar to that of the TMZ only arm. It is possible that the non-responder tumors developed resistance to TMZ by DSB formation avoidance.

To the best of our knowledge, this is the first time that a compound was shown to potently inhibit both ATM and DNA-PKcs *in vivo* and result in such striking radiosensitization as observed by us and others (Konstantinidou et al., 2009). In a proof-of-principle manner, this demonstrates that it may be possible to significantly improve GBM therapy by combining IR and possibly TMZ with potent and bioavailable DNA repair inhibitors like NVP-BEZ235. As mentioned before, NVP-BEZ235 was evaluated in clinical trials as a monotherapy for the treatment of solid malignancies including GBM; however due to excessive toxicities, Novartis decided to stop marketing NVP-BEZ235. Because of the striking effects as a radiosensitizer we recommend the clinical testing of low-dose NVP-BEZ235 combined with radiotherapy to evaluate its

radiosensitizing effects. We hope that lower doses may decrease the toxicities and still result in radiosensitization. Importantly, as DNA damage repair is such a basic and essential process for cell viability, it is likely that NVP-BEZ235 radiosensitization will be beneficial for other cancer types, especially since augmented repair pathways have been reported in a variety of cancers as a mechanism for radioresistance. As with all radiosensitizers, abrogation of radiation toxicity due to sensitization of normal tissues is always a concern. With NVP-BEZ235 in our mouse model, we did not observe a dramatically impaired repair of DSBs in the cortex, cerebellum, and neurogenic regions (SVZ and SGZ) after whole brain irradiations. Although we did not test these, the lack of an effect in the brain could be attributed to a poorer drug delivery to the brain compared to the tumor, which may have a leaky blood brain barrier and higher dependence on DNA repair pathways. It remains to be seen if this is true for humans as well. More importantly, radiotherapy-dependent, long-term neurological effects such as inflammation, white matter necrosis, and demyelination need to be tested when radiation is administered in combination with NVP-BEZ235.

BIBLIOGRAPHY

(2008). Comprehensive genomic characterization defines human glioblastoma genes and core pathways. Nature *455*, 1061-1068.

Ammirati, M., Vick, N., Liao, Y.L., Ciric, I., and Mikhael, M. (1987). Effect of the extent of surgical resection on survival and quality of life in patients with supratentorial glioblastomas and anaplastic astrocytomas. Neurosurgery *21*, 201-206.

Bao, S., Wu, Q., McLendon, R.E., Hao, Y., Shi, Q., Hjelmeland, A.B., Dewhirst, M.W., Bigner, D.D., and Rich, J.N. (2006). Glioma stem cells promote radioresistance by preferential activation of the DNA damage response. Nature *444*, 756-760.

Bartkova, J., Hamerlik, P., Stockhausen, M.T., Ehrmann, J., Hlobilkova, A., Laursen, H., Kalita, O., Kolar, Z., Poulsen, H.S., Broholm, H.*, et al.* (2010). Replication stress and oxidative damage contribute to aberrant constitutive activation of DNA damage signalling in human gliomas. Oncogene *29*, 5095-5102.

Batey, M.A., Zhao, Y., Kyle, S., Richardson, C., Slade, A., Martin, N.M., Lau, A., Newell, D.R., and Curtin, N.J. (2013). Preclinical evaluation of a novel ATM inhibitor, KU59403, in vitro and in vivo in p53 functional and dysfunctional models of human cancer. Mol Cancer Ther.

Begg, A.C., Stewart, F.A., and Vens, C. (2011). Strategies to improve radiotherapy with targeted drugs. Nat Rev Cancer *11*, 239-253.

Bhattacharyya, N.P., Skandalis, A., Ganesh, A., Groden, J., and Meuth, M. (1994). Mutator phenotypes in human colorectal carcinoma cell lines. Proceedings of the National Academy of Sciences of the United States of America *91*, 6319-6323.

Biddlestone-Thorpe, L., Sajjad, M., Rosenberg, E., Beckta, J.M., Valerie, N.C., Tokarz, M., Adams, B.R., Wagner, A.F., Khalil, A., Gilfor, D.*, et al.* (2013). ATM kinase inhibition preferentially sensitizes p53 mutant glioma to ionizing radiation. Clin Cancer Res.

Blaiss, C.A., Yu, T.S., Zhang, G., Chen, J., Dimchev, G., Parada, L.F., Powell, C.M., and Kernie, S.G. (2011). Temporally specified genetic ablation of neurogenesis impairs cognitive recovery after traumatic brain injury. The Journal of neuroscience : the official journal of the Society for Neuroscience *31*, 4906-4916.

Bleehen, N.M., and Stenning, S.P. (1991). A Medical Research Council trial of two radiotherapy doses in the treatment of grades 3 and 4 astrocytoma. The Medical Research Council Brain Tumour Working Party. Br J Cancer *64*, 769-774.

Brachmann, S.M., Hofmann, I., Schnell, C., Fritsch, C., Wee, S., Lane, H., Wang, S., Garcia-Echeverria, C., and Maira, S.M. (2009). Specific apoptosis induction by the dual PI3K/mTor inhibitor NVP-BEZ235 in HER2 amplified and PIK3CA mutant breast cancer cells. Proceedings of the National Academy of Sciences of the United States of America *106*, 22299-22304.

Branzei, D., and Foiani, M. (2008). Regulation of DNA repair throughout the cell cycle. Nat Rev Mol Cell Biol *9*, 297-308.

Brown, N.R., Korolchuk, S., Martin, M.P., Stanley, W.A., Moukhametzianov, R., Noble, M.E., and Endicott, J.A. (2015). CDK1 structures reveal conserved and unique features of the essential cell cycle CDK. Nature communications *6*, 6769.

Buatti, J., Ryken, T.C., Smith, M.C., Sneed, P., Suh, J.H., Mehta, M., and Olson, J.J. (2008). Radiation therapy of pathologically confirmed newly diagnosed glioblastoma in adults. Journal of neuro-oncology *89*, 313-337.

Budke, B., Logan, H.L., Kalin, J.H., Zelivianskaia, A.S., Cameron McGuire, W., Miller, L.L., Stark, J.M., Kozikowski, A.P., Bishop, D.K., and Connell, P.P. (2012). RI-1: a chemical inhibitor of RAD51 that disrupts homologous recombination in human cells. Nucleic Acids Res *40*, 7347-7357.

Buis, J., Stoneham, T., Spehalski, E., and Ferguson, D.O. (2012). Mre11 regulates CtIP-dependent double-strand break repair by interaction with CDK2. Nature structural & molecular biology *19*, 246-252.

Cahill, D.P., Levine, K.K., Betensky, R.A., Codd, P.J., Romany, C.A., Reavie, L.B., Batchelor, T.T., Futreal, P.A., Stratton, M.R., Curry, W.T.*, et al.* (2007). Loss of the mismatch repair protein MSH6 in human glioblastomas is associated with tumor progression during temozolomide treatment. Clin Cancer Res *13*, 2038-2045.

Campeau, E., Ruhl, V.E., Rodier, F., Smith, C.L., Rahmberg, B.L., Fuss, J.O., Campisi, J., Yaswen, P., Cooper, P.K., and Kaufman, P.D. (2009). A versatile viral system for expression and depletion of proteins in mammalian cells. PLoS ONE *4*, e6529.

Carbain, B., Paterson, D.J., Anscombe, E., Campbell, A.J., Cano, C., Echalier, A., Endicott, J.A., Golding, B.T., Haggerty, K., Hardcastle, I.R.*, et al.* (2014). 8-Substituted O(6)-cyclohexylmethylguanine CDK2 inhibitors: using structure-based inhibitor design to optimize an alternative binding mode. J Med Chem *57*, 56-70.

Cerniglia, G.J., Karar, J., Tyagi, S., Christofidou-Solomidou, M., Rengan, R., Koumenis, C., and Maity, A. (2012). Inhibition of autophagy as a strategy to augment radiosensitization by the dual phosphatidylinositol 3-kinase/mammalian target of rapamycin inhibitor NVP-BEZ235. Mol Pharmacol *82*, 1230-1240.

Chang, C.H., Horton, J., Schoenfeld, D., Salazer, O., Perez-Tamayo, R., Kramer, S., Weinstein, A., Nelson, J.S., and Tsukada, Y. (1983). Comparison of postoperative radiotherapy and combined postoperative radiotherapy and chemotherapy in the multidisciplinary management of malignant gliomas. A joint Radiation Therapy Oncology Group and Eastern Cooperative Oncology Group study. Cancer *52*, 997-1007.

Chanthery, Y.H., Gustafson, W.C., Itsara, M., Persson, A., Hackett, C.S., Grimmer, M., Charron, E., Yakovenko, S., Kim, G., Matthay, K.K.*, et al.* (2012). Paracrine signaling through MYCN enhances tumor-vascular interactions in neuroblastoma. Sci Transl Med *4*, 115ra113.

Chen, R., Nishimura, M.C., Bumbaca, S.M., Kharbanda, S., Forrest, W.F., Kasman, I.M., Greve, J.M., Soriano, R.H., Gilmour, L.L., Rivers, C.S.*, et al.* (2010). A hierarchy of self-renewing tumor-initiating cell types in glioblastoma. Cancer Cell *17*, 362-375.

Chiarini, F., Grimaldi, C., Ricci, F., Tazzari, P.L., Evangelisti, C., Ognibene, A., Battistelli, M., Falcieri, E., Melchionda, F., Pession, A.*, et al.* (2010). Activity of the novel dual phosphatidylinositol 3-kinase/mammalian target of rapamycin inhibitor NVP-BEZ235 against T-cell acute lymphoblastic leukemia. Cancer research *70*, 8097-8107.

Cho, D.C., Cohen, M.B., Panka, D.J., Collins, M., Ghebremichael, M., Atkins, M.B., Signoretti, S., and Mier, J.W. (2010). The efficacy of the novel dual PI3-kinase/mTOR inhibitor NVP-BEZ235 compared with rapamycin in renal cell carcinoma. Clin Cancer Res *16*, 3628-3638.

Conway, A.B., Lynch, T.W., Zhang, Y., Fortin, G.S., Fung, C.W., Symington, L.S., and Rice, P.A. (2004). Crystal structure of a Rad51 filament. Nature structural & molecular biology *11*, 791-796.

Davies, O.R., and Pellegrini, L. (2007). Interaction with the BRCA2 C terminus protects RAD51-DNA filaments from disassembly by BRC repeats. Nature structural & molecular biology *14*, 475-483.

Dean, M., Fojo, T., and Bates, S. (2005). Tumour stem cells and drug resistance. Nat Rev Cancer *5*, 275-284.

Dietmaier, W., Wallinger, S., Bocker, T., Kullmann, F., Fishel, R., and Ruschoff, J. (1997a). Diagnostic microsatellite instability: definition and correlation with mismatch repair protein expression. Cancer research *57*, 4749-4756.

Dietmaier, W., Wallinger, S., Bocker, T., Kullmann, F., Fishel, R., and Rüschoff, J. (1997b). Diagnostic microsatellite instability: definition and correlation with mismatch repair protein expression. Cancer research *57*, 4749-4756.

Dolan, M.E., Mitchell, R.B., Mummert, C., Moschel, R.C., and Pegg, A.E. (1991). Effect of O6-Benzylguanine Analogues on Sensitivity of Human Tumor Cells to the Cytotoxic Effects of Alkylating Agents. Cancer research *51*, 3367-3372.

Dunn, G.P., Rinne, M.L., Wykosky, J., Genovese, G., Quayle, S.N., Dunn, I.F., Agarwalla, P.K., Chheda, M.G., Campos, B., Wang, A.*, et al.* (2012). Emerging insights into the molecular and cellular basis of glioblastoma. Genes Dev *26*, 756-784.

Eichhorn, P.J., Gili, M., Scaltriti, M., Serra, V., Guzman, M., Nijkamp, W., Beijersbergen, R.L., Valero, V., Seoane, J., Bernards, R.*, et al.* (2008). Phosphatidylinositol 3-kinase hyperactivation results in lapatinib resistance that is reversed by the mTOR/phosphatidylinositol 3-kinase inhibitor NVP-BEZ235. Cancer research *68*, 9221-9230.

Engelman, J.A., Chen, L., Tan, X., Crosby, K., Guimaraes, A.R., Upadhyay, R., Maira, M., McNamara, K., Perera, S.A., Song, Y.*, et al.* (2008). Effective use of PI3K and MEK inhibitors to treat mutant Kras G12D and PIK3CA H1047R murine lung cancers. Nat Med *14*, 1351-1356.

Esashi, F., Christ, N., Gannon, J., Liu, Y., Hunt, T., Jasin, M., and West, S.C. (2005). CDK-dependent phosphorylation of BRCA2 as a regulatory mechanism for recombinational repair. Nature *434*, 598-604.

Estrada-Bernal, A., Lawler, S.E., Nowicki, M.O., Ray Chaudhury, A., and Van Brocklyn, J.R. (2011). The role of sphingosine kinase-1 in EGFRvIII-regulated growth and survival of glioblastoma cells. Journal of neuro-oncology *102*, 353-366.

Fadul, C., Wood, J., Thaler, H., Galicich, J., Patterson, R.H., Jr., and Posner, J.B. (1988). Morbidity and mortality of craniotomy for excision of supratentorial gliomas. Neurology *38*, 1374-1379.

Falck, J., Forment, J.V., Coates, J., Mistrik, M., Lukas, J., Bartek, J., and Jackson, S.P. (2012). CDK targeting of NBS1 promotes DNA-end resection, replication restart and homologous recombination. EMBO reports *13*, 561-568.

Felsberg, J., Thon, N., Eigenbrod, S., Hentschel, B., Sabel, M.C., Westphal, M., Schackert, G., Kreth, F.W., Pietsch, T., Löffler, M.*, et al.* (2011). Promoter methylation and expression of MGMT and the DNA mismatch repair genes MLH1, MSH2, MSH6 and PMS2 in paired primary and recurrent glioblastomas. International Journal of Cancer *129*, 659-670.

Finlay, M.R., and Griffin, R.J. (2012). Modulation of DNA repair by pharmacological inhibitors of the PIKK protein kinase family. Bioorganic & medicinal chemistry letters *22*, 5352-5359.

Fokas, E., Yoshimura, M., Prevo, R., Higgins, G., Hackl, W., Maira, S.M., Bernhard, E.J., McKenna, W.G., and Muschel, R.J. (2012). NVP-BEZ235 and NVP-BGT226, dual phosphatidylinositol 3-kinase/mammalian target of rapamycin inhibitors, enhance tumor and endothelial cell radiosensitivity. Radiat Oncol *7*, 48.

Franceschi, E., Cavallo, G., Lonardi, S., Magrini, E., Tosoni, A., Grosso, D., Scopece, L., Blatt, V., Urbini, B., Pession, A.*, et al.* (2007). Gefitinib in patients with progressive high-grade gliomas: a multicentre phase II study by Gruppo Italiano Cooperativo di Neuro-Oncologia (GICNO). Br J Cancer *96*, 1047-1051.

Friedman, H.S., Kerby, T., and Calvert, H. (2000). Temozolomide and Treatment of Malignant Glioma. Clin Cancer Res *6*, 2585-2597.

Friedman, H.S., Prados, M.D., Wen, P.Y., Mikkelsen, T., Schiff, D., Abrey, L.E., Yung, W.K., Paleologos, N., Nicholas, M.K., Jensen, R.*, et al.* (2009). Bevacizumab alone and in combination with irinotecan in recurrent glioblastoma. J Clin Oncol *27*, 4733-4740.

Fu, D., Calvo, J.A., and Samson, L.D. (2012). Balancing repair and tolerance of DNA damage caused by alkylating agents. Nat Rev Cancer *12*, 104-120.

Garcia-Echeverria, C., and Sellers, W.R. (2008). Drug discovery approaches targeting the PI3K/Akt pathway in cancer. Oncogene *27*, 5511-5526.

Gilbert, M.R., Dignam, J.J., Armstrong, T.S., Wefel, J.S., Blumenthal, D.T., Vogelbaum, M.A., Colman, H., Chakravarti, A., Pugh, S., Won, M.*, et al.* (2014). A randomized trial of bevacizumab for newly diagnosed glioblastoma. N Engl J Med *370*, 699-708.

Halazonetis, T.D., Gorgoulis, V.G., and Bartek, J. (2008). An oncogene-induced DNA damage model for cancer development. Science *319*, 1352-1355.

Hambardzumyan, D., Becher, O.J., Rosenblum, M.K., Pandolfi, P.P., Manova-Todorova, K., and Holland, E.C. (2008). PI3K pathway regulates survival of cancer stem cells residing in the perivascular niche following radiation in medulloblastoma in vivo. Genes Dev *22*, 436-448.

Happold, C., Roth, P., Wick, W., Schmidt, N., Florea, A.-M., Silginer, M., Reifenberger, G., and Weller, M. (2012). Distinct molecular mechanisms of acquired resistance to temozolomide in glioblastoma cells. J Neurochem *122*, 444-455.

Hegi, M.E., Diserens, A.-C., Gorlia, T., Hamou, M.-F., de Tribolet, N., Weller, M., Kros, J.M., Hainfellner, J.A., Mason, W., Mariani, L.*, et al.* (2005a). MGMT Gene Silencing and Benefit from Temozolomide in Glioblastoma. New England Journal of Medicine *352*, 997-1003.

Hegi, M.E., Diserens, A.C., Gorlia, T., Hamou, M.F., de Tribolet, N., Weller, M., Kros, J.M., Hainfellner, J.A., Mason, W., Mariani, L.*, et al.* (2005b). MGMT gene silencing and benefit from temozolomide in glioblastoma. N Engl J Med *352*, 997-1003.

Helleday, T., Petermann, E., Lundin, C., Hodgson, B., and Sharma, R.A. (2008). DNA repair pathways as targets for cancer therapy. Nat Rev Cancer *8*, 193-204.

Huang, F., Mazina, O.M., Zentner, I.J., Cocklin, S., and Mazin, A.V. (2012). Inhibition of homologous recombination in human cells by targeting RAD51 recombinase. J Med Chem *55*, 3011-3020.

Huang, P.H., Xu, A.M., and White, F.M. (2009). Oncogenic EGFR signaling networks in glioma. Science signaling *2*, re6.

Huertas, P., and Jackson, S.P. (2009). Human CtIP mediates cell cycle control of DNA end resection and double strand break repair. The Journal of biological chemistry *284*, 9558-9565.

Hunter, C., Smith, R., Cahill, D.P., Stephens, P., Stevens, C., Teague, J., Greenman, C., Edkins, S., Bignell, G., Davies, H.*, et al.* (2006). A hypermutation phenotype and somatic MSH6 mutations in recurrent human malignant gliomas after alkylator chemotherapy. Cancer research *66*, 3987-3991.

Jackson, S.P., and Bartek, J. (2009). The DNA-damage response in human biology and disease. Nature *461*, 1071-1078.

Johnson, B.E., Mazor, T., Hong, C., Barnes, M., Aihara, K., McLean, C.Y., Fouse, S.D., Yamamoto, S., Ueda, H., Tatsuno, K.*, et al.* (2014a). Mutational analysis reveals the origin and therapy-driven evolution of recurrent glioma. Science *343*, 189-193.

Johnson, B.E., Mazor, T., Hong, C., Barnes, M., Aihara, K., McLean, C.Y., Fouse, S.D., Yamamoto, S., Ueda, H., Tatsuno, K.*, et al.* (2014b). Mutational analysis reveals the origin and therapy-driven evolution of recurrent glioma. Science *343*, 189-193.

Kaina, B., Christmann, M., Naumann, S., and Roos, W.P. (2007). MGMT: key node in the battle against genotoxicity, carcinogenicity and apoptosis induced by alkylating agents. DNA Repair (Amst) *6*, 1079-1099.

Keime-Guibert, F., Chinot, O., Taillandier, L., Cartalat-Carel, S., Frenay, M., Kantor, G., Guillamo, J.S., Jadaud, E., Colin, P., Bondiau, P.Y.*, et al.* (2007). Radiotherapy for glioblastoma in the elderly. N Engl J Med *356*, 1527-1535.

Keles, G.E., Anderson, B., and Berger, M.S. (1999). The effect of extent of resection on time to tumor progression and survival in patients with glioblastoma multiforme of the cerebral hemisphere. Surgical neurology *52*, 371-379.

Kesavabhotla, K., Schlaff, C.D., Shin, B., Mubita, L., Kaplan, R., Tsiouris, A.J., Pannullo, S.C., Christos, P., Lavi, E., Scheff, R.*, et al.* (2012). Phase I/II study of oral erlotinib for treatment of relapsed/refractory glioblastoma multiforme and anaplastic astrocytoma. Journal of experimental therapeutics & oncology *10*, 71-81.

Kirkpatrick, D.B. (1984). The first primary brain-tumor operation. Journal of neurosurgery *61*, 809-813.

Kitange, G.J., Mladek, A.C., Carlson, B.L., Schroeder, M.A., Pokorny, J.L., Cen, L., Decker, P.A., Wu, W., Lomberk, G.A., Gupta, S.K.*, et al.* (2012). Inhibition of Histone Deacetylation Potentiates the Evolution of Acquired Temozolomide Resistance Linked to MGMT Upregulation in Glioblastoma Xenografts. Clin Cancer Res *18*, 4070-4079.

Kiyohara, E., Tamai, K., Katayama, I., and Kaneda, Y. (2012). The combination of chemotherapy with HVJ-E containing Rad51 siRNA elicited diverse anti-tumor effects and synergistically suppressed melanoma. Gene therapy *19*, 734-741.

Konstantinidou, G., Bey, E.A., Rabellino, A., Schuster, K., Maira, M.S., Gazdar, A.F., Amici, A., Boothman, D.A., and Scaglioni, P.P. (2009). Dual phosphoinositide 3-kinase/mammalian target of rapamycin blockade is an effective radiosensitizing strategy for the treatment of non-small cell lung cancer harboring K-RAS mutations. Cancer research *69*, 7644-7652.

Krejci, L., Altmannova, V., Spirek, M., and Zhao, X. (2012). Homologous recombination and its regulation. Nucl Acids Res *40*, 5795-5818.

Lacroix, M., Abi-Said, D., Fourney, D.R., Gokaslan, Z.L., Shi, W., DeMonte, F., Lang, F.F., McCutcheon, I.E., Hassenbusch, S.J., Holland, E.*, et al.* (2001). A multivariate analysis of 416 patients with glioblastoma multiforme: prognosis, extent of resection, and survival. Journal of neurosurgery *95*, 190-198.

Liang, B.C., Thornton, A.F., Jr., Sandler, H.M., and Greenberg, H.S. (1991). Malignant astrocytomas: focal tumor recurrence after focal external beam radiation therapy. Journal of neurosurgery *75*, 559-563.

Liu, T.J., Koul, D., LaFortune, T., Tiao, N., Shen, R.J., Maira, S.M., Garcia-Echevrria, C., and Yung, W.K. (2009). NVP-BEZ235, a novel dual phosphatidylinositol 3-kinase/mammalian target of rapamycin inhibitor, elicits multifaceted antitumor activities in human gliomas. Mol Cancer Ther *8*, 2204-2210.

Lord, C.J., and Ashworth, A. (2012). The DNA damage response and cancer therapy. Nature *481*, 287-294.

Louis, D.N., Ohgaki, H., Wiestler, O.D., Cavenee, W.K., Burger, P.C., Jouvet, A., Scheithauer, B.W., and Kleihues, P. (2007). The 2007 WHO classification of tumours of the central nervous system. Acta neuropathologica *114*, 97-109.

Luo, J., Solimini, N.L., and Elledge, S.J. (2009). Principles of cancer therapy: oncogene and non-oncogene addiction. Cell *136*, 823-837.

Maira, S.M., Stauffer, F., Brueggen, J., Furet, P., Schnell, C., Fritsch, C., Brachmann, S., Chene, P., De Pover, A., Schoemaker, K.*, et al.* (2008). Identification and characterization of NVP-BEZ235, a new orally available dual phosphatidylinositol 3-kinase/mammalian target of rapamycin inhibitor with potent in vivo antitumor activity. Mol Cancer Ther *7*, 1851-1863.

McEllin, B., Camacho, C.V., Mukherjee, B., Hahm, B., Tomimatsu, N., Bachoo, R.M., and Burma, S. (2010). PTEN loss compromises homologous recombination repair in astrocytes: implications for glioblastoma therapy with temozolomide or poly(ADP-ribose) polymerase inhibitors. Cancer research *70*, 5457-5464.

McNeill, R.S., Vitucci, M., Wu, J., and Miller, C.R. (2014). Contemporary murine models in preclinical astrocytoma drug development. Neuro Oncol.

Meyer, M., Reimand, J., Lan, X., Head, R., Zhu, X., Kushida, M., Bayani, J., Pressey, J.C., Lionel, A.C., Clarke, I.D.*, et al.* (2015). Single cell-derived clonal analysis of human glioblastoma links functional and genomic heterogeneity. PNAS *112*, 851-856.

Miller, C.R., and Perry, A. (2007). Glioblastoma. Arch Pathol Lab Med *131*, 397-406.

Miyazaki, T., Bressan, D.A., Shinohara, M., Haber, J.E., and Shinohara, A. (2004). In vivo assembly and disassembly of Rad51 and Rad52 complexes during double-strand break repair. Embo j *23*, 939-949.

Mukherjee, B., Choy, H., Nirodi, C., and Burma, S. (2010). Targeting nonhomologous end-joining through epidermal growth factor receptor inhibition: rationale and strategies for radiosensitization. Semin Radiat Oncol *20*, 250-257.

Mukherjee, B., McEllin, B., Camacho, C.V., Tomimatsu, N., Sirasanagandala, S., Nannepaga, S., Hatanpaa, K.J., Mickey, B., Madden, C., Maher, E.*, et al.* (2009). EGFRvIII and DNA double-strand break repair: a molecular mechanism for radioresistance in glioblastoma. Cancer research *69*, 4252-4259.

Mukherjee, B., Tomimatsu, N., Amancherla, K., Camacho, C.V., Pichamoorthy, N., and Burma, S. (2012). The dual PI3K/mTOR inhibitor NVP-BEZ235 is a potent inhibitor of ATM- and DNA-PKCs-mediated DNA damage responses. Neoplasia *14*, 34-43.

Munck, J.M., Batey, M.A., Zhao, Y., Jenkins, H., Richardson, C.J., Cano, C., Tavecchio, M., Barbeau, J., Bardos, J., Cornell, L.*, et al.* (2012). Chemosensitization of cancer cells by KU-0060648, a dual inhibitor of DNA-PK and PI-3K. Mol Cancer Ther *11*, 1789-1798.

Muranen, T., Selfors, L.M., Worster, D.T., Iwanicki, M.P., Song, L., Morales, F.C., Gao, S., Mills, G.B., and Brugge, J.S. (2012). Inhibition of PI3K/mTOR leads to adaptive resistance in matrix-attached cancer cells. Cancer Cell *21*, 227-239.

Nguyen, S.A., Stechishin, O.D.M., Luchman, H.A., Lun, X.Q., Senger, D.L., Robbins, S.M., Cairncross, G., and Weiss, S. (2014). Novel MSH6 mutations in treatment naïve glioblastoma and anaplastic oligodendroglioma influence temozolomide resistance independently of MGMT methylation. Clin Cancer Res.

Ochs, K., and Kaina, B. (2000). Apoptosis induced by DNA damage O6-methylguanine is Bcl-2 and caspase-9/3 regulated and Fas/caspase-8 independent. Cancer research *60*, 5815-5824.

Ohba, S., Mukherjee, J., See, W.L., and Pieper, R.O. (2014). Mutant IDH1-driven cellular transformation increases RAD51-mediated homologous recombination and temozolomide resistance. Cancer research.

Ohgaki, H., Burger, P., and Kleihues, P. (2014). Definition of primary and secondary glioblastoma--response. Clin Cancer Res *20*, 2013.

Parsons, D.W., Jones, S., Zhang, X., Lin, J.C., Leary, R.J., Angenendt, P., Mankoo, P., Carter, H., Siu, I.M., Gallia, G.L.*, et al.* (2008). An integrated genomic analysis of human glioblastoma multiforme. Science *321*, 1807-1812.

Patel, A.P., Tirosh, I., Trombetta, J.J., Shalek, A.K., Gillespie, S.M., Wakimoto, H., Cahill, D.P., Nahed, B.V., Curry, W.T., Martuza, R.L.*, et al.* (2014). Single-cell RNA-seq highlights intratumoral heterogeneity in primary glioblastoma. Science *344*, 1396-1401.

Perry, J.R., Belanger, K., Mason, W.P., Fulton, D., Kavan, P., Easaw, J., Shields, C., Kirby, S., Macdonald, D.R., Eisenstat, D.D.*, et al.* (2010). Phase II trial of continuous dose-intense temozolomide in recurrent malignant glioma: RESCUE study. J Clin Oncol *28*, 2051-2057.

Peters, K.B., Lou, E., Desjardins, A., Reardon, D.A., Lipp, E.S., Miller, E., Herndon, J.E., 2nd, McSherry, F., Friedman, H.S., and Vredenburgh, J.J. (2015). Phase II Trial of Upfront Bevacizumab, Irinotecan, and Temozolomide for Unresectable Glioblastoma. The oncologist.

Peterson, S.R., Jesch, S.A., Chamberlin, T.N., Dvir, A., Rabindran, S.K., Wu, C., and Dynan, W.S. (1995). Stimulation of the DNA-dependent protein kinase by RNA

polymerase II transcriptional activator proteins. The Journal of biological chemistry *270*, 1449-1454.

Peyton, J.D., Ahnert, J.R., Burris, H., Britten, C., Chen, L.C., Taberno, J., Duval, V., Rouyrre, N., Silva, A.P., Quadt, C.*, et al.* (2011). A dose-escalation study with the novel formulation of the oral pan-class I PI3K inhibitor BEZ235, solid dispersion system (SDS) sachet, in patients with advanced solid tumors. J Clin Oncol *29*, .

Puliyappadamba, V.T., Chakraborty, S., Chauncey, S.S., Li, L., Hatanpaa, K.J., Mickey, B., Noorani, S., Shu, H.K., Burma, S., Boothman, D.A.*, et al.* (2013). Opposing effect of EGFRWT on EGFRvIII-mediated NF-kappaB activation with RIP1 as a cell death switch. Cell Rep *4*, 764-775.

Raderschall, E., Stout, K., Freier, S., Suckow, V., Schweiger, S., and Haaf, T. (2002). Elevated levels of Rad51 recombination protein in tumor cells. Cancer research *62*, 219-225.

Raizer, J.J., Abrey, L.E., Lassman, A.B., Chang, S.M., Lamborn, K.R., Kuhn, J.G., Yung, W.K., Gilbert, M.R., Aldape, K.A., Wen, P.Y.*, et al.* (2010). A phase II trial of erlotinib in patients with recurrent malignant gliomas and nonprogressive glioblastoma multiforme postradiation therapy. Neuro Oncol *12*, 95-103.

Razis, E., Selviaridis, P., Labropoulos, S., Norris, J.L., Zhu, M.J., Song, D.D., Kalebic, T., Torrens, M., Kalogera-Fountzila, A., Karkavelas, G.*, et al.* (2009). Phase II study of neoadjuvant imatinib in glioblastoma: evaluation of clinical and molecular effects of the treatment. Clin Cancer Res *15*, 6258-6266.

Restle, A., Farber, M., Baumann, C., Bohringer, M., Scheidtmann, K.H., Muller-Tidow, C., and Wiesmuller, L. (2008). Dissecting the role of p53 phosphorylation in homologous recombination provides new clues for gain-of-function mutants. Nucleic Acids Res *36*, 5362-5375.

Reya, T., Morrison, S.J., Clarke, M.F., and Weissman, I.L. (2001). Stem cells, cancer, and cancer stem cells. Nature *414*, 105-111.

Roos, W.P., Batista, L.F., Naumann, S.C., Wick, W., Weller, M., Menck, C.F., and Kaina, B. (2007). Apoptosis in malignant glioma cells triggered by the temozolomide-induced DNA lesion O6-methylguanine. Oncogene *26*, 186-197.

Ryken, T.C., Frankel, B., Julien, T., and Olson, J.J. (2008). Surgical management of newly diagnosed glioblastoma in adults: role of cytoreductive surgery. Journal of neuro-oncology *89*, 271-286.

Sanai, N., and Berger, M.S. (2008). Glioma extent of resection and its impact on patient outcome. Neurosurgery *62*, 753-764; discussion 264-756.

Santiskulvong, C., Konecny, G.E., Fekete, M., Chen, K.Y., Karam, A., Mulholland, D., Eng, C., Wu, H., Song, M., and Dorigo, O. (2011). Dual Targeting of Phosphoinositide 3-Kinase and Mammalian Target of Rapamycin Using NVP-BEZ235 as a Novel Therapeutic Approach in Human Ovarian Carcinoma. Clin Cancer Res *17*, 2373-2384.

Sarkaria, J.N., Kitange, G.J., James, C.D., Plummer, R., Calvert, H., Weller, M., and Wick, W. (2008). Mechanisms of chemoresistance to alkylating agents in malignant glioma. Clin Cancer Res *14*, 2900-2908.

Schnell, C.R., Stauffer, F., Allegrini, P.R., O'Reilly, T., McSheehy, P.M., Dartois, C., Stumm, M., Cozens, R., Littlewood-Evans, A., Garcia-Echeverria, C*., et al.* (2008). Effects of the dual phosphatidylinositol 3-kinase/mammalian target of rapamycin inhibitor NVP-BEZ235 on the tumor vasculature: implications for clinical imaging. Cancer research *68*, 6598-6607.

Serra, V., Markman, B., Scaltriti, M., Eichhorn, P.J., Valero, V., Guzman, M., Botero, M.L., Llonch, E., Atzori, F., Di Cosimo, S*., et al.* (2008). NVP-BEZ235, a dual PI3K/mTOR inhibitor, prevents PI3K signaling and inhibits the growth of cancer cells with activating PI3K mutations. Cancer research *68*, 8022-8030.

Shiloh, Y., and Ziv, Y. (2013). The ATM protein kinase: regulating the cellular response to genotoxic stress, and more. Nat Rev Mol Cell Biol *14*, 197-210.

Shinohara, E.T., Geng, L., Tan, J., Chen, H., Shir, Y., Edwards, E., Halbrook, J., Kesicki, E.A., Kashishian, A., and Hallahan, D.E. (2005). DNA-dependent protein kinase is a molecular target for the development of noncytotoxic radiation-sensitizing drugs. Cancer research *65*, 4987-4992.

Short, S.C., Giampieri, S., Worku, M., Alcaide-German, M., Sioftanos, G., Bourne, S., Lio, K.I., Shaked-Rabi, M., and Martindale, C. (2011). Rad51 inhibition is an effective means of targeting DNA repair in glioma models and CD133+ tumor-derived cells. Neuro Oncol *13*, 487-499.

Singh, S.K., Hawkins, C., Clarke, I.D., Squire, J.A., Bayani, J., Hide, T., Henkelman, R.M., Cusimano, M.D., and Dirks, P.B. (2004). Identification of human brain tumour initiating cells. Nature *432*, 396-401.

Sonoda, Y., Ozawa, T., Hirose, Y., Aldape, K.D., McMahon, M., Berger, M.S., and Pieper, R.O. (2001). Formation of intracranial tumors by genetically modified human astrocytes defines four pathways critical in the development of human anaplastic astrocytoma. Cancer research *61*, 4956-4960.

Sottoriva, A., Spiteri, I., Piccirillo, S.G., Touloumis, A., Collins, V.P., Marioni, J.C., Curtis, C., Watts, C., and Tavare, S. (2013). Intratumor heterogeneity in human

glioblastoma reflects cancer evolutionary dynamics. Proceedings of the National Academy of Sciences of the United States of America *110*, 4009-4014.

Stupp, R., Hegi, M.E., Mason, W.P., van den Bent, M.J., Taphoorn, M.J., Janzer, R.C., Ludwin, S.K., Allgeier, A., Fisher, B., Belanger, K.*, et al.* (2009a). Effects of radiotherapy with concomitant and adjuvant temozolomide versus radiotherapy alone on survival in glioblastoma in a randomised phase III study: 5-year analysis of the EORTC-NCIC trial. Lancet Oncol *10*, 459-466.

Stupp, R., Hegi, M.E., Mason, W.P., van den Bent, M.J., Taphoorn, M.J.B., Janzer, R.C., Ludwin, S.K., Allgeier, A., Fisher, B., Belanger, K.*, et al.* (2009b). Effects of radiotherapy with concomitant and adjuvant temozolomide versus radiotherapy alone on survival in glioblastoma in a randomised phase III study: 5-year analysis of the EORTC-NCIC trial. The Lancet Oncology *10*, 459-466.

Stupp, R., Mason, W.P., van den Bent, M.J., Weller, M., Fisher, B., Taphoorn, M.J., Belanger, K., Brandes, A.A., Marosi, C., Bogdahn, U.*, et al.* (2005). Radiotherapy plus concomitant and adjuvant temozolomide for glioblastoma. N Engl J Med *352*, 987-996.

Sung, P. (1994). Catalysis of ATP-dependent homologous DNA pairing and strand exchange by yeast RAD51 protein. Science *265*, 1241-1243.

Symington, L.S., and Gautier, J. (2011). Double-strand break end resection and repair pathway choice. Annu Rev Genet *45*, 247-271.

Takaku, M., Kainuma, T., Ishida-Takaku, T., Ishigami, S., Suzuki, H., Tashiro, S., van Soest, R.W., Nakao, Y., and Kurumizaka, H. (2011). Halenaquinone, a chemical compound that specifically inhibits the secondary DNA binding of RAD51. Genes to cells : devoted to molecular & cellular mechanisms *16*, 427-436.

Toledo, L.I., Murga, M., Zur, R., Soria, R., Rodriguez, A., Martinez, S., Oyarzabal, J., Pastor, J., Bischoff, J.R., and Fernandez-Capetillo, O. (2011). A cell-based screen identifies ATR inhibitors with synthetic lethal properties for cancer-associated mutations. Nature structural & molecular biology *18*, 721-727.

Tomimatsu, N., Mukherjee, B., Catherine Hardebeck, M., Ilcheva, M., Vanessa Camacho, C., Louise Harris, J., Porteus, M., Llorente, B., Khanna, K.K., and Burma, S. (2014). Phosphorylation of EXO1 by CDKs 1 and 2 regulates DNA end resection and repair pathway choice. Nature communications *5*, 3561.

van den Bent, M.J., Brandes, A.A., Rampling, R., Kouwenhoven, M.C., Kros, J.M., Carpentier, A.F., Clement, P.M., Frenay, M., Campone, M., Baurain, J.F.*, et al.* (2009). Randomized phase II trial of erlotinib versus temozolomide or carmustine in recurrent glioblastoma: EORTC brain tumor group study 26034. J Clin Oncol *27*, 1268-1274.

Verhaak, R.G., Hoadley, K.A., Purdom, E., Wang, V., Qi, Y., Wilkerson, M.D., Miller, C.R., Ding, L., Golub, T., Mesirov, J.P.*, et al.* (2010). Integrated genomic analysis identifies clinically relevant subtypes of glioblastoma characterized by abnormalities in PDGFRA, IDH1, EGFR, and NF1. Cancer Cell *17*, 98-110.

Vredenburgh, J.J., Desjardins, A., Herndon, J.E., 2nd, Marcello, J., Reardon, D.A., Quinn, J.A., Rich, J.N., Sathornsumetee, S., Gururangan, S., Sampson, J.*, et al.* (2007). Bevacizumab plus irinotecan in recurrent glioblastoma multiforme. J Clin Oncol *25*, 4722-4729.

Walker, M.D., Alexander, E., Jr., Hunt, W.E., MacCarty, C.S., Mahaley, M.S., Jr., Mealey, J., Jr., Norrell, H.A., Owens, G., Ransohoff, J., Wilson, C.B.*, et al.* (1978). Evaluation of BCNU and/or radiotherapy in the treatment of anaplastic gliomas. A cooperative clinical trial. Journal of neurosurgery *49*, 333-343.

Wang, C., and Lees-Miller, S.P. (2013). Detection and Repair of Ionizing Radiation-Induced DNA Double Strand Breaks: New Developments in Nonhomologous End Joining. Int J Radiat Oncol Biol Phys.

Wang, H., Shi, L.Z., Wong, C.C., Han, X., Hwang, P.Y., Truong, L.N., Zhu, Q., Shao, Z., Chen, D.J., Berns, M.W.*, et al.* (2013). The interaction of CtIP and Nbs1 connects CDK and ATM to regulate HR-mediated double-strand break repair. PLoS genetics *9*, e1003277.

Ward, A., Khanna, K.K., and Wiegmans, A.P. (2015). Targeting homologous recombination, new pre-clinical and clinical therapeutic combinations inhibiting RAD51. Cancer treatment reviews *41*, 35-45.

Wedge, S.R., Porteous, J.K., and Newlands, E.S. (1996a). 3-aminobenzamide and/or O6-benzylguanine evaluated as an adjuvant to temozolomide or BCNU treatment in cell lines of variable mismatch repair status and O6-alkylguanine-DNA alkyltransferase activity. Br J Cancer *74*, 1030-1036.

Wedge, S.R., Porteus, J.K., May, B.L., and Newlands, E.S. (1996b). Potentiation of temozolomide and BCNU cytotoxicity by O(6)-benzylguanine: a comparative study in vitro. Br J Cancer *73*, 482-490.

Wiewrodt, D., Nagel, G., Dreimüller, N., Hundsberger, T., Perneczky, A., and Kaina, B. (2008). MGMT in primary and recurrent human glioblastomas after radiation and chemotherapy and comparison with p53 status and clinical outcome. International Journal of Cancer *122*, 1391-1399.

Yamaguchi, M., Saito, H., Suzuki, M., and Mori, K. (2000). Visualization of neurogenesis in the central nervous system using nestin promoter-GFP transgenic mice. Neuroreport *11*, 1991-1996.

Yip, S., Miao, J., Cahill, D.P., Iafrate, A.J., Aldape, K., Nutt, C.L., and Louis, D.N. (2009). MSH6 Mutations Arise in Glioblastomas during Temozolomide Therapy and Mediate Temozolomide Resistance. Clin Cancer Res *15*, 4622-4629.

Yun, M.H., and Hiom, K. (2009). CtIP-BRCA1 modulates the choice of DNA double-strand-break repair pathway throughout the cell cycle. Nature *459*, 460-463.

Yung, W.K., Vredenburgh, J.J., Cloughesy, T.F., Nghiemphu, P., Klencke, B., Gilbert, M.R., Reardon, D.A., and Prados, M.D. (2010). Safety and efficacy of erlotinib in first-relapse glioblastoma: a phase II open-label study. Neuro Oncol *12*, 1061-1070.

Zhao, Y., Thomas, H.D., Batey, M.A., Cowell, I.G., Richardson, C.J., Griffin, R.J., Calvert, A.H., Newell, D.R., Smith, G.C., and Curtin, N.J. (2006). Preclinical evaluation of a potent novel DNA-dependent protein kinase inhibitor NU7441. Cancer research *66*, 5354-5362.

Zhu, J., Zhou, L., Wu, G., Konig, H., Lin, X., Li, G., Qiu, X.L., Chen, C.F., Hu, C.M., Goldblatt, E.*, et al.* (2013). A novel small molecule RAD51 inactivator overcomes imatinib-resistance in chronic myeloid leukaemia. EMBO Mol Med *5*, 353-365.